RUNNING TITLE: Effect of proliferation on RPE phenotype

TITLE: Targeting the cAMP and TGFβ pathway increases proliferation to promote re-epithelialization of human stem cell derived retinal pigment epithelium

AUTHORS: Parul Choudhary[1], Alex Gutteridge[1], Emma Impey[1], R. Ian Storer[2], Robert M. Owen[2], Paul J. Whiting[1], Magda Bictash[1,3], Caroline L. Benn[1,3]

[1]Pfizer Neuroscience and Pain Research Unit, The Portway, Granta Park, Great Abington, Cambridge CB21 6GS, UK.

[2]Pfizer Worldwide Medicinal Chemistry, The Portway, Granta Park, Great Abington, Cambridge CB21 6GS, UK.

[3]These authors contributed equally to this work

AUTHOR CONTRIBUTIONS:

Parul Choudhary: Conception and design, Collection and/or assembly of data, Data analysis and interpretation, Manuscript writing, Final approval of manuscript

Alex Gutteridge: Data analysis and interpretation

Emma Impey: Collection and/or assembly of data

R. Ian Storer: Data analysis and interpretation

Robert M. Owen: Data analysis and interpretation

Paul J. Whiting: Financial support, Final approval of manuscript

Magda Bictash: Conception and design, Data analysis and interpretation, Final approval of manuscript

Caroline L. Benn: Conception and design, Manuscript writing, Final approval of manuscript

Address correspondence to: Parul Choudhary, PhD, The Portway, Granta Park, Great Abington, Cambridge CB21 6GS, UK. Tel: +44 (0)1304 640689; Fax: +44 (0)1304 641573; E-mail: parul.choudhary@pfizer.com; parulc83@gmail.com

KEY WORDS: Retinal Pigment Epithelium, Stem Cells, Proliferation, cAMP, TGFβ

ABSTRACT

Retinal pigment epithelium (RPE) cell integrity is critical to the maintenance of retinal function. Many retinopathies such as age-related macular degeneration (AMD) are caused by the degeneration or malfunction of the RPE cell layer. Replacement of diseased RPE with healthy, stem cell derived RPE is a potential therapeutic strategy for treating AMD. Human embryonic stem cells (hESC) differentiated into RPE progeny have potential to provide an unlimited supply of cells for transplantation but challenges around scalability and efficiency of the differentiation process still remain. Using hESC-derived RPE as a cellular model, we sought to understand mechanisms that could be modulated to increase RPE yield following differentiation. We show that RPE epithelialization is a density-dependent process and cells seeded at low density fail to epithelialize. We demonstrate that activation of the cAMP pathway increases proliferation of dissociated RPE in culture, in part through inhibition of TGFβ signalling. This in turn results in enhanced uptake of epithelial identity even in cultures seeded at low density. In line with these findings, targeted manipulation of the TGFβ pathway with small molecules produces an increase in efficiency of RPE re-epithelialization. Taken together, these data highlight mechanisms that promote epithelial fate acquisition in stem cell derived RPE. Modulation of these pathways has potential to favorably impact upon scalability and clinical translation of hESC-derived RPE as a cell therapy.

INTRODUCTION

Retinal pigment epithelium cells are a highly specialised, polarised cell type situated as a tightly packed monolayer between photoreceptors and the choroid. RPE cells help to maintain homeostasis and photoreceptor function in the retina via a range of processes including metabolism and storage of retinoid, phagocytosis of rod outer segments, scattered light absorption, barrier activity and ion transport [1]. Loss of RPE function is associated with diseases such as Age-Related Macular Degeneration (AMD), Retinitis Pigmentosa, proliferative vitreoretinopathy (PVR) and diabetic retinopathies among others, which often result in loss of vision [2]. The prevalence of AMD is on the

rise with increasing population longevity [3], which necessitates the development of new therapeutic approaches to treat this disease. A potential treatment for at least some of these ocular pathologies is the replacement of the dysfunctional RPE with healthy RPE including RPE derived from pluripotent stem cells [4]. Several studies have demonstrated successful derivation of mature RPE from human embryonic stem cells (hESC) or human induced pluripotent stem cells (hiPSC) using a range of differentiation protocols which produce RPE at varying levels of efficiency and time scales [5-7]. Stem cell derived RPE are functional [8-10] and have a gene expression signature equivalent to primary RPE [11-13]. Furthermore, their transplantation shows long-term protective effects leading to restored visual function in animal models of retinal dystrophy [14-17]. However, manufacture of transplantation-ready RPE cells with high yield and purity under conditions compatible with good manufacturing practices (GMP) still remains a significant challenge that needs to be overcome in order to successfully use this approach more widely.

RPE cells are normally quiescent in the adult eye. However, *in vitro* dissociation and passaging procedures release RPE from cell cycle arrest and induce proliferation. This is accompanied by an epithelial-mesenchymal transition (EMT) where cells deviate from an epithelial state and acquire a mesenchymal phenotype. This is followed by a FOXM1 dependent mesenchymal-epithelial transition (MET) that results in re-uptake of epithelial characteristics [18]. The proliferative capacity of RPE allows serial expansion of cells in culture, albeit limited to a few passages, as cells lose key cytological and functional attributes with extended passage [19]. This limits the capacity of expansion of RPE with respect to manufacturing cells at scale for therapy. In this report, we sought to further understand the molecular mechanisms underpinning the acquisition of RPE cell fate and investigate the contribution of cellular proliferation together with cellular density to this process. Manipulation of these mechanisms would potentially allow better control of the differentiation and expansion process which might favourably impact cell production for clinical applications.

Cyclic AMP (cAMP) is a second messenger used in intracellular signal transduction and can regulate the function of protein kinases which in turn phosphorylate other proteins including transcription

factors such as CREB. Activation of cAMP-inducible genes regulate cellular processes such as differentiation and proliferation in a variety of cell types [20]. In RPE cells, cAMP has been shown to promote differentiation and maturation purportedly via proliferation-independent mechanisms such as promoting melanosome and pigmentation related pathways [21-24]. Approaches to increase cAMP e.g with the use of Vasointestinal Peptide, a hormone that raises intracellular cAMP, have been utilized in directing differentiation of embryonic stem cells towards the RPE lineage [9]. Similarly, review of the literature suggests that cAMP signalling controls migratory and fibrotic responses similar to those seen in PVR [25-27]. Therefore, we sought to determine whether cAMP treatment impacted gain of RPE identity during *in vitro* dissociation and culture of hESC-derived RPE. Interestingly, we observed that treatment with dibutyryl-cAMP (dbcAMP, Bucladesine), a cell permeable synthetic analogue of cAMP or use of molecules such as forskolin that increase intracellular cAMP through activation of Adenylyl cyclase, promote re-acquisition of RPE fate across a range of seeding densities in a proliferation dependent manner. Investigation into the underlying molecular pathways further suggested that interplay between cAMP signalling and the TGFβ pathway might be responsible for the phenotypic effects observed.

The TGFβ pathway plays a central role in several cellular processes where it transduces extracellular signals into intracellular transcriptional responses that control cell growth, apoptosis, and differentiation. The TGFβ superfamily of endogenous signaling ligands consists of more than 25 different ligands including BMPs, growth and differentiation factors and activins. TGFβ ligands (TGFβ1, β2 and β3) recruit TGFβ type II receptors (TGFβR2, ACTRIIA, or ACTRIIB) with a set of type I receptors (ALK4, ALK5, or ALK7). Receptor dimerization together with phosphorylation of SMADs 2/3 due to the receptor serine/threonine kinase activity leads to SMAD nuclear translocation and downstream regulation of transcription resulting in signal propagation [28]. In this report, we show that inhibition of TGFβ signalling, in particular through inhibition of ALK5 kinase activity, with the use of small molecule tools results in an increase in epithelial phenotype of RPE. This suggests that signaling through TGFβ type I receptors, is an important determinant of epithelial cell fate.

In summary, this study furthers our understanding of the biology of stem cell derived RPE and additionally highlights potential points of intervention in pathways that could be targeted to increase efficiency of generating RPE suitable for transplantation.

MATERIALS AND METHODS

1. *Cell culture and manipulations:* RPE were generated from the hESC line SHEF1 (obtained from Axordia Ltd, also available in the UK Stem Cell Bank with the accession number R-05-007) using the spontaneous differentiation method described previously [7]. Pluripotent cells were cultured as feeder-free colonies on hESC-qualified Matrigel (BD Biosciences) using mTesR1 media (StemCell Technologies). RPE foci (Passage 0, P0) were excised with a scalpel and dissociated into a single cell suspension using Accutase (Gibco) and plated onto CellStart (Invitrogen) coated surfaces for expansion for a period of 8 weeks. For all experiments, the starting population of cells used were at P1 or P2 such that each round of expansion led to 3-4 population doublings. For experiments involving culture of cells in transwells, cells at P1 were plated on Vitronectin (AMS Bio) coated transwells at a density of 362500 cells/cm^2 and cultured for a period of 3 weeks. Quantification of VEGF and PEDF in the cell culture supernatant was performed on the Mesoscale discovery platform using commercially available kits (MS6000, Human VEGF PEDF duplex assay). Bead phagocytosis assay was performed using FluoSpheres polystyrene microspheres (1.0µm Red; Invitrogen) following a published protocol [29]. Where required, media was supplemented with 10µM Forskolin (Sigma), 0.5mM dbcAMP (Sigma), 10ng/ml TGFβ1 or 10µg/ml 1D11 (R&D Biosystems) at the time of seeding. For screening, compounds were obtained from the Pfizer library, solubilized in 100% DMSO and serially diluted such that final assay and vehicle concentration was 0.1% DMSO. ALK2 inhibitors DMH1 and LDN-212854 were purchased from Tocris. For all treatments, media was replenished three times per week.

2. RNA extraction, cDNA synthesis and quantitative PCR: Total RNA was extracted from RPE cells using the RNEasy Mini or Micro Kit (Qiagen) with on-column DNase digestion. cDNA was synthesized

using the High Capacity cDNA Synthesis kit (Applied Biosystems). Individual gene expression was assessed using predesigned Taqman assays and the reactions were carried out on the ABI7900 or CFX96 platform. Gene expression in all instances was quantified by the Relative quantification method of $2^{-\Delta\Delta Ct}$ and normalized to geometric means of housekeeping genes.

3. Microarray analysis: mRNA was hybridized on Illumina HT-12v4 BeadChips according to manufacturer's instructions. Raw microarray data was log transformed and quantile normalised using the beadarray package in Bioconductor. Differential expression analysis was performed using limma and geneset enrichment analysis with camera. All other analysis was performed with standard Bioconductor/R packages. Standard hierarchical clustering algorithms were used to achieve visual clarity of the heatmaps. The microarray data are available in the ArrayExpress database under accessions E-MTAB-854 and E-MTAB-3878.

4. *Immunocytochemistry*: Samples were fixed in 4% paraformaldehyde in PBS for 15 min followed by blocking and permeabilization using 0.3% Triton X-100 in PBS and 10% normal donkey serum. Primary antibodies used in this study are: mouse anti-PMEL17 (1:25, Dako M0634), rabbit anti-Ki67 (1:500, VectorLabs VP-K451), rabbit anti-ZO1 (1:100, Zymed 187430), mouse anti-αSMA (1:1000, Sigma A5228), mouse anti-CRALBP (1:200, Affinity Biosciences MA1-813), rabbit anti-MERTK (1:50, Abcam ab52968). For EdU incorporation, cells were treated with 10μM EdU 18 hours prior to fixation. EdU incorporation was measured using the Click-iT 488 Imaging kit (Life Technologies) according to manufacturer's instructions. Nuclei were counterstained with the nuclear dye 4',6-diamidino-2-phenylindole (DAPI). For immunocytochemistry of transwell sections, the transwell membrane was fixed and frozen in a cryomold containing M1 embedding matrix and 10μm sections were prepared using a cryostat and immunostained. Images were captured and analyzed on the ImageXpress platform (Molecular devices) or on a confocal microscope (Leica).

RESULTS

1. RPE epithelialization is a density-dependent process.

Although RPE are differentiated epithelial cells, they retain the ability to change state into a mesenchymal phenotype when dissociated and cultured. This transitional state then undergoes a mesenchymal-epithelial transition to re-differentiate into an epithelial phenotype (Figure 1A) [18]. Successful epithelialization is critically reliant on seeding density such that cells seeded at high density successfully re-epithelialize whereas cells seeded at low density remain mesenchymal. In order to gain further insight into this density dependent process, we used whole genome microarrays to analyse a transcriptional profile time course of cells seeded either at high (100000 cells/cm^2) or low (8000 cells/cm^2) density. Strikingly, the expression patterns of most genes clustered into two distinct, symmetrical groups (Figure 1B). Genes in the first cluster exhibit relatively high expression in the starting RPE sample (D0), but show an immediate drop in expression following dissociation. These genes then steadily increase in expression towards the starting level in the high density culture but remain suppressed in the low density cultures. The second cluster shows the opposite pattern: initially low in expression, these genes immediately rise following dissociation before decreasing to their D0 level in the high density culture, whereas their expression tends to remain high in the low density cultures. Importantly, we note that the transcriptional state of the cells seeded at high density returns towards that of the starting RPE population, whereas cells seeded at low density remain distinct. The list of genes belonging to clusters 1 and 2 can be seen in Supplementary Table 1.

We further examined the expression of epithelial and mesenchymal markers and, consistent with visual observations, there was an initial upregulation of mesenchymal markers concomitant with a decrease in epithelial and RPE specific markers upon dissociation. This was followed by a re-expression of epithelial markers in high density cultures with time indicating a successful mesenchymal-epithelial transition. In contrast, cells seeded at low density retained high expression of mesenchymal markers and low expression of epithelial markers throughout the timecourse (Figure 1C). Immunostaining for representative RPE markers PMEL17, RLBP1 and ZO1 and the mesenchymal marker α-SMA was consistent with the mRNA expression pattern confirming that low

density cultures did not display an epithelial phenotype (Figure 1D). Taken together, this analysis strongly suggests that an appropriately high seeding density is required for successful epithelialization. In addition, we confirmed that the RPE obtained following re-epithelialization were polarized and functional in terms of phagocytosis and ability to secrete trophic factors such as VEGF and PEDF, which are key features of native RPE. RPE were seeded on transwell inserts and cultured for a period of 3 weeks. Cross-sections of the insert were immunostained for the RPE markers ZO1, MERTK and PMEL17 (Supplementary figure 1A). The expression of ZO1 was restricted to the cell junctions, MERTK to the apical surface and PMEL17 throughout the cell body consistent with cell polarization. Furthermore, RPE were capable of phagocytosing fluorescently labelled beads (Supplementary figure 1B) which serves as a surrogate measure of ability to phagocytose rod outer segments [30]. Finally, we measured the ability of RPE to secrete VEGF and PEDF. Spent media was collected from RPE cultured on transwells and compared to ARPE19 cells cultured under identical conditions. We observed an increase in VEGF and PEDF secretion by RPE with time in culture (e.g at day 21 vs. day 4) indicative of attainment of polarisation and functionality upon re-epithelialization (Supplementary figure 1C). In contrast, ARPE19 did not secrete detectable levels of PEDF consistent with the notion that they do not replicate all aspects of native RPE function.

2. Increasing cAMP levels promotes acquisition of RPE identity in a time- and density- dependent manner

We have shown a density-dependent effect on re-acquisition of epithelial identity where cells seeded at high density readily differentiate back into a RPE state over a period of time but cells seeded at a lower density do not. Next, we wanted to understand the pathways underlying RPE epithelialization and identify their putative modulators. Given the literature suggesting effects of cAMP signalling on RPE characteriscs [21-25], we selected forskolin (FSK) as a tool to increase intracellular cAMP levels. We found that treatment with 10μM FSK led to a consistent increase in pigmentation and epithelial characteristics across a range of seeding densities (Figure 2A,

Supplementary figure 2). This prompted us to ask whether FSK treatment modulated the gene expression profile of cells during the time course of RPE culture. Taqman low density arrays (TLDA) were used to perform qPCR with a panel of 24 genes indicative of epithelial or mesenchymal identity (Supplementary figure 3). We performed a principal component analysis on this multivariate data and found that the first principal component correlated with high expression of epithelial genes and low expression of mesenchymal genes. We used the first principal component as a univariate weighted score of RPE identity and therefore used it to measure the effect of FSK at a range of seeding densities (2.5k, 10k, 15k, 20k, 25k, 27.5k, 30k, 38k; k=x1000cells/cm^2) after 63 days in culture. This showed that treatment with FSK led to an increase in 'RPE-score' i.e acquisition of the RPE phenotype, at every plating density tested (Figure 2B).

A limitation of the TLDA-based approach is the comparatively limited set of genes profiled. Due to this, we were limited in our ability to generate unbiased hypotheses about the underlying mechanism of increased epithelialization with increased cAMP levels. We therefore sought to extend these initial qPCR-based observations to global gene expression profiling. In order to generate a comprehensive dataset, we used microarrays to assess the effect of increased cAMP signalling on cells seeded at 10000, 20000 and 40000 cells/cm^2 over time (3, 15 and 34 days in culture). The stable, cell permeant cAMP analogue, dbcAMP, was used to enhance intracellular cAMP signalling in this study. Interestingly, principal component analysis showed that at every timepoint sampled, the gene expression signature of cells treated with 0.5mM dbcAMP was equivalent to cells seeded at double the density in media alone (Figure 3A). For example, the expression profile of cells seeded at 10000 cells/cm^2 with dbcAMP was equivalent to that of cells at 20000 cells/cm^2 without dbcAMP. Similarly, the expression profile of cAMP-treated cells at 20000 cells/cm^2 was comparable to cells at 40000 cells/cm^2 without supplementation. A clustered heatmap representation of the top 1% variable genes reiterates the same observation of a 'doubling effect' of density in cells exposed to dbcAMP where cells treated with dbcAMP clustered with cells seeded at twice the density without dbcAMP exposure (Figure 3B). We next looked at the expression of specific RPE markers and found

240 them to be consistent with the profiles seen with the whole genome analyses (Figure 3C). These
241 expression patterns were further confirmed by gene specific qPCR for representative genes
242 (Supplementary figure 4A) together with immunostaining for protein expression (Supplementary
243 figure 4B). Additionally, we determined that a dose of at least 0.5mM dbcAMP was required to see
244 this effect (Supplementary fig 4C). In summary, these data show that intracellular elevation of cAMP
245 signalling leads to an increase in acquisition of RPE phenotype.
246
247 **3. Increasing cAMP levels promotes RPE proliferation**
248 In order to gain insight into the molecular mechanisms by which cAMP positively modulates RPE
249 fate, we performed geneset enrichment analyses (GSEA) of the dbcAMP induced expression
250 changes. Besides markers of the RPE phenotype, there was enhanced representation of sets of
251 genes associated with increased proliferation (Figure 4A, Supplementary table 2). This suggested
252 that the increased epithelial phenotype could occur as a result of increased proliferation. In order to
253 test this hypothesis, we assessed proliferation in cells treated with or without dbcAMP, using the
254 incorporation of EdU, a modified thymidine analogue, which can be visualized using 'Click' chemistry
255 dependent imaging [31]. We found an increase in proliferating cells upon supplementation with
256 dbcAMP on days 7, 14 and 21 of culture (Figure 4B). Importantly, with increased time e.g at day 56,
257 there was no significant difference in proliferation between cells supplemented with dbcAMP or not
258 (Figure 4B). This suggests that although intracellular cAMP elevation promotes proliferation, it is not
259 an uncontrolled feature and homeostatic RPE mechanisms are in play to achieve quiescence after
260 the initial phase of proliferation upregulation. An increase in proliferation, measured by
261 immunostaining for Ki67, was seen upon treatment of cells with FSK (Figure 4C) showing that
262 intracellular cAMP elevation by different methods resulted in a similar effect. We also determined
263 the optimum period of dbcAMP exposure required to observe effects on proliferation. Cells were
264 seeded at a density of 38000 cells/cm^2 and cultured for a period of 8 weeks with continuous dbcAMP
265 treatment for either 2 weeks, 3 weeks or the entire duration of 8 weeks. The increase in

proliferation resulted in an increased number of cells whose nuclei stained positive for the nuclear specific fluorescent dye DAPI. Using DAPI count as a surrogate for cell number estimation, we observed no difference in cell number between the dbcAMP exposure times tested (Figure 4D). From this data, we conclude that exposure of cells to dbcAMP for the first 2 weeks post dissociation and seeding is sufficient to result in increased proliferation.

4. Activation of cAMP signalling suppresses the TGFβ pathway to promote successful epithelialization

To understand mode of cAMP action, causal reasoning analysis [32] of the gene expression dataset was performed to predict molecular regulators of the observed gene expression changes. We compared the gene expression profiles of cultures seeded at 20000 cells/cm^2 in the presence or absence of dbcAMP at day 34 and observed that TGFβ signalling was a key mechanism being supressed by dbcAMP treatment ($p = 7.95x10^{-17}$). In order to further decipher the interplay between cAMP-TGFβ pathways, we made use of information available in the literature. It is known that activation of the TGFβ pathway leads to downstream activation of SMADs 2/3 which then directly affect gene expression by binding to gene promoters. We identified genes that are directly bound by SMAD3 using a publically available ChIP-Seq dataset [33]. We then investigated how the expression of these genes changed upon dbcAMP treatment. Interestingly, we observed a significantly decreased expression of SMAD3 responsive genes in RPE cells treated with dbcAMP ($p < 1x10^{-10}$) (Figure 5A). Taken together, these two lines of evidence support the notion that active cAMP signalling, which promotes proliferation and epithelialization, is associated with inhibition of the TGFβ pathway in RPE.

In order to explore the role of TGFβ signalling more deeply, we looked at the expression profile of TGFβ ligands as well as genes downstream of type 1 and 2 TGFβ receptor activation in high vs low density cultures. This demonstrated that high density cultures, which epithelialize normally, have low expression TGFβ pathway members (Supplementary figure 5). This is in line with the hypothesis

that TGFβ signalling is suppressed for successful epithelialization. In order to further verify this observation, we asked whether exogenous activation of the TGFβ pathway in high density cultures, which would normally have supressed TGFβ signalling, would lead to a decrease in epithelial phenotype acquisition. Recombinant TGFβ1 was added to cultures seeded at a high density of 100000 cells/cm^2 and maintained in the media for a period of 5 days. An increase in transcript expression of mesenchymal markers along with a decrease in expression of epithelial markers as measured by qPCR, was observed which suggested that activation of TGFβ signalling indeed prevented successful epithelialization (Figure 5B). This was also verified by immunostaining for expression of epithelial (PMEL17) and mesenchymal (αSMA) proteins (Figure 5C, 5D). We next tested whether the effect on phenotype was a consequence of change in cellular proliferation. Consistent with the effects seen with dbcAMP supplementation, activation of TGFβ signalling by addition of recombinant TGFβ1 protein led to a decrease in proliferation as measured by immunostaining for Ki67 (Figure 5C, 5D). Taken together, our data supports the hypothesis that TGFβ signalling and its associated anti-proliferative effect is supressed in RPE cultures seeded at high density that acquire an epithelial phenotype.

5. Screen for small molecules that positively modulate epithelialization

A key requirement for a successful RPE cell replacement therapy is the scalable and efficient generation of RPE with a differentiated epithelial phenotype. In this context, identification of small molecules that could promote consistent acquisition of an epithelial phenotype even at low densities would be particularly advantageous. Therefore, we sought to leverage and extend our initial observations and look for small molecule tools that would promote epithelial phenotype acquisition at low density, a condition where RPE would not normally epithelialize. We generated a bespoke library consisting of 1000 small molecules that were known agonists or antagonists of proteins within pathways likely to affect RPE fate based on hypotheses posed by expression data or published literature indications. This included signalling pathways such as BMP, Wnt, TGFβ etc. FSK

was used as a positive control compound known to promote re-epithelialization as shown by our dbcAMP data. We established a high content immunocytochemistry based assay for PMEL17, a marker of mature pigmented RPE, in a 384 well format to allow compound screening at sufficiently high throughput with modest cell requirements. Primary screening was performed using compounds at a concentration of 10μM. A positive hit was defined as a molecule that increased % positive PMEL17 expression to greater than 3 standard deviations above the DMSO vehicle control. Effect on DAPI measurement, which is indicative of cell number, was also quantified. Data generated using these parameters allowed us to identify whether positive hits function potentially through a proliferative mode of action. Compounds that led to a significant decrease in DAPI compared to vehicle control with no effect on PMEL17 were considered toxic and ruled out from additional analysis. Data deconvolution demonstrated significant effects on PMEL17 caused by multiple inhibitors of the type 1 TGFβ receptors with a preponderance of compounds with activity against ALK5 kinase. These compounds appeared to promote epithelialization through increasing cell proliferation (i.e having an effect of increased DAPI count concomitant with increased %PMEL17). However, we did not find any mechanisms other than TGFβ signalling in this investigation.

In order to verify primary hits, we extended our investigation to a broader set of ALK5 inhibitors and generated dose-response curves to measure impact on RPE phenotype by immunocytochemistry for PMEL17 (Figure 6A). We included a further assessment of cellular proliferation by quantifying the level of incorporation of EdU measured by imaging, and determined effect of compound dose on this output (Figure 6B). We determined EC_{50} values for both measures and noted a close correlation (R^2=0.8) between EC_{50} for %PMEL17 positive and %EdU positive cells for all ALK5 inhibitors tested (Figure 6C) supporting the notion that ALK5 inhibition promotes cellular proliferation and attainment of RPE phenotype. The observed EC_{50} values for both PMEL17 and EdU were broadly in the same rank order as the published potencies against ALK5 for the compounds tested (Supplementary fig. 6). However, this is limited by the fact that the ALK5 potencies have not been re-measured in parallel, instead relying on literature values across different assay formats which can introduce variability.

We were also able to rule out off-target effects due to particular compound chemotypes as a consistent effect on RPE phenotype was observed with ALK5 inhibitor compounds from different chemical series. In addition, it is noteworthy that inhibitors of ALK2, a receptor for BMP ligands that signal through a distinct arm in the TGFβ cascade, had no effect on RPE phenotype indicating specificity of the ALK5 mechanism (Compound 8 (DMH1) and Compound 9 (LDN-212854) in Figure 6A, 6B).

To confirm that the output measure of immunostaining for PMEL17 was indicative of a true increase in epithelial RPE characteristics, we performed qPCR to measure expression of a panel of epithelial and mesenchymal markers. Compounds 6 and 7 (EC_{50}=1.27 μM and 0.1 μM for PMEL17 respectively) were chosen as representative examples for this broader analysis. RPE were seeded at 15,000 cells/cm^2 and treated with compounds at three concentrations (10, 1 and 0.1 μM). A consistent increase in several RPE markers (*BEST1*, *LRAT*, *MERTK*, *RPE65*, *RLBP1*) was seen along with decrease in a marker indicative of a mesenchymal phenotype (*GREM1*) (Supplementary figure. 7). Measurement of these multiple endpoints provide further support to the notion that ALK5 inhibitors promote acquisition of the RPE phenotype.

6. Validation of TGFβ mechanism

Following on from compound screening, we wanted to independently verify the TGFβ mechanism through an orthogonal, non-chemical based interrogation. To enable this, we selected 1D11, a well-characterized monoclonal pan–TGFβ-neutralizing antibody [34] to inhibit endogenous TGFβ signalling. RPE were seeded at low density of 15000 cells/cm^2 where TGFβ signalling should be active, and treated with neutralizing antibody for a period of 14 days. An increase in epithelial markers with an accompanying decrease in mesenchymal markers was observed at both the transcript (Figure 7A) and protein level (Figure 7B), measured by qPCR and immunocytochemistry respectively, indicating enhanced uptake of epithelial characteristics. We also observed an increase in proliferation as measured by imaging of EdU incorporation, confirming that suppression of TGFβ

signalling led to enhanced proliferation (Figure 7B). Taken together, our data is consistent with the hypothesis that TGFβ signalling serves to impede epithelial phenotype acquisition in RPE and that its inhibition can lead to enhanced uptake of epithelial identity.

DISCUSSION:

Stem cells provide a potentially unlimited source of cells for regenerative therapy in a range of human disorders including retinal diseases such as age-related macular degeneration (AMD). AMD is the leading cause of blindness in people over the age of 65 in the developed world. It is a progressive disease caused by death and dysfunction of the retinal pigment epithelium (RPE) which in turn leads to photoreceptor loss. The specific loss of the RPE monolayer, combined with other advantages of targeting this particular tissue (immune privileged niche, ease of accessibility, separation from systemic circulation, well established methods for diagnosis and monitoring progression) suggests AMD as a prime candidate for exploring replacement of the damaged RPE monolayer with stem cell derived healthy RPE as a therapy [35-38].

The RPE monolayer, formed in the early embryo, is a terminally differentiated cell sheet which develops with a centre to periphery gradient such that only the peripheral cells retain low levels of proliferation whereas the remainder remains non-proliferative throughout life [39, 40]. However, in culture, their normal quiescence can be released resulting in a re-entry into the cell-cycle accompanied by proliferation. This results in trans-differentiation where cells deviate from an epithelial state and instead express hallmarks of a fusiform, mesenchymal state. This is followed by a mesenchymal-epithelial transition (MET) regulated by the transcription factor FOXM1 which results in re-epithelialization [18]. However, this process is density dependent, where cells seeded at an appropriately high density, successfully acquire an epithelial phenotype. Cultures seeded at low density fail to attain the epithelial state and instead continue to remain mesenchymal. Taking advantage of the critical seeding-density dependent nature of the culture, we wanted to gain further understanding of the signalling pathways that control the transition and acquisition of the epithelial

phenotype. This would allow us to interrogate pathways of interest and hence promote epithelial fate achievement and increased RPE yield.

In the first instance, we have shown that manipulating cAMP levels significantly impacts on the re-attainment of the RPE phenotype in a time- and density-dependent manner. Published literature suggested that cAMP exerts direct effects on RPE phenotypes such as pigmentation and phagocytosis while inhibiting RPE proliferation [25, 26]. We show that elevating cAMP levels in dissociated RPE cells through FSK treatment or use of the cell permeant cAMP analogue dbcAMP, increases acquisition of RPE phenotype through increasing proliferation. Remarkably, global gene expression profiling suggests that dbcAMP supplementation promotes RPE epithelialization to mimic a doubling of seeding density compared to cells without supplementation. This is of particular relevance in terms of RPE yield while manufacturing cells for a clinical application e.g culturing transplantation-ready cells under GMP compatible conditions for a clinical trial. In such a case, modulation of cAMP signalling through the use of dbcAMP could equate to a 100% increase in cell yield and consequently affect cost and feasibility of the cell replacement therapy approach. It is important to appreciate that, instead of uncontrolled proliferation, our data is consistent with the interpretation that *in vitro* RPE culture is a homeostatic system where cell contact signals the cells to terminate proliferation and achieve quiescence [40]. This is distinct from contexts where increased proliferation could lead to potentially detrimental impacts, e.g. when RPE cell monolayers are not anchored and cells at the edge of a monolayer could proliferate and acquire a mesenchymal identity without these critical inhibitory signals from other RPE cells. An ocular pathology where this occurs is PVR, where proliferation of cell types including RPE, together with the appearance of a mesenchymal, migratory RPE state, results in the formation of a fibrotic, contractile scar tissue which inhibits vision [41]. Interestingly, one of the key pathways that have been implicated in PVR formation and progression is TGFβ signalling [42, 43]. TGFβ acts as a potent driver of fibrosis progression through the induction of epithelial–mesenchymal transition (EMT), in which epithelial cells acquire mesenchymal phenotypes, leading to enhanced motility and invasion [44]. Given the

precedence of TGFβ in pathogenesis of PVR, we were intrigued that analysis of gene expression upon cAMP elevation identified a potential role of this pathway in epithelial fate acquisition. We chose to investigate this in the context of a phenotypic screening approach where RPE seeded at low density, which would normally not epithelialize, were challenged with a focused library of small molecules targeting signalling pathways of interest, including but not limited to TGFβ signalling. We then looked for those molecules which could promote acquisition of the epithelial phenotype at low density and retrospectively used their known target activities to inform on the signalling pathway that could be involved. To our knowledge, this study provides the first example of use of hESC-derived RPE cells for high throughput phenotypic screening, successfully miniaturized to a 384 well format, and highlights that this clinically applied cell type is amenable to such interrogations. This approach led us to confirm the role of the TGFβ pathway, specifically signalling through the ALK5 receptor, as being key to RPE epithelial fate acquisition. TGFβ signalling controls a plethora of cellular responses and plays an important role in animal development. Its biological activity has been implicated in epithelial-mesenchymal interactions, e.g., in branching morphogenesis of the lung, kidney, mammary gland, and in inductive events between mammary epithelium and stroma [28, 45, 46]. Several studies in diverse cell types show that activation of TGFβ signalling leads to inhibition of cell proliferation and an increase in migration and uptake of mesenchymal characteristics [47, 48]. Polarized, functional RPE express and secrete low levels of TGFβ ligands to maintain the normal physiology of the subretinal space. Pathological conditions such as PVR lead to loss of polarity which manifests in high level of TGFβ secretion and loss of epithelial integrity and function [49, 50]. Our results suggest that inhibition of the TGFβ pathway via ALK5 signalling with small molecules effectively promotes the attainment of the epithelial state of RPE in a proliferation-dependent manner which potentially allows more favourable cell-cell contacts and promotes epithelialization in a manner akin to that of cAMP. Additionally, use of multiple compound chemotypes as well as recapitulating the same results with an orthogonal, antibody based neutralization method further lends support to the key role of TGFβ signalling. Based on our data which shows that TGFβ signalling

is downregulated in high density cultures, we propose that use of ALK5 inhibitors will promote proliferation and yield when used in cultures at low density, where this signalling pathway is active. This would translate to a *bonafide* increase in RPE yield as these cultures would normally not re-epithelialize in the absence of these compounds. However, further work is needed to fully characterize the activity of molecules and to understand their potency and specificity for the various TGFβ receptor subtypes in a head-to-head comparison. It also remains to be tested how cAMP elevation mechanistically inhibits the TGFβ pathway to potentiate RPE re-epithelialization. It is possible that increased cAMP signalling leads to PKA activation which in turn antagonizes the ras/MEK/ERK signaling cascade leading to attenuation of TGFβ signalling, as has been described in other cellular models [51–55]. This hypothesis requires further investigation to be validated. Another area that warrants further exploration is to test whether additional pathways that control TGFβ signalling e.g the Hippo and Crumbs pathway which are key sensors of cell density [56] and hence may be relevant to cell contact dependent RPE epithelialization, also play a role in this process. This will help to fully comprehend how proliferation dependent cell-cell contacts signal the initiation of the epithelialization program and how a network of signalling pathways feed into it.

CONCLUSION

To conclude, in order to transition to a successful and efficacious cell replacement therapy, stem cell derived RPE need to be produced at scale with high yield and under GMP conditions. Presence of trans-differentiated RPE exhibiting mesenchymal characteristics that develop upon seeding cultures at low density can potentially compromise the functionality of the cell population. Given the intricate link between seeding density and epithelial fate outcome, the use of small molecule tools for e.g dbcAMP or inhibitors of TGFβ signalling as demonstrated in this report, could support large scale manufacturing of functional RPE with high yield which would be advantageous for successful clinical translation and therapeutic output.

ACKNOWLEDGEMENTS

We would like to acknowledge Maria Isabel Rosa, Juliette Steer, Anna Wilbrey and Julie Kerby for help with RPE foci dissection and for initial workup of RPE culture; Mary-Ann Madsen and Christos Michaeledes for initial work with forskolin; Lawrence Welch for help with qPCR; Anna Ashton and members of the Pfizer DSRD group for optimizing methods for RPE characterization and Nicole E. Bodycombe for help with deconvolution of screening data.

DISCLOSURE OF POTENTIAL CONFLICTS OF INTEREST

All authors are employees of Pfizer Ltd. Parul Choudhary and Paul J. Whiting are co-inventors on a patent titled 'Method for producing Retinal Pigment Epithelium Cells' (US Pub No US2015/0159134 A1), which describe some of these data.

REFERENCES

1. Strauss O. The retinal pigment epithelium in visual function. **Physiological reviews**. 2005;85:845-881.
2. da Cruz L, Chen FK, Ahmado A et al. RPE transplantation and its role in retinal disease. **Progress in retinal and eye research**. 2007;26:598-635.
3. Lindekleiv H, Erke MG. Projected prevalence of age-related macular degeneration in Scandinavia 2012-2040. **Acta ophthalmologica**. 2013;91:307-311.
4. Nazari H, Zhang L, Zhu D et al. Stem cell based therapies for age-related macular degeneration: The promises and the challenges. **Progress in retinal and eye research**. 2015.
5. Leach LL, Clegg DO. Concise Review: Making Stem Cells Retinal: Methods for Deriving Retinal Pigment Epithelium and Implications for Patients With Ocular Disease. **Stem cells**. 2015;33:2363-2373.
6. Maruotti J, Sripathi SR, Bharti K et al. Small-molecule-directed, efficient generation of retinal pigment epithelium from human pluripotent stem cells. **Proceedings of the National Academy of Sciences of the United States of America**. 2015.
7. Vugler A, Carr AJ, Lawrence J et al. Elucidating the phenomenon of HESC-derived RPE: anatomy of cell genesis, expansion and retinal transplantation. **Experimental neurology**. 2008;214:347-361.
8. Maeda T, Lee MJ, Palczewska G et al. Retinal pigmented epithelial cells obtained from human induced pluripotent stem cells possess functional visual cycle enzymes in vitro and in vivo. **The Journal of biological chemistry**. 2013;288:34484-34493.
9. Buchholz DE, Hikita ST, Rowland TJ et al. Derivation of functional retinal pigmented epithelium from induced pluripotent stem cells. **Stem cells**. 2009;27:2427-2434.
10. Idelson M, Alper R, Obolensky A et al. Directed differentiation of human embryonic stem cells into functional retinal pigment epithelium cells. **Cell stem cell**. 2009;5:396-408.

11. Strunnikova NV, Maminishkis A, Barb JJ et al. Transcriptome analysis and molecular signature of human retinal pigment epithelium. **Human molecular genetics**. 2010;19:2468-2486.
12. Liao JL, Yu J, Huang K et al. Molecular signature of primary retinal pigment epithelium and stem-cell-derived RPE cells. **Human molecular genetics**. 2010;19:4229-4238.
13. Klimanskaya I, Hipp J, Rezai KA et al. Derivation and comparative assessment of retinal pigment epithelium from human embryonic stem cells using transcriptomics. **Cloning and stem cells**. 2004;6:217-245.
14. Guha S, Baltazar GC, Tu LA et al. Stimulation of the D5 dopamine receptor acidifies the lysosomal pH of retinal pigmented epithelial cells and decreases accumulation of autofluorescent photoreceptor debris. **Journal of neurochemistry**. 2012;122:823-833.
15. Lu B, Malcuit C, Wang S et al. Long-term safety and function of RPE from human embryonic stem cells in preclinical models of macular degeneration. **Stem cells**. 2009;27:2126-2135.
16. Lund RD, Wang S, Klimanskaya I et al. Human embryonic stem cell-derived cells rescue visual function in dystrophic RCS rats. **Cloning and stem cells**. 2006;8:189-199.
17. Plaza Reyes A, Petrus-Reurer S, Antonsson L et al. Xeno-Free and Defined Human Embryonic Stem Cell-Derived Retinal Pigment Epithelial Cells Functionally Integrate in a Large-Eyed Preclinical Model. **Stem cell reports**. 2015.
18. Choudhary P, Dodsworth BT, Sidders B et al. A FOXM1 Dependent Mesenchymal-Epithelial Transition in Retinal Pigment Epithelium Cells. **PloS one**. 2015;10:e0130379.
19. Croze RH, Buchholz DE, Radeke MJ et al. ROCK Inhibition Extends Passage of Pluripotent Stem Cell-Derived Retinal Pigmented Epithelium. **Stem cells translational medicine**. 2014;3:1066-1078.
20. Della Fazia MA, Servillo G, Sassone-Corsi P. Cyclic AMP signalling and cellular proliferation: regulation of CREB and CREM. **FEBS letters**. 1997;410:22-24.
21. Kokkinaki M, Abu-Asab M, Gunawardena N et al. Klotho regulates retinal pigment epithelial functions and protects against oxidative stress. **The Journal of neuroscience : the official journal of the Society for Neuroscience**. 2013;33:16346-16359.
22. Kojima A, Nakahama K, Ohno-Matsui K et al. Connexin 43 contributes to differentiation of retinal pigment epithelial cells via cyclic AMP signaling. **Biochemical and biophysical research communications**. 2008;366:532-538.
23. Koh SM. VIP enhances the differentiation of retinal pigment epithelium in culture: from cAMP and pp60(c-src) to melanogenesis and development of fluid transport capacity. **Progress in retinal and eye research**. 2000;19:669-688.
24. Hecquet C, Lefevre G, Valtink M et al. cAMP inhibits the proliferation of retinal pigmented epithelial cells through the inhibition of ERK1/2 in a PKA-independent manner. **Oncogene**. 2002;21:6101-6112.
25. Hackett S, Friedman Z, Campochiaro PA. Cyclic 3',5'-adenosine monophosphate modulates retinal pigment epithelial cell migration in vitro. **Archives of ophthalmology**. 1986;104:1688-1692.
26. Smith-Thomas LC, Richardson PS, Rennie IG et al. Influence of pigment content, intracellular calcium and cyclic AMP on the ability of human retinal pigment epithelial cells to contract collagen gels. **Current eye research**. 2000;21:518-529.
27. Huang W, Wang L, Yuan M et al. Adrenomedullin affects two signal transduction pathways and the migration in retinal pigment epithelial cells. **Investigative ophthalmology & visual science**. 2004;45:1507-1513.
28. Massague J. TGFbeta signalling in context. **Nature reviews Molecular cell biology**. 2012;13:616-630.
29. Carr AJ, Vugler A, Lawrence J et al. Molecular characterization and functional analysis of phagocytosis by human embryonic stem cell-derived RPE cells using a novel human retinal assay. **Molecular vision**. 2009;15:283-295.

30. Osakada F, Ikeda H, Mandai M et al. Toward the generation of rod and cone photoreceptors from mouse, monkey and human embryonic stem cells. **Nature biotechnology**. 2008;26:215-224.
31. Chehrehasa F, Meedeniya AC, Dwyer P et al. EdU, a new thymidine analogue for labelling proliferating cells in the nervous system. **Journal of neuroscience methods**. 2009;177:122-130.
32. Chindelevitch L, Ziemek D, Enayetallah A et al. Causal reasoning on biological networks: interpreting transcriptional changes. **Bioinformatics**. 2012;28:1114-1121.
33. Zhang Y, Handley D, Kaplan T et al. High throughput determination of TGFbeta1/SMAD3 targets in A549 lung epithelial cells. **PloS one**. 2011;6:e20319.
34. Dasch JR, Pace DR, Waegell W et al. Monoclonal antibodies recognizing transforming growth factor-beta. Bioactivity neutralization and transforming growth factor beta 2 affinity purification. **Journal of immunology**. 1989;142:1536-1541.
35. Brandl C, Grassmann F, Riolfi J et al. Tapping Stem Cells to Target AMD: Challenges and Prospects. **Journal of clinical medicine**. 2015;4:282-303.
36. Schwartz SD, Hubschman JP, Heilwell G et al. Embryonic stem cell trials for macular degeneration: a preliminary report. **Lancet**. 2012;379:713-720.
37. Schwartz SD, Regillo CD, Lam BL et al. Human embryonic stem cell-derived retinal pigment epithelium in patients with age-related macular degeneration and Stargardt's macular dystrophy: follow-up of two open-label phase 1/2 studies. **Lancet**. 2015;385:509-516.
38. Kamao H, Mandai M, Okamoto S et al. Characterization of human induced pluripotent stem cell-derived retinal pigment epithelium cell sheets aiming for clinical application. **Stem cell reports**. 2014;2:205-218.
39. Al-Hussaini H, Kam JH, Vugler A et al. Mature retinal pigment epithelium cells are retained in the cell cycle and proliferate in vivo. **Molecular vision**. 2008;14:1784-1791.
40. Kokkinopoulos I, Shahabi G, Colman A et al. Mature peripheral RPE cells have an intrinsic capacity to proliferate; a potential regulatory mechanism for age-related cell loss. **PloS one**. 2011;6:e18921.
41. Pastor JC, Rojas J, Pastor-Idoate S et al. Proliferative vitreoretinopathy: A new concept of disease pathogenesis and practical consequences. **Progress in retinal and eye research**. 2015.
42. Nassar K, Grisanti S, Tura A et al. A TGF-beta receptor 1 inhibitor for prevention of proliferative vitreoretinopathy. **Experimental eye research**. 2014;123:72-86.
43. Hoerster R, Muether PS, Vierkotten S et al. Upregulation of TGF-ss1 in experimental proliferative vitreoretinopathy is accompanied by epithelial to mesenchymal transition. **Graefe's archive for clinical and experimental ophthalmology = Albrecht von Graefes Archiv fur klinische und experimentelle Ophthalmologie**. 2014;252:11-16.
44. Chen X, Xiao W, Wang W et al. The complex interplay between ERK1/2, TGFbeta/Smad, and Jagged/Notch signaling pathways in the regulation of epithelial-mesenchymal transition in retinal pigment epithelium cells. **PloS one**. 2014;9:e96365.
45. Derynck R, Muthusamy BP, Saeteurn KY. Signaling pathway cooperation in TGF-beta-induced epithelial-mesenchymal transition. **Current opinion in cell biology**. 2014;31:56-66.
46. Leask A, Abraham DJ. TGF-beta signaling and the fibrotic response. **FASEB journal : official publication of the Federation of American Societies for Experimental Biology**. 2004;18:816-827.
47. Dunfield LD, Nachtigal MW. Inhibition of the antiproliferative effect of TGFbeta by EGF in primary human ovarian cancer cells. **Oncogene**. 2003;22:4745-4751.
48. Takehara K, LeRoy EC, Grotendorst GR. TGF-beta inhibition of endothelial cell proliferation: alteration of EGF binding and EGF-induced growth-regulatory (competence) gene expression. **Cell**. 1987;49:415-422.

49. Hirsch L, Nazari H, Sreekumar PG et al. TGF-beta2 secretion from RPE decreases with polarization and becomes apically oriented. **Cytokine**. 2015;71:394-396.
50. Holtkamp GM, De Vos AF, Peek R et al. Analysis of the secretion pattern of monocyte chemotactic protein-1 (MCP-1) and transforming growth factor-beta 2 (TGF-beta2) by human retinal pigment epithelial cells. **Clinical and experimental immunology**. 1999;118:35-40.
51. Davis MI, Ronesi J, Lovinger DM. A predominant role for inhibition of the adenylate cyclase/protein kinase A pathway in ERK activation by cannabinoid receptor 1 in N1E-115 neuroblastoma cells. **The Journal of biological chemistry**. 2003;278:48973-48980.
52. Cook SJ, McCormick F. Inhibition by cAMP of Ras-dependent activation of Raf. **Science**. 1993;262:1069-1072.
53. Dumaz N, Marais R. Integrating signals between cAMP and the RAS/RAF/MEK/ERK signalling pathways. Based on the anniversary prize of the Gesellschaft fur Biochemie und Molekularbiologie Lecture delivered on 5 July 2003 at the Special FEBS Meeting in Brussels. **The FEBS journal**. 2005;272:3491-3504.
54. Xie L, Law BK, Chytil AM et al. Activation of the Erk pathway is required for TGF-beta1-induced EMT in vitro. **Neoplasia**. 2004;6:603-610.
55. Mulder KM. Role of Ras and Mapks in TGFbeta signaling. **Cytokine & growth factor reviews**. 2000;11:23-35.
56. Varelas X, Samavarchi-Tehrani P, Narimatsu M et al. The Crumbs complex couples cell density sensing to Hippo-dependent control of the TGF-beta-SMAD pathway. **Developmental cell**. 2010;19:831-844.
57. Rena G, Bain J, Elliott M et al. D4476, a cell-permeant inhibitor of CK1, suppresses the site-specific phosphorylation and nuclear exclusion of FOXO1a. **EMBO reports**. 2004;5:60-65.
58. Callahan JF, Burgess JL, Fornwald JA et al. Identification of novel inhibitors of the transforming growth factor beta1 (TGF-beta1) type 1 receptor (ALK5). **Journal of medicinal chemistry**. 2002;45:999-1001.
59. Surmacz B, Fox H, Gutteridge A et al. Directing differentiation of human embryonic stem cells toward anterior neural ectoderm using small molecules. **Stem cells**. 2012;30:1875-1884.
60. Boys ML, Bian F, Kramer JB et al. Discovery of a series of 2-(1H-pyrazol-1-yl)pyridines as ALK5 inhibitors with potential utility in the prevention of dermal scarring. **Bioorganic & medicinal chemistry letters**. 2012;22:3392-3397.
61. Mohedas AH, Xing X, Armstrong KA et al. Development of an ALK2-biased BMP type I receptor kinase inhibitor. **ACS chemical biology**. 2013;8:1291-1302.

FIGURE LEGENDS

Fig 1: Cell-density dependent effects on re-epithelialization in stem-cell derived RPE

A. Schematic representation of density-dependent RPE culture where RPE seeded at high density undergo proliferation and successfully epithelialize whereas RPE seeded at low density remain mesenchymal.

B. Heatmap of expression profiles of the top 250 expressed genes ranked by the significance of their expression changes over time in high (100000 cells/cm^2) and low (8000 cells/cm^2) density cultures.

Raw expression data are mean centred and scaled to unit variance prior to clustering. The genes cluster into two groups (1 & 2) based on the observed expression pattern. Cluster 1 genes show initial downregulation whereas Cluster 2 genes show initial upregulation upon dissociation and culture. Genes from both clusters return to basal levels with time upon high density seeding but not upon low density seeding.

C. Heatmap showing changes in gene expression of a panel of representative epithelial and mesenchymal markers over a timecourse of RPE culture where cells are seeded as in Figure 1B.

D. Representative images showing immunocytochemistry for epithelial (CRALBP, ZO1, PMEL17) and mesenchymal markers (α-SMA) at day 42 in cultures seeded as in Figure 1B.

Fig 2: Increasing cAMP signalling promotes acquisition of RPE identity across multiple cell densities.

A. Representative brightfield images showing RPE seeded at multiple densities in the presence or absence of 10μM forskolin treatment at day 63 in culture

B. 'The RPE Score' (see main text) of each sample in the presence (blue) and absence (red) of 10μM FSK at day 63 is plotted against the seeding density (2.5k, 10k, 15k, 20k, 25k, 27.5k, 30k, 38k; k=x1000cells/cm^2). The shaded area represents 95% confidence intervals and the solid circles represent biological replicates at the given density.

Fig 3: Gene expression analysis of dbcAMP treated RPE.

A. Principal component analysis of the microarray gene expression data is shown for samples obtained from three different seeding densities (indicated by the shape of each point: circle= 10000 cells/cm^2; square= 20000 cells/cm^2 and diamond= 40000 cells/cm^2) in the presence (blue) or absence (red) of dbcAMP. The data from four time points (Day 0, 3, 15 and 34 post-seeding) is indicated by the shading of each point and the labelled ellipses such that colour intensity increases with increasing time in culture. The day 0 samples are indicated as black points and the proportion of the

total variance captured by each principal component is indicated in the axis title. This shows that at each time point tested, there is a 'doubling effect' i.e clustering of samples seeded at half the density in the presence of dbcAMP with samples at double the density but without dbcAMP. k= x1000 cells/cm^2.

B. Heatmap of gene expression levels for the top 1% most variable genes (rows) observed at day 34 in culture. The seeding density and dbcAMP treatment status each sample is indicated by the labels at the bottom of the heatmap (k= x1000 cells/cm^2). Expression levels are shown mean centred and scaled to unit variance for each gene. Clustering of samples consistent with the doubling effect can be seen.

C. Heatmap of gene expression levels for selected RPE markers across all timepoints, seeding density and dbcAMP treatment is shown.

Fig 4: dbcAMP increases proliferation of RPE cells

A. Exemplar gene ontology (GO) terms, derived from comparison of cultures in the presence vs. absence of dbcAMP at Day34 (20000 cells/cm^2 seeding density), alongside their gene set test significance p values ($p < 0.05$). D= Downregulated, U= Upregulated. FDR= False discovery rate.

B. Representative images showing EdU incorporation in the presence or absence of dbcAMP in RPE seeded at 38000 cells/cm^2 at different timepoints in culture. The quantification of EdU incorporation is shown below. Bars represent Mean + SD (n=8).

C. Representative images showing immunocytochemistry for Ki67 in the presence or absence of 10µM FSK in RPE seeded at 38000 cells/cm^2 at different timepoints in culture. The quantification of images is shown below. Bars represent Mean + SD (n=3).

D. Representative images showing nuclei stained with DAPI in RPE treated seeded at 38000 cells/cm2 and cultured for a period of 8 weeks with different periods of exposure to dbcAMP Quantification of cell number, measured by DAPI positive nuclei per frame imaged is shown below.

(Vehicle: media alone, 2+6: 2wk dbcAMP+ 6wk media, 3+5: 3wk dbcAMP+ 5wk media, 8: 8wk dbcAMP). Bars represent Mean + SD (n=3).

Fig 5: Role of TGFβ signalling in RPE

A. Histogram showing change in expression of SMAD3 bound genes in dbcAMP vs control cultures at day 34 (20000 cells/cm^2 seeding density) . The frequency of genes is plotted on the y axis and the log fold change is plotted on the x axis (No change= 0 log fold change). The leftward shift of the distribution indicates a significant decrease in expression of SMAD3 responsive genes with dbcAMP treatment.

B. qPCR based measurement of transcript expression of a panel of epithelial (*CRB3, BEST1, PMEL*) and mesenchymal (*CDH2, MMP2, GREM1*) markers in cells seeded at 100000 cells/cm^2 and exposed to 10ng/ml TGFβ1 for 5 days. *ATP5B* and *CYC1* are used as housekeeping genes. Bars represent Mean + SD (n=3). $P<0.05$ (Student's t-test).

C Representative images showing immunocytochemistry for indicated markers (in cells seeded at high density and exposed to TGFβ1 for 5 days.

D. Quantification of Figure 5C

Fig 6: Effect of ALK5 inhibitors on RPE phenotype and proliferation

Cells were seeded at 15000 cells/cm^2 and treated with compounds for 14 days. Immunocytochemistry was performed and dose response curves were generated measuring % of DAPI positive cells staining positive for PMEL17 (A) and EdU (B). Forskolin (FSK) was used as the positive control. Correlation between EC_{50} for both measures for all ALK5 inhibitors screened is shown in (C).

Fig 7: Inhibition of TGFβ signalling promotes RPE phenotype

A. qPCR based measurement of transcript expression of a panel of epithelial *(BEST1, PMEL, LRAT, MERTK, RPE65, RLBP1*) and mesenchymal (*GREM1*) markers in RPE seeded at 5000 cells/cm^2 and treated with 10µg/ml Anti-TGFβ antibody (1D11) for a period of 14 days. Data is normalized to expression of vehicle control. *HPRT1* is used as a housekeeping gene. Bars represent Mean + SD (n=3). P<0.05 (Student's t-test).

B. Representative images showing immunocytochemistry for indicated markers along with their quantification in cells seeded at 5000 cells/cm^2 and exposed to 10µg/ml Anti-TGFβ for 14 days.

SUPPLEMENTARY FIGURE LEGENDS

Supplementary Figure1

A. Representative confocal images of X-Z cross-sections of RPE cells cultured on transwells immunostained for ZO1, MERTK and PMEL17 (green). Nuclei are stained with DAPI (blue). Autofluorescence can also be seen from the polyester membrane of the transwell and has been indicated within dotted white lines.

B. Representative confocal image showing phagocytosis of fluorescent bead (red) by RPE. RPE grown on transwells were incubated with polystyrene beads for a period of 24h at 37^{o}C. The transwell membrane was immunostained for CRALBP (green) to show RPE coverage membrane and sectioned. The beads can be seen within the CRALBP positive area but outside the nuclei stained with DAPI (blue) indicating internalization by phagocytosis.

C. Spent media was collected from RPE and ARPE19 cultures seeded on transwells at Day 4 (RPE) and Day 21 (RPE, ARPE19). VEGF and PEDF were quantified to show that their secretion increases with time in culture. Bars represent Mean$\pm$ SD (n=4-6). P<0.05, Student's t-test.

Supplementary Figure2:

Increasing cAMP signalling promotes acquisition of RPE identity across multiple cell densities. Increased pigmentation and cell coverage with forskolin treatment are evident in cells and cell lysates. (K= x1000)

Supplementary Figure 3:

A. Heatmap showing clustering of expression of epithelial and mesenchymal markers, as measured by qPCR, where epithelial marker genes cluster together and are distinct from mesenchymal markers. qPCR data from samples seeded at 38000 cells/cm^2 in media at Day63 in culture were used to generate this heatmap. Gene specific qPCR showing effect of FSK on expression of epithelial (B, C) and mesenchymal markers (D, E) across a range of densities at Day63 is shown.

Supplementary Figure 4:

A. qPCR based measurement of transcript expression of a panel of RPE markers in cells seeded at different densities (10k, 20k, 40k; k=1000 cells/cm^2) at day 3, 15, 34 (D3, D15, D34) in culture in the presence (+) or absence (-) of 0.5mM dbcAMP. *GAPDH* and *ACT* are used as a housekeeping genes. Bars represent Mean $\pm$ SD (n=3). $P<0.05$ (Student's t-test).

B. Representative images showing immunocytochemistry for epithelial marker PMEL17 (green) at day 15 in cultures seeded as above in the presence or absence of dbcAMP. Nuclei are counterstained with DAPI (blue).

C. dbcAMP dose of at least 0.5mM is required to observe effect on RPE phenotype. RPE were seeded at 20000 cells/cm^2 and treated with different concentrations of dbcAMP for a period of 14 days. Immunocytochemistry was performed for PMEL17 which showed that a concentration of at least 0.5mM dbcAMP was required to observe an upregulation of this marker of RPE phenotype. (n=3, Bars= $\pm$ SD)

Supplementary Figure 5:

Schematic of the TGFβ signalling pathway. The downstream signalling effectors are coloured according to their differential expression in high density vs low density cultures. Red indicates decreased expression and green indicates increased expression in high vs. low density cultures with the intensity of the shade indicating fold change. Low expression of TGFβ and its downstream effectors, as seen by red shading, suggests suppression of the TGFβ pathway in high density cultures compared to low density cultures.

Supplementary Figure 6:

Table summarizing published IC_{50} values against ALK5 and ALK2 for compounds tested [57-61], compound structures and EC_{50} values for effect on %PMEL17 and %EdU measured by immunocytochemistry (calculated in this study).

Supplementary Figure 7:

qPCR based measurement of transcript expression of a panel of epithelial (*BEST1, LRAT, MERTK, RPE65, RLBP1*) and mesenchymal (*GREM1*) markers in RPE seeded at 15000 cells/cm^2 and treated with Compound #6 and #7 at a concentration of 10μM, 1μM and 0.1μM for a period of 14 days. Data is normalized to expression of vehicle control. *GAPDH* and *HPRT1* are used as housekeeping genes.

Supplementary Table 1:

Table showing list of genes in Cluster 1 and Cluster 2 from Figure 1B.

Supplementary Table 2:

Table showing list of GO terms upregulated in the presence of dbcAMP in cultures seeded at 20000 cells/cm^2 at Day 34.

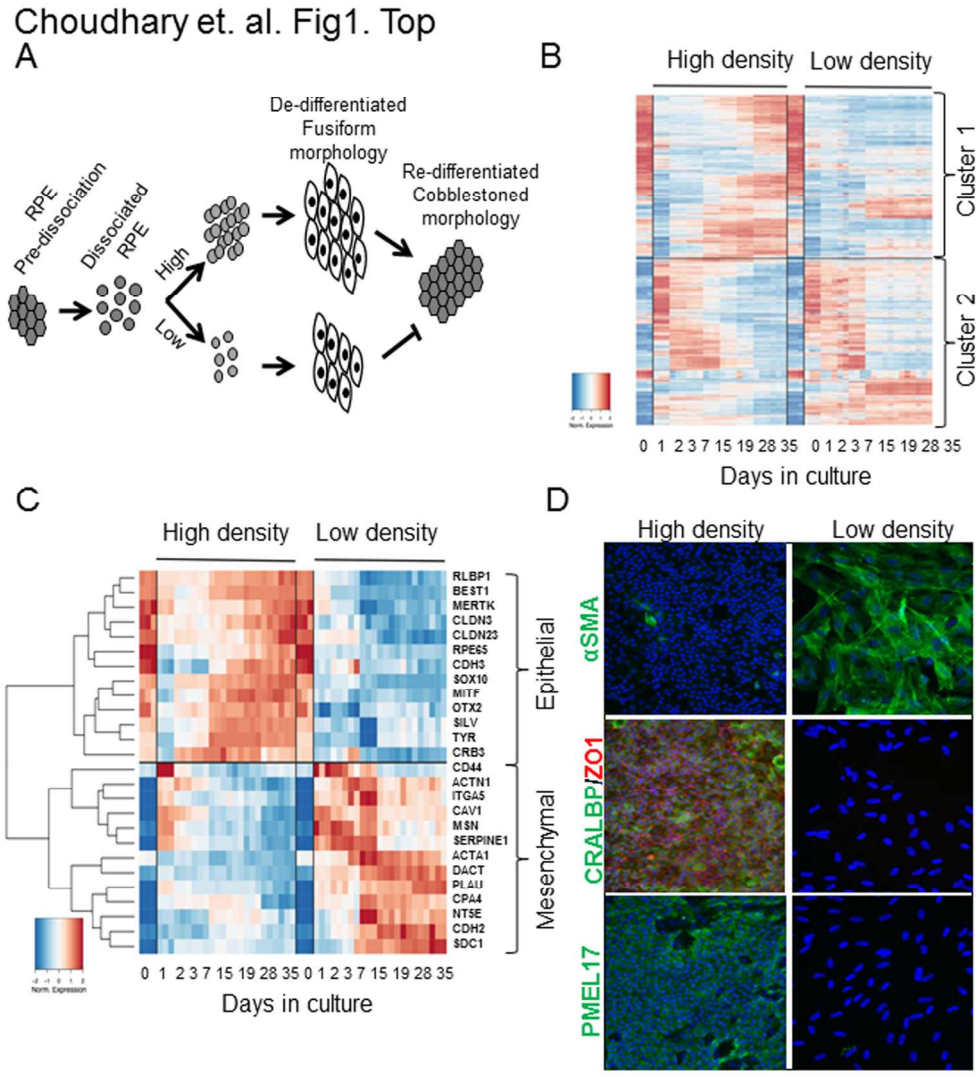

Fig1_R1
147x160mm (300 x 300 DPI)

Choudhary et. al. Fig 2. Top

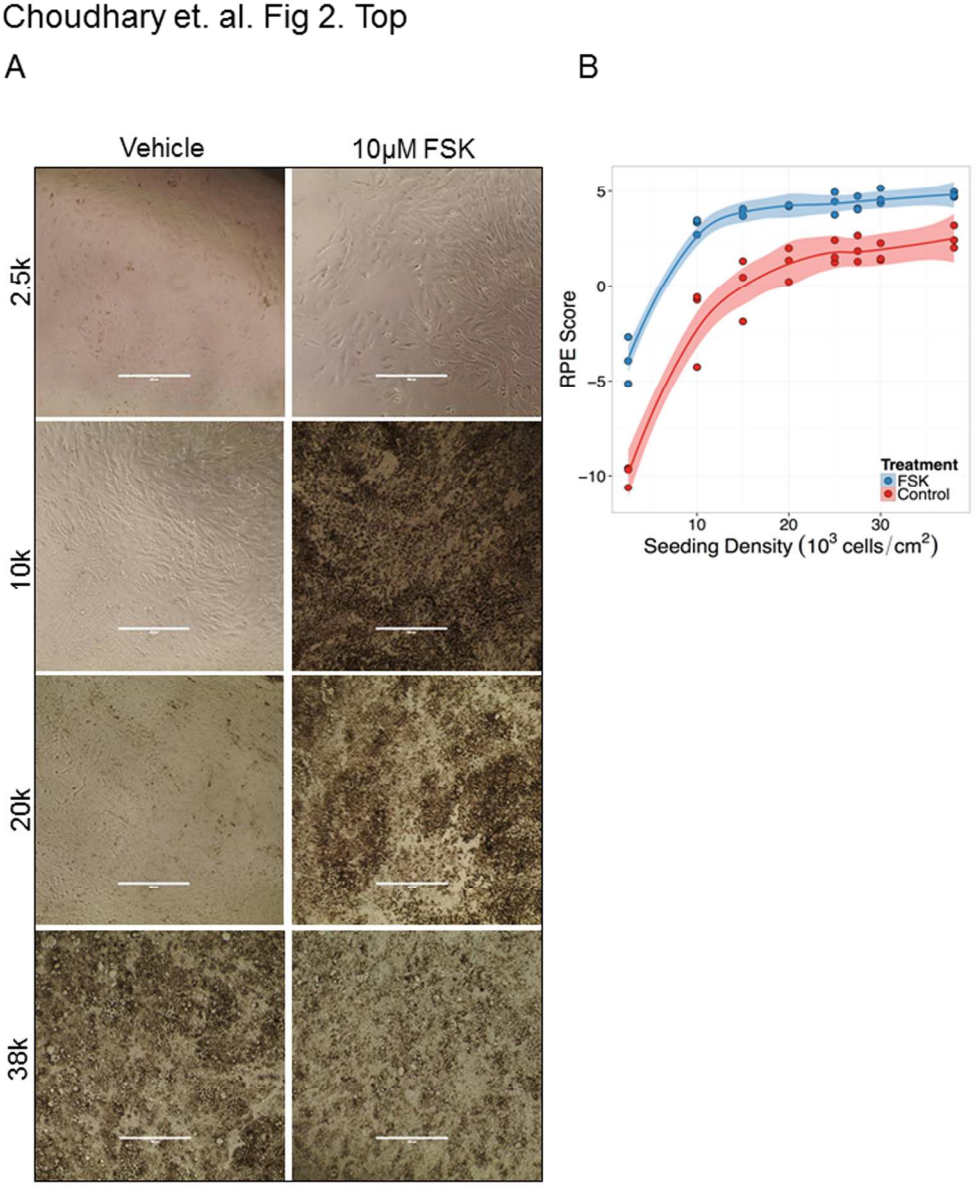

Fig2_R1
147x179mm (300 x 300 DPI)

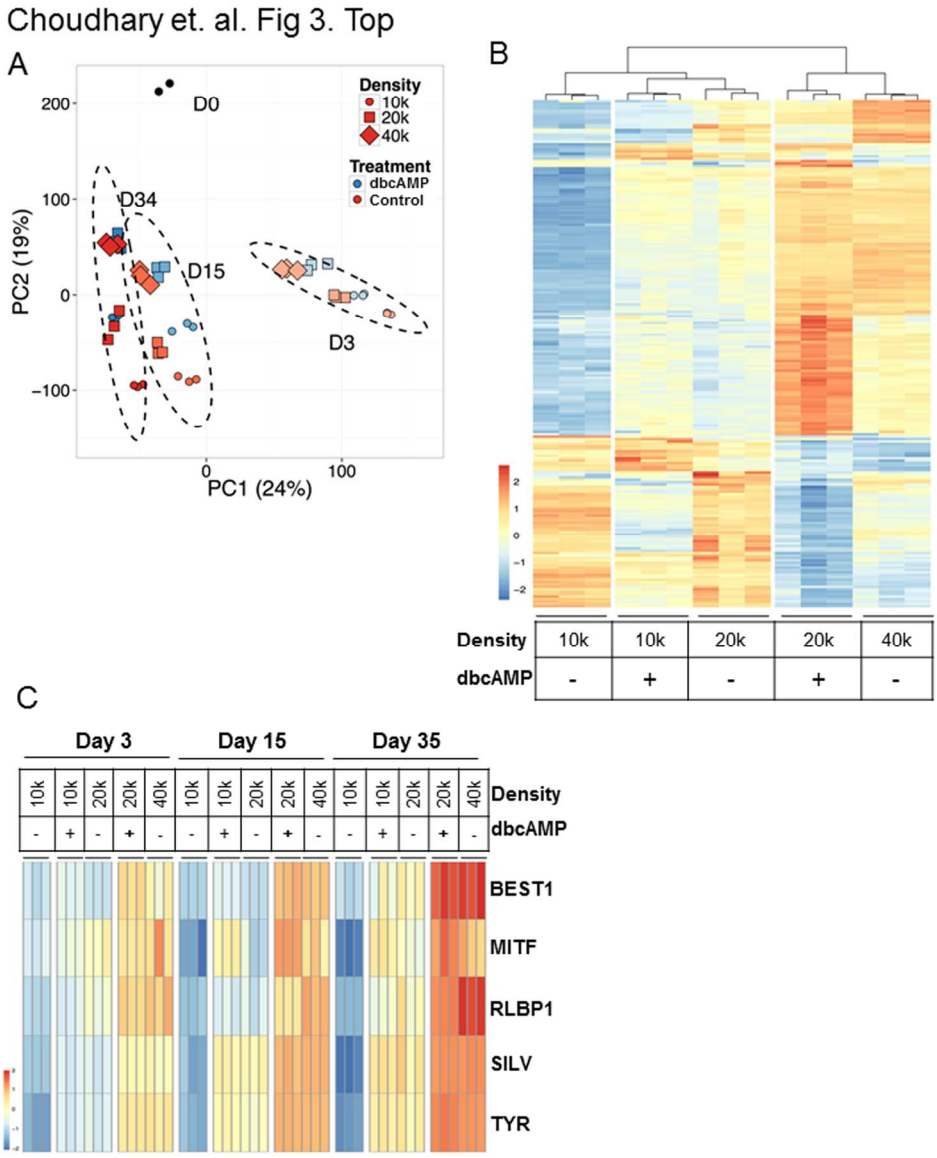

Fig3_R1
145x183mm (300 x 300 DPI)

Choudhary et. al. Fig 4. Top

A

GO ID	Term	Direction	FDR
GO:0006986	Response to unfolded protein	D	1.56E-10
GO:0030198	Extracellular matrix organization	D	3.51E-10
GO:0007059	Chromosome segregation	U	2.00E-07
GO:0007067	Mitotic nuclear division	U	2.77E-07
GO:0050953	Sensory perception of light stimulus	U	4.08E-05
GO:0007601	Visual perception	U	5.31E-05
GO:0042440	Pigment metabolic process	U	9.10E-05
GO:0042438	Melanin biosynthetic process	U	0.003339

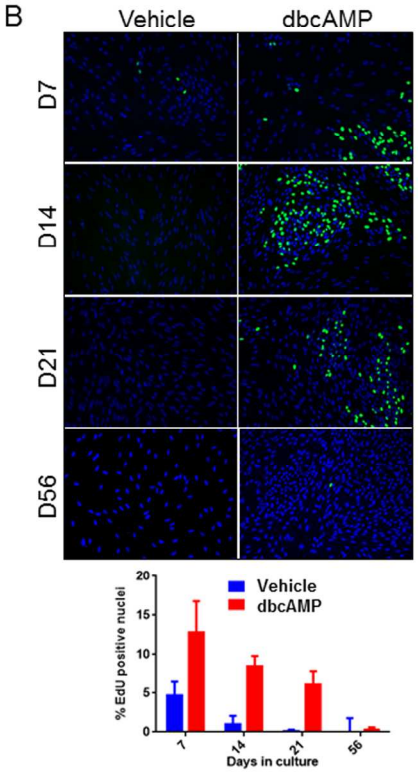

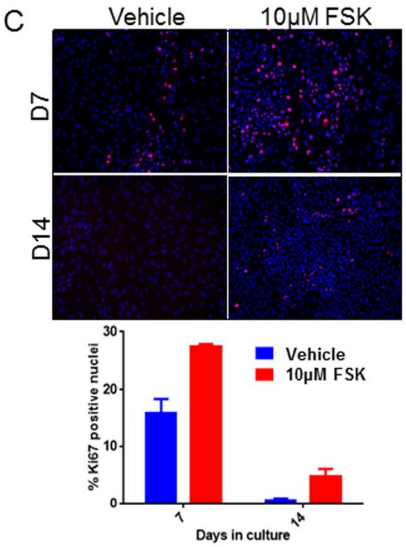

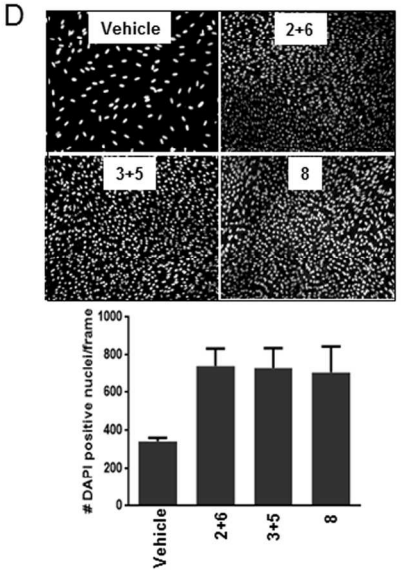

Fig4_R1
147x197mm (300 x 300 DPI)

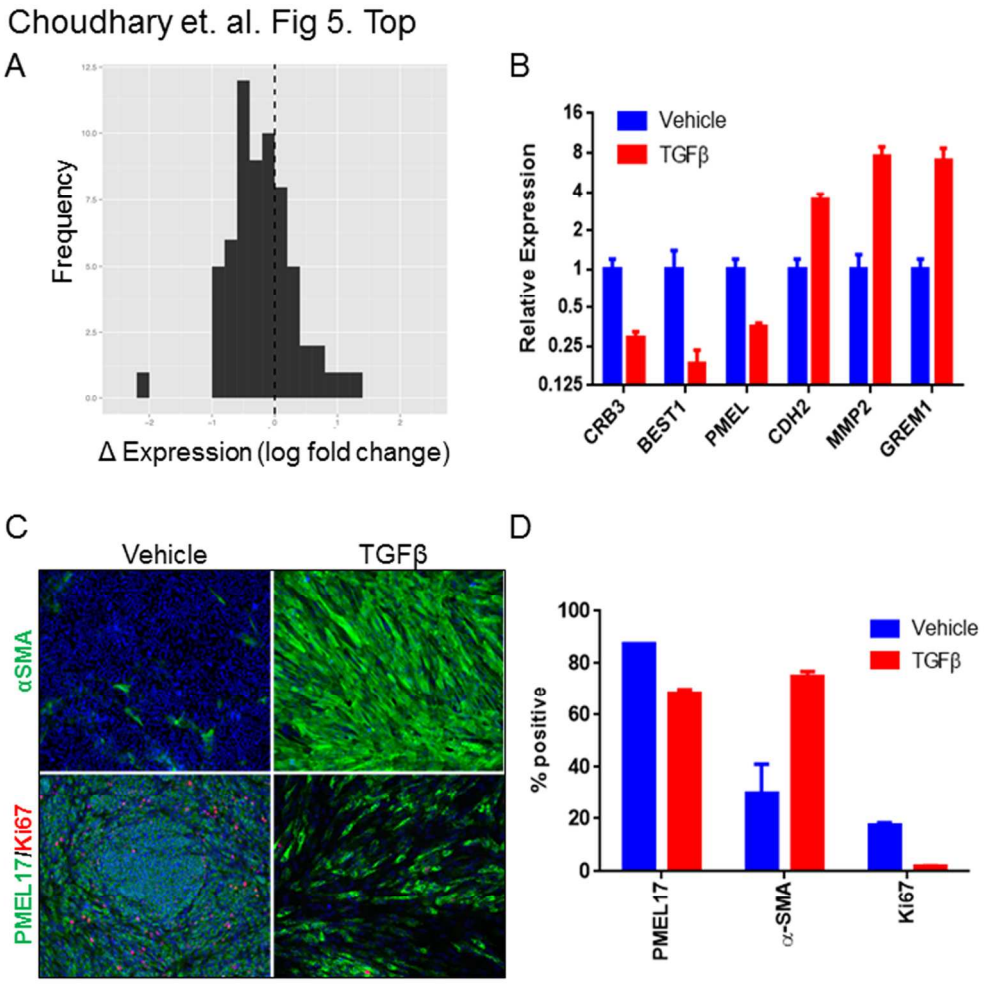

Fig5_R1
147x147mm (300 x 300 DPI)

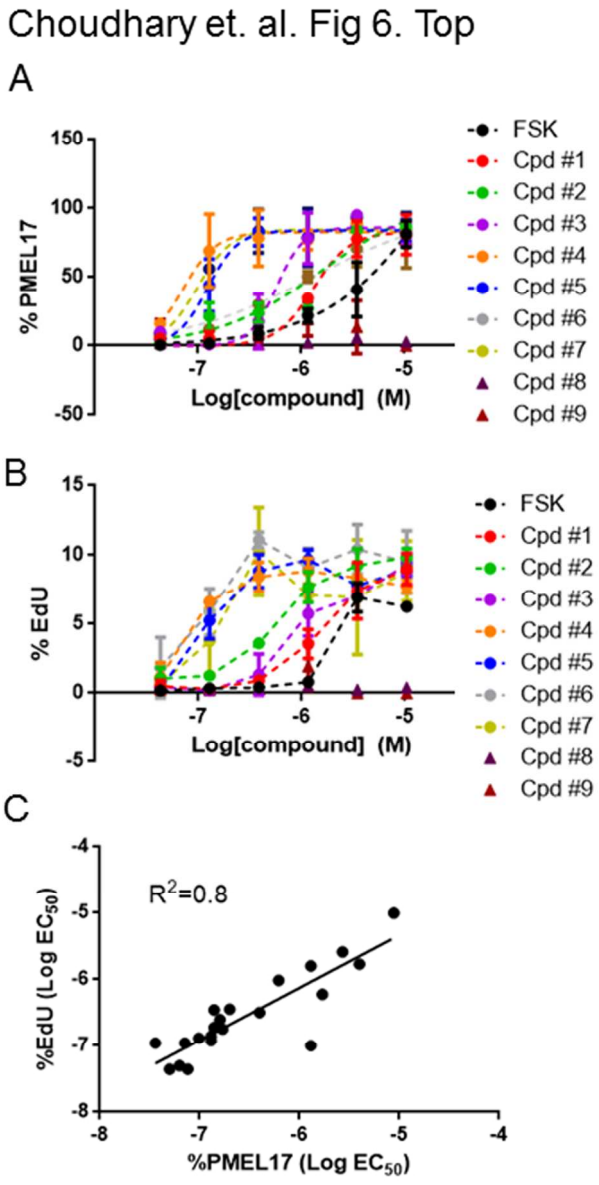

Fig6_R1
82x156mm (300 x 300 DPI)

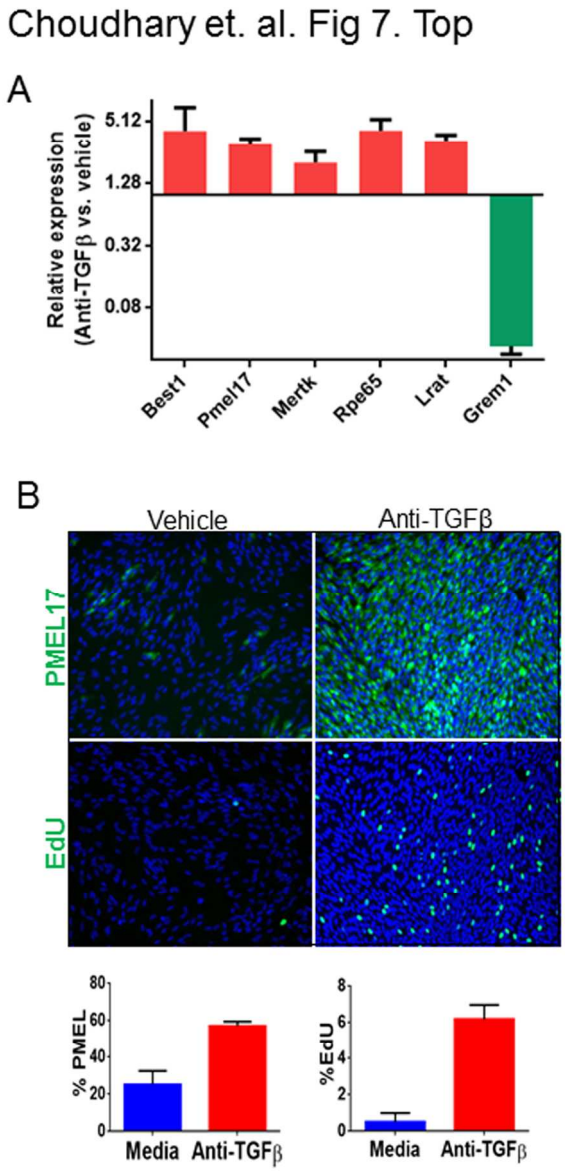

Fig7_R1
113x217mm (300 x 300 DPI)

Choudhary et. al. Supplementary figure 1. Top

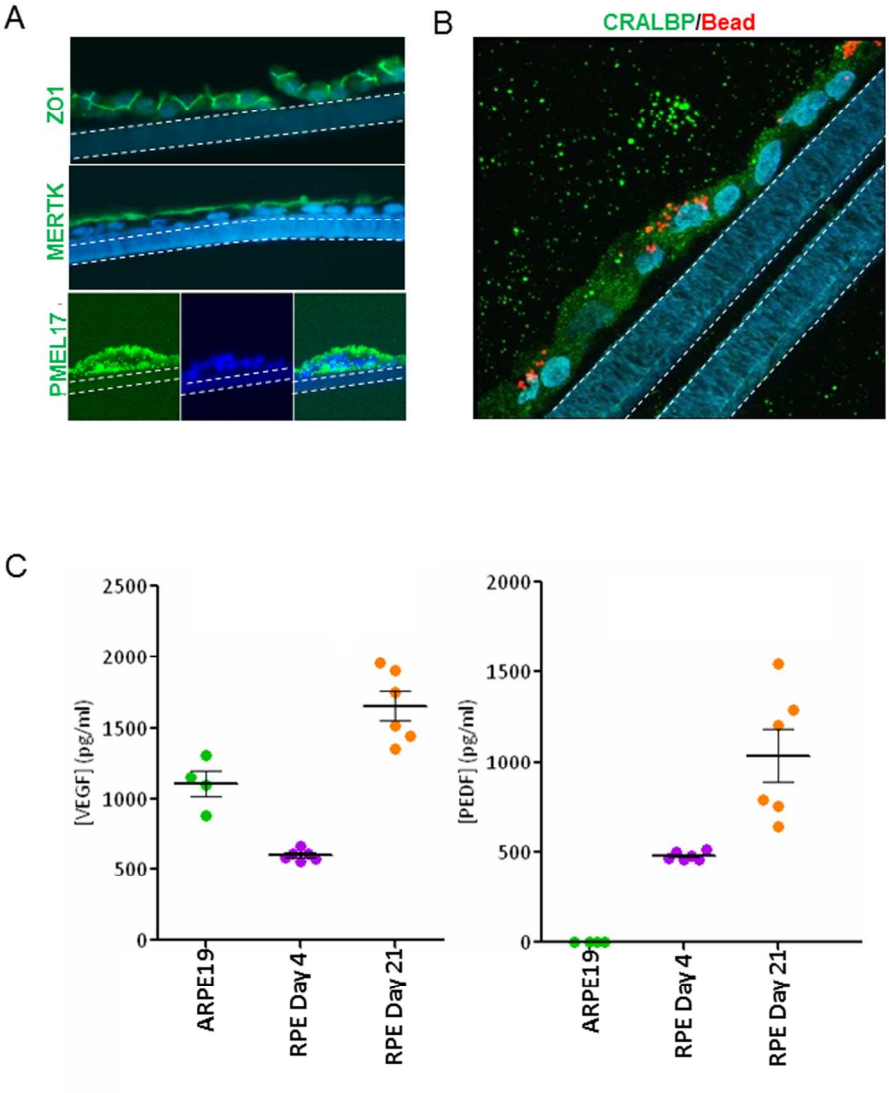

147x190mm (300 x 300 DPI)

Choudhary et. al. Supplementary figure 2. Top

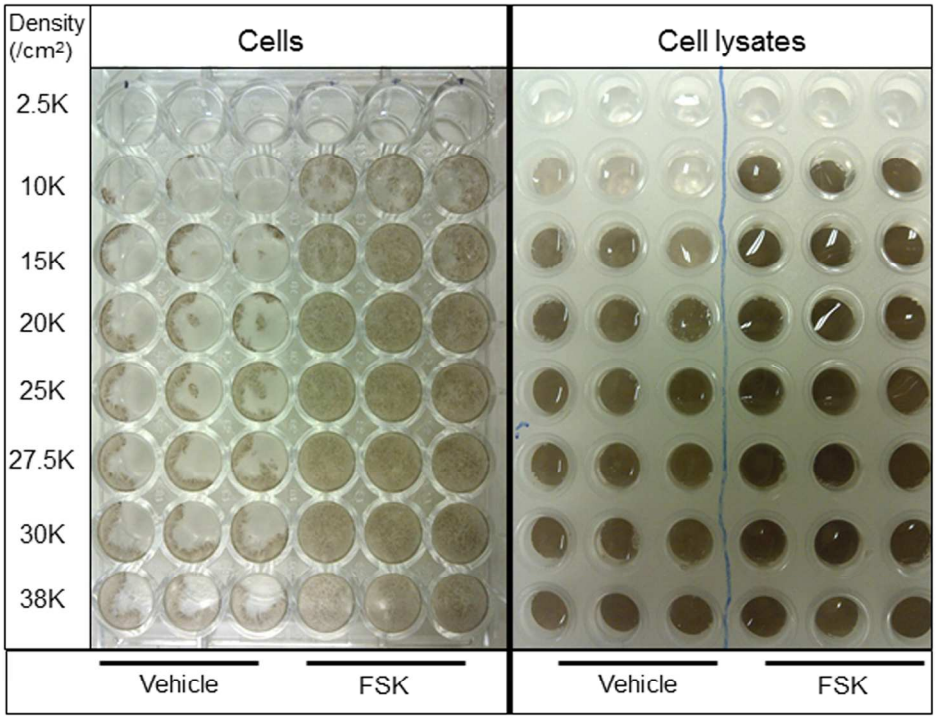

147x139mm (300 x 300 DPI)

Choudhary et. al. Supplementary figure 3. Top

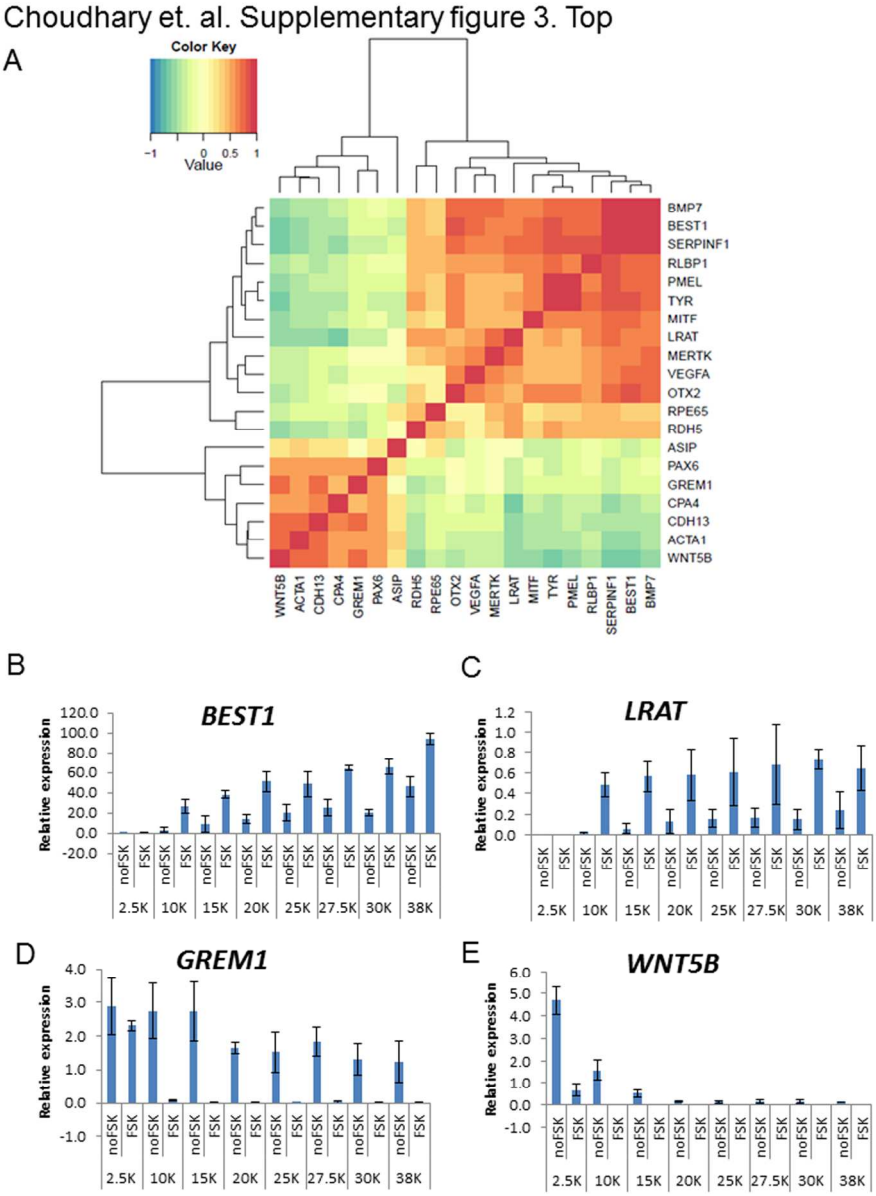

147x197mm (300 x 300 DPI)

Choudhary et. al. Supplementary figure 4. Top

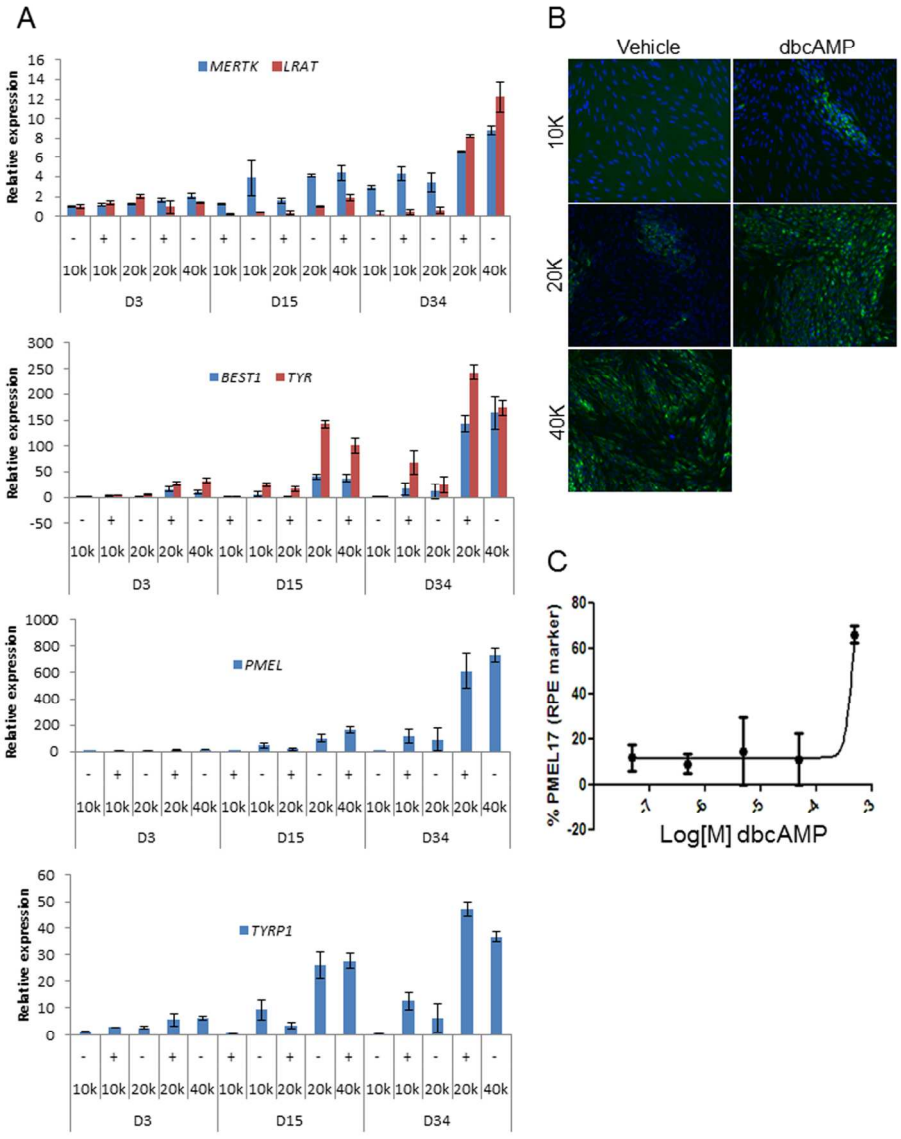

147x197mm (300 x 300 DPI)

Choudhary et. al. Supplementary figure 5. Top

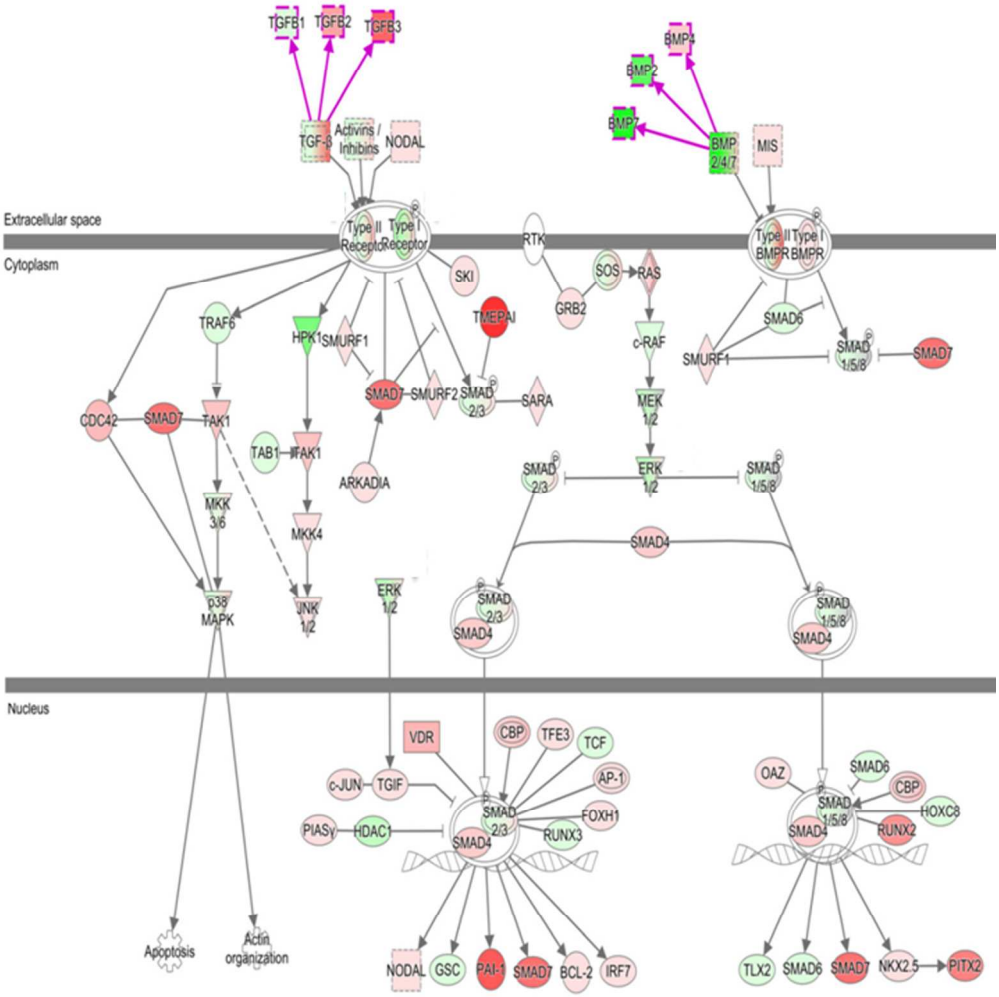

147x171mm (300 x 300 DPI)

Choudhary et. al. Supplementary figure 6. Top

Cpd #	Structure	ALK5 IC_{50}	ALK2 IC_{50}	Pmel EC_{50}	Edu EC_{50}	Reference
1	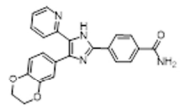	500nM	n.d.	1.3µM	1.6µM	Patent:WO200061576. [57]. Also related to [58].
2	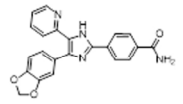	150nM	22µM	1.7µM	600nM	Compound 14 [56], [59]
3	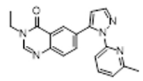	69nM	n.d.	600nM	1.0µM	[60](Compound 10)
4	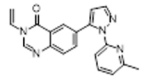	4nM	n.d.	70nM	100nM	[60](Compound 3)
5	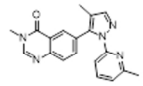	4nM	n.d.	100nM	100nM	[60](Compound 4)
6	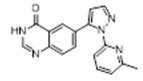	1nM	n.d.	1.3µM	100nM	[60](Compound 6)
7	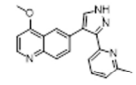	Not published	n.d.	100nM	130nM	Patent:WO200426306
8	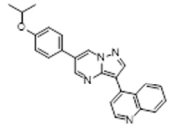	5.9µM	12.6nM	n.a.	n.a.	DMH1 [61]
9	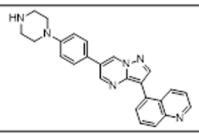	9.2µM	1.3nM	n.a.	n.a.	LDN-212854 [61]

147x185mm (300 x 300 DPI)

Choudhary et. al. Supplementary figure 7. Top

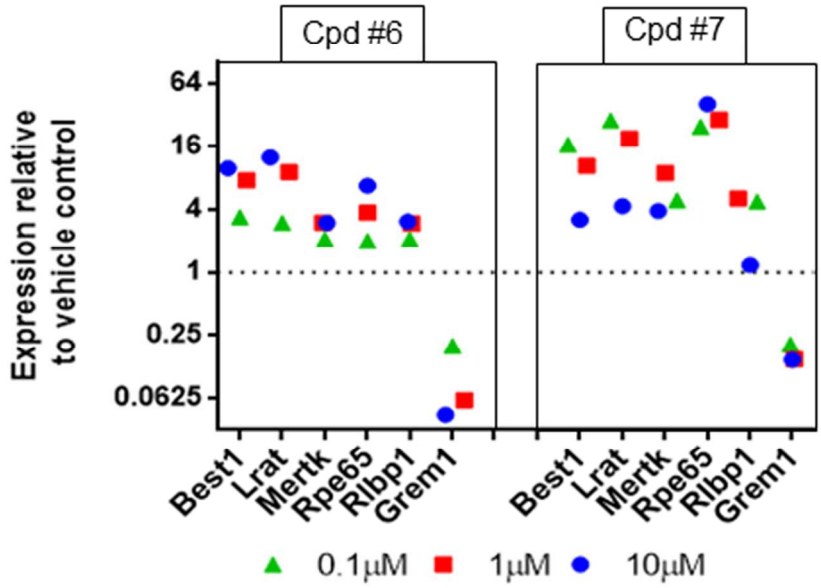

82x66mm (300 x 300 DPI)

PROBE_ID	SYMBOL	Entrez Gen	Cluster
ILMN_1794	ABCA4	24	1
ILMN_1658	ABCB5	340273	1
ILMN_1687	ABCB7	22	1
ILMN_1794	ABHD14A	25864	1
ILMN_2227	ABHD14B	84836	1
ILMN_1695	ABHD9	79852	1
ILMN_1761	ACAD11	84129	1
ILMN_1778	ACADM	34	1
ILMN_1795	ACADS	35	1
ILMN_1775	ACCN1	40	1
ILMN_1765	ACCN2	41	1
ILMN_2333	ACHE	43	1
ILMN_1654	ACO2	50	1
ILMN_1735	ACOT11	26027	1
ILMN_1685	ACOX2	8309	1
ILMN_2078	ACP5	54	1
ILMN_2234	ACP6	51205	1
ILMN_1706	ACPL2	92370	1
ILMN_2227	ACSBG1	23205	1
ILMN_3236	ACSF2	80221	1
ILMN_1752	ACSS1	84532	1
ILMN_1671	ACTA2	59	1
ILMN_1745	ADAD2	161931	1
ILMN_2384	ADAM15	8751	1
ILMN_1673	ADAMTS1	9510	1
ILMN_1681	ADAMTS5	11096	1
ILMN_1805	ADAMTS9	56999	1
ILMN_1721	ADAMTSL2	9719	1
ILMN_1798	ADAMTSL3	57188	1
ILMN_1687	ADAMTSL4	54507	1
ILMN_1702	ADHFE1	137872	1
ILMN_1708	ADM	133	1
ILMN_2080	ADNP2	22850	1
ILMN_1703	ADORA2B	136	1
ILMN_1695	ADRB2	154	1
ILMN_1775	AFF3	3899	1
ILMN_1802	AGA	175	1
ILMN_1794	AGPAT9	84803	1
ILMN_1712	AHCYL2	23382	1
ILMN_3246	AIF1L	83543	1
ILMN_1797	AIG1	51390	1
ILMN_1688	AIM1	202	1
ILMN_1713	AKR1C3	8644	1
ILMN_2096	ALDH1A1	216	1
ILMN_1807	ALDH1A3	220	1
ILMN_1793	ALDH2	217	1

ILMN_1785	ALDH6A1	4329	1
ILMN_1687	ALDH7A1	501	1
ILMN_1755	ALDOC	230	1
ILMN_2078	ALPK1	80216	1
ILMN_1701	ALPL	249	1
ILMN_1792	AMOT	154796	1
ILMN_1665	AMT	275	1
ILMN_1696	ANG	283	1
ILMN_1772	ANGPTL2	23452	1
ILMN_1674	ANGPTL4	51129	1
ILMN_1813	ANKDD1A	348094	1
ILMN_1784	ANKMY2	57037	1
ILMN_1687	ANKRA2	57763	1
ILMN_1675	ANKRD16	54522	1
ILMN_1768	ANKRD24	170961	1
ILMN_2075	ANKRD29	147463	1
ILMN_1667	ANKRD33	341405	1
ILMN_1756	ANKRD37	353322	1
ILMN_1776	ANKRD38	163782	1
ILMN_1779	ANKRD43	134548	1
ILMN_1712	ANKRD46	157567	1
ILMN_1724	ANKRD57	65124	1
ILMN_1766	AP1S2	8905	1
ILMN_1662	APC	324	1
ILMN_1659	APC2	10297	1
ILMN_1767	APH1B	83464	1
ILMN_2396	APLP1	333	1
ILMN_2081	APLP2	334	1
ILMN_1789	APOC1	341	1
ILMN_1740	APOE	348	1
ILMN_1723	APOLD1	81575	1
ILMN_2404	APP	351	1
ILMN_1776	AQP1	358	1
ILMN_1663	ARHGAP9	64333	1
ILMN_1669	ARHGEF16	27237	1
ILMN_1666	ARHGEF4	50649	1
ILMN_1803	ARHGEF6	9459	1
ILMN_1813	ARL1	400	1
ILMN_2120	ARL5B	221079	1
ILMN_1777	ARL9	132946	1
ILMN_1689	ARMC10	83787	1
ILMN_1697	ARMC5	79798	1
ILMN_2334	ARMCX3	51566	1
ILMN_2198	ARRDC3	57561	1
ILMN_1684	ASAH1	427	1
ILMN_1685	ASAP3	55616	1
ILMN_1654	ASB13	79754	1

ILMN_1701	ASCL1	429	1
ILMN_1791	ASIP	434	1
ILMN_1804	ASMTL	8623	1
ILMN_1692	ASPA	443	1
ILMN_1708	ASS1	445	1
ILMN_1684	ASTN1	460	1
ILMN_2374	ATF3	467	1
ILMN_1698	ATP10B	23120	1
ILMN_1731	ATP1A1	476	1
ILMN_1658	ATP1B1	481	1
ILMN_1747	ATP1B2	482	1
ILMN_1802	ATP2B2	491	1
ILMN_1693	ATP2B3	492	1
ILMN_2079	ATP5L	10632	1
ILMN_1755	ATP6AP1L	92270	1
ILMN_1660	ATP6V1C2	245973	1
ILMN_1654	ATP6V1G2	534	1
ILMN_1725	ATPGD1	57571	1
ILMN_1749	AUTS2	26053	1
ILMN_1724	AXIN2	8313	1
ILMN_1703	AXUD1	64651	1
ILMN_2148	B2M	567	1
ILMN_1690	B3GALT4	8705	1
ILMN_3246	B3GNT1	11041	1
ILMN_2326	BACE2	25825	1
ILMN_1703	BAIAP2L1	55971	1
ILMN_1720	BAZ2B	29994	1
ILMN_1733	BCAS1	8537	1
ILMN_1766	BCAT1	586	1
ILMN_2176	BCHE	590	1
ILMN_1716	BCL10	8915	1
ILMN_1665	BCL11B	64919	1
ILMN_1710	BCL3	602	1
ILMN_1814	BCMO1	53630	1
ILMN_1734	BDKRB1	623	1
ILMN_1668	BEGAIN	57596	1
ILMN_3237	BEND5	79656	1
ILMN_1718	BEST1	7439	1
ILMN_1690	BFSP2	8419	1
ILMN_1768	BHLHB2	8553	1
ILMN_1726	BHLHB3	79365	1
ILMN_2182	BIRC2	329	1
ILMN_1695	BMF	90427	1
ILMN_1722	BMP2	650	1
ILMN_1740	BMP4	652	1
ILMN_1741	BMP7	655	1
ILMN_1751	BNC1	646	1

ILMN_1724	BNIP3	664	1
ILMN_2045	BNIP3L	665	1
ILMN_1803	BOC	91653	1
ILMN_1665	BRF2	55290	1
ILMN_1774	BSCL2	26580	1
ILMN_3247	BSPRY	54836	1
ILMN_1723	BST2	684	1
ILMN_2081	BTC	685	1
ILMN_1695	BTD	686	1
ILMN_1775	BTG1	694	1
ILMN_1770	BTG2	7832	1
ILMN_1700	BTN3A2	11118	1
ILMN_2373	BTN3A3	10384	1
ILMN_1767	C10orf10	11067	1
ILMN_1783	C10orf11	83938	1
ILMN_1777	C10orf65	112817	1
ILMN_1715	C10orf67	256815	1
ILMN_2213	C11orf54	28970	1
ILMN_1798	C11orf75	56935	1
ILMN_1811	C11orf9	745	1
ILMN_1804	C12orf23	90488	1
ILMN_2105	C12orf32	83695	1
ILMN_1772	C12orf34	84915	1
ILMN_1772	C12orf44	60673	1
ILMN_1798	C12orf47	51275	1
ILMN_1658	C13orf15	28984	1
ILMN_1713	C14orf132	56967	1
ILMN_1721	C14orf159	80017	1
ILMN_1693	C14orf180	400258	1
ILMN_2157	C14orf19	280655	1
ILMN_1807	C14orf28	122525	1
ILMN_1724	C14orf93	60686	1
ILMN_1793	C15orf39	56905	1
ILMN_1681	C17orf44	284029	1
ILMN_2398	C17orf58	284018	1
ILMN_1743	C17orf69	147081	1
ILMN_1671	C18orf10	25941	1
ILMN_1796	C18orf56	494514	1
ILMN_1754	C1orf162	128346	1
ILMN_1761	C1orf168	199920	1
ILMN_1797	C1orf21	81563	1
ILMN_1793	C1orf51	148523	1
ILMN_1702	C1orf54	79630	1
ILMN_1748	C1orf55	163859	1
ILMN_1759	C1orf61	10485	1
ILMN_1716	C1QL1	10882	1
ILMN_1744	C1QTNF5	114902	1

ILMN_173	C1RL	51279	1
ILMN_167	C1S	716	1
ILMN_204	C20orf111	51526	1
ILMN_170	C20orf186	149954	1
ILMN_175	C20orf46	55321	1
ILMN_241	C21orf57	54059	1
ILMN_169	C21orf63	59271	1
ILMN_176	C21orf94	246705	1
ILMN_173	C22orf36	388886	1
ILMN_324	C2CD4B	388125	1
ILMN_167	C2orf40	84417	1
ILMN_168	C2orf64	493753	1
ILMN_176	C3	718	1
ILMN_179	C3orf58	205428	1
ILMN_324	C3orf71	646450	1
ILMN_217	C4A	720	1
ILMN_181	C4B	721	1
ILMN_181	C4orf33	132321	1
ILMN_323	C4orf47	441054	1
ILMN_207	C4orf49	84709	1
ILMN_172	C4orf7	260436	1
ILMN_168	C5orf13	9315	1
ILMN_177	C5orf41	153222	1
ILMN_168	C5orf53	492311	1
ILMN_324	C6orf124	653483	1
ILMN_166	C6orf192	116843	1
ILMN_228	C6orf48	50854	1
ILMN_167	C7orf41	222166	1
ILMN_165	C7orf68	29923	1
ILMN_168	C8orf13	83648	1
ILMN_181	C8orf34	116328	1
ILMN_165	C8orf4	56892	1
ILMN_213	C8orf47	203111	1
ILMN_324	C8orf83	286144	1
ILMN_170	C9orf127	51754	1
ILMN_171	C9orf40	55071	1
ILMN_178	C9orf5	23731	1
ILMN_166	C9orf75	286262	1
ILMN_167	C9orf95	54981	1
ILMN_174	CA11	770	1
ILMN_174	CA14	23632	1
ILMN_166	CA2	760	1
ILMN_167	CA5B	11238	1
ILMN_172	CA9	768	1
ILMN_173	CABC1	56997	1
ILMN_175	CABP7	164633	1
ILMN_239	CACNA1H	8912	1

ILMN_240(	CACNB2	783	1
ILMN_219[	CACNB3	784	1
ILMN_181[	CADM4	199731	1
ILMN_179[	CAMK2N1	55450	1
ILMN_166[	CAMTA1	23261	1
ILMN_173[	CAPN5	726	1
ILMN_324[	CAPN6	827	1
ILMN_180[	CARHSP1	23589	1
ILMN_236[	CASP6	839	1
ILMN_168[	CBLB	868	1
ILMN_172[	CBX4	8535	1
ILMN_165[	CBX7	23492	1
ILMN_176[	CCBL1	883	1
ILMN_170(	CCDC136	64753	1
ILMN_167[	CCDC14	64770	1
ILMN_179(	CCDC28A	25901	1
ILMN_177(	CCDC28B	79140	1
ILMN_168[	CCDC33	80125	1
ILMN_174[	CCDC5	115106	1
ILMN_234[	CCNB1IP1	57820	1
ILMN_166[	CCND2	894	1
ILMN_169[	CCNG1	900	1
ILMN_209[	CCNL1	57018	1
ILMN_167(	CCNO	10309	1
ILMN_168[	CCRN4L	25819	1
ILMN_239(	CD14	929	1
ILMN_206(	CD24	1E+08	1
ILMN_172(	CD248	57124	1
ILMN_171[	CD68	968	1
ILMN_173(	CD74	972	1
ILMN_236(	CD79B	974	1
ILMN_204[	CD84	8832	1
ILMN_167(	CDC2L6	23097	1
ILMN_174[	CDC42EP4	23580	1
ILMN_177[	CDC42EP5	148170	1
ILMN_179[	CDH10	1008	1
ILMN_170[	CDH3	1001	1
ILMN_172[	CDKN1B	1027	1
ILMN_171[	CDKN1C	1028	1
ILMN_177[	CDKN2AIP	55602	1
ILMN_165(	CDKN2C	1031	1
ILMN_175[	CDO1	1036	1
ILMN_169[	CDRT4	284040	1
ILMN_180[	CDS1	1040	1
ILMN_171[	CEBPA	1050	1
ILMN_169[	CEBPB	1051	1
ILMN_178[	CEBPD	1052	1

ILMN_3177	CECR4	1E+08	1
ILMN_1723	CEL	1056	1
ILMN_1711	CELSR2	1952	1
ILMN_1741	CEP70	80321	1
ILMN_1774	CFB	629	1
ILMN_1777	CFD	1675	1
ILMN_1810	CFH	3075	1
ILMN_1727	CFI	3426	1
ILMN_1739	CHAC1	79094	1
ILMN_3238	CHADL	150356	1
ILMN_1740	CHCHD10	400916	1
ILMN_1785	CHCHD6	84303	1
ILMN_1740	CHD3	1107	1
ILMN_2106	CHES1	1112	1
ILMN_1678	CHN1	1123	1
ILMN_1794	CHRNA3	1136	1
ILMN_1663	CITED2	10370	1
ILMN_1787	CITED4	163732	1
ILMN_1764	CKMT2	1160	1
ILMN_2328	CLCC1	23155	1
ILMN_1787	CLCNKA	1187	1
ILMN_1750	CLDN19	149461	1
ILMN_1725	CLDN23	137075	1
ILMN_1723	CLDN3	1365	1
ILMN_2077	CLDND2	125875	1
ILMN_1789	CLIP3	25999	1
ILMN_1778	CLN5	1203	1
ILMN_1682	CLOCK	9575	1
ILMN_1731	CLSTN2	64084	1
ILMN_1734	CLSTN3	9746	1
ILMN_1798	CLU	1191	1
ILMN_2382	CLUL1	27098	1
ILMN_1663	CLYBL	171425	1
ILMN_1709	CMBL	134147	1
ILMN_1750	CNGB3	54714	1
ILMN_1748	CNKSR3	154043	1
ILMN_2400	CNTN1	1272	1
ILMN_1718	CNTN2	6900	1
ILMN_1717	CNTN3	5067	1
ILMN_1692	CNTNAP1	8506	1
ILMN_1806	COL18A1	80781	1
ILMN_1742	COL4A5	1287	1
ILMN_1732	COL6A1	1291	1
ILMN_1809	COL6A2	1292	1
ILMN_2102	COL8A2	1296	1
ILMN_1685	COL9A2	1298	1
ILMN_1689	COLEC12	81035	1

ILMN_1813	CP	1356	1
ILMN_1703	CPD	1362	1
ILMN_1731	CPE	1363	1
ILMN_1722	CPEB4	80315	1
ILMN_1792	CPS1	1373	1
ILMN_1773	CPT1C	126129	1
ILMN_1678	CPT2	1376	1
ILMN_2400	CPVL	54504	1
ILMN_1741	CPXM2	119587	1
ILMN_1705	CPZ	8532	1
ILMN_1690	CRABP2	1382	1
ILMN_2140	CRIPAK	285464	1
ILMN_1753	CRISPLD1	83690	1
ILMN_1658	CRTAC1	55118	1
ILMN_3260	CRTC3	64784	1
ILMN_1719	CRX	1406	1
ILMN_1796	CRY2	1408	1
ILMN_1711	CRYAA	1409	1
ILMN_1714	CRYL1	51084	1
ILMN_1686	CSF1R	1436	1
ILMN_1775	CSMD2	114784	1
ILMN_1723	CSNK2A2	1459	1
ILMN_1688	CSPG5	10675	1
ILMN_1660	CSRP2	1466	1
ILMN_1800	CST3	1471	1
ILMN_2144	CTBS	1486	1
ILMN_2392	CTDSPL	10217	1
ILMN_2305	CTH	1491	1
ILMN_1716	CTNND2	1501	1
ILMN_1674	CTSD	1509	1
ILMN_2390	CTSH	1512	1
ILMN_1758	CTSK	1513	1
ILMN_1755	CUBN	8029	1
ILMN_1654	CX3CL1	6376	1
ILMN_1787	CXCL1	2919	1
ILMN_1748	CXCL14	9547	1
ILMN_1682	CXCL2	2920	1
ILMN_2320	CXCR4	7852	1
ILMN_1763	CXXC4	80319	1
ILMN_1696	CYB5D2	124936	1
ILMN_1739	CYB5R2	51700	1
ILMN_1744	CYBA	1535	1
ILMN_1712	CYBRD1	79901	1
ILMN_1758	CYGB	114757	1
ILMN_1704	CYP27A1	1593	1
ILMN_2188	CYR61	3491	1
ILMN_2201	CYTL1	54360	1

ILMN_1812	CYYR1	116159	1
ILMN_1787	DAAM1	23002	1
ILMN_1752	DAAM2	23500	1
ILMN_1687	DAPL1	92196	1
ILMN_1715	DBP	1628	1
ILMN_1729	DCDC5	196296	1
ILMN_1683	DCN	1634	1
ILMN_1701	DCT	1638	1
ILMN_1665	DCUN1D3	123879	1
ILMN_1676	DDIT3	1649	1
ILMN_1661	DDIT4	54541	1
ILMN_1696	DDIT4L	115265	1
ILMN_1812	DDR1	780	1
ILMN_1720	DECR1	1666	1
ILMN_1768	DEDD2	162989	1
ILMN_1686	DEFB1	1672	1
ILMN_1738	DEXI	28955	1
ILMN_1689	DHDH	27294	1
ILMN_1790	DHRS13	147015	1
ILMN_1678	DHX58	79132	1
ILMN_1737	DIO2	1734	1
ILMN_1655	DKFZp434N	84222	1
ILMN_2390	DKFZP564J	25854	1
ILMN_1768	DLG4	1742	1
ILMN_1743	DLL1	28514	1
ILMN_1655	DMRTA1	63951	1
ILMN_1775	DNAJB1	3337	1
ILMN_2222	DNAJB4	11080	1
ILMN_1773	DNAJB9	4189	1
ILMN_2269	DNAJC12	56521	1
ILMN_1749	DNAJC22	79962	1
ILMN_1810	DNAJC27	51277	1
ILMN_1687	DNAJC4	3338	1
ILMN_1796	DNASE2	1777	1
ILMN_1770	DPH5	51611	1
ILMN_1672	DPYSL2	1808	1
ILMN_1792	DPYSL4	10570	1
ILMN_2112	DRD4	1815	1
ILMN_2402	DSC1	1823	1
ILMN_1663	DSC2	1824	1
ILMN_1781	DUSP1	1843	1
ILMN_1759	DUSP10	11221	1
ILMN_1712	DUSP2	1844	1
ILMN_1667	DUSP26	78986	1
ILMN_1656	DUSP5	1847	1
ILMN_2396	DUSP6	1848	1
ILMN_1743	DUSP8	1850	1

ILMN_2137	DVL3	1857	1
ILMN_1697	DYNLRB2	83657	1
ILMN_1681	DYRK4	8798	1
ILMN_1653	ECH1	1891	1
ILMN_2072	ECHDC3	79746	1
ILMN_1653	EDG1	1901	1
ILMN_1689	EDIL3	10085	1
ILMN_1796	EDNRA	1909	1
ILMN_2108	EEF1A2	1917	1
ILMN_1789	EEF2K	29904	1
ILMN_1653	EFEMP2	30008	1
ILMN_1779	EFHD1	80303	1
ILMN_1695	EFNB3	1949	1
ILMN_1690	EGF	1950	1
ILMN_1798	EGFR	1956	1
ILMN_1762	EGR1	1958	1
ILMN_1743	EGR2	1959	1
ILMN_1722	EGR3	1960	1
ILMN_3244	EHBP1L1	254102	1
ILMN_2318	EIF5	1983	1
ILMN_1769	ELF3	1999	1
ILMN_1757	ELN	2006	1
ILMN_1737	ELOVL4	6785	1
ILMN_1709	ELP2	55250	1
ILMN_3240	EML2	24139	1
ILMN_1699	ENDOD1	23052	1
ILMN_1765	ENO2	2026	1
ILMN_1660	ENPP5	59084	1
ILMN_2416	ENTPD8	377841	1
ILMN_1746	EPC1	80314	1
ILMN_1675	EPDR1	54749	1
ILMN_1672	EPHA4	2043	1
ILMN_1709	EPHX2	2053	1
ILMN_1665	EPO	2056	1
ILMN_2388	EPSTI1	94240	1
ILMN_1769	ERC2	26059	1
ILMN_1682	ERMN	57471	1
ILMN_1751	ERMP1	79956	1
ILMN_1698	ERN1	2081	1
ILMN_1744	ERO1L	30001	1
ILMN_1806	ESPN	83715	1
ILMN_1684	ETFB	2109	1
ILMN_2244	ETNK1	55500	1
ILMN_2388	EXTL2	2135	1
ILMN_1733	FAM100A	124402	1
ILMN_1743	FAM107A	11170	1
ILMN_2410	FAM111A	63901	1

ILMN_173	FAM117B	150864	1
ILMN_172	FAM119B	25895	1
ILMN_166	FAM132A	388581	1
ILMN_324	FAM150B	285016	1
ILMN_324	FAM156B	727866	1
ILMN_180	FAM162A	26355	1
ILMN_165	FAM174B	400451	1
ILMN_166	FAM38B	63895	1
ILMN_216	FAM40B	57464	1
ILMN_174	FAM46A	55603	1
ILMN_171	FAM46C	54855	1
ILMN_174	FAM53C	51307	1
ILMN_330	FAM69A	388650	1
ILMN_323	FAM74A3	728495	1
ILMN_171	FAM89A	375061	1
ILMN_173	FASTKD5	60493	1
ILMN_178	FAT3	120114	1
ILMN_222	FBLN5	10516	1
ILMN_167	FBN2	2201	1
ILMN_180	FBP2	8789	1
ILMN_324	FBRS	64319	1
ILMN_175	FBXO15	201456	1
ILMN_166	FBXO33	254170	1
ILMN_324	FBXO45	200933	1
ILMN_180	FBXW5	54461	1
ILMN_170	FCGRT	2217	1
ILMN_220	FER1L4	80307	1
ILMN_177	FGD3	89846	1
ILMN_171	FGF11	2256	1
ILMN_179	FGFRL1	53834	1
ILMN_176	FHIT	2272	1
ILMN_172	FIBCD1	84929	1
ILMN_165	FILIP1	27145	1
ILMN_217	FLJ10916	55258	1
ILMN_326	FLJ30594	150622	1
ILMN_211	FLJ31568	150244	1
ILMN_167	FLJ35220	284131	1
ILMN_169	FLJ35934	400579	1
ILMN_326	FLJ37644	400618	1
ILMN_179	FLJ41603	389337	1
ILMN_166	FLJ41821	401011	1
ILMN_173	FLJ42875	440556	1
ILMN_176	FLJ45244	400242	1
ILMN_172	FLOT2	2319	1
ILMN_180	FLRT3	23767	1
ILMN_220	FLVCR2	55640	1
ILMN_168	FMO1	2326	1

ILMN_1732	FMO2	2327	1
ILMN_1677	FMO4	2329	1
ILMN_1661	FOLR1	2348	1
ILMN_1669	FOS	2353	1
ILMN_1751	FOSB	2354	1
ILMN_1705	FOXC2	2303	1
ILMN_1712	FOXO4	4303	1
ILMN_1773	FOXP4	116113	1
ILMN_1788	FRAT2	23401	1
ILMN_1753	FRMPD3	84443	1
ILMN_1716	FRZB	2487	1
ILMN_1808	FSCN1	6624	1
ILMN_1683	FTH1	2495	1
ILMN_1792	FUT4	2526	1
ILMN_1741	FUT8	2530	1
ILMN_1696	FZD1	8321	1
ILMN_1743	FZD4	8322	1
ILMN_1729	FZD8	8325	1
ILMN_2410	GAA	2548	1
ILMN_2151	GABARAPL	23710	1
ILMN_1729	GAL3ST1	9514	1
ILMN_1738	GALNT13	114805	1
ILMN_1722	GALNT14	79623	1
ILMN_1756	GAMT	2593	1
ILMN_1794	GAP43	2596	1
ILMN_1772	GAS1	2619	1
ILMN_2148	GBP1	2633	1
ILMN_1774	GBP2	2634	1
ILMN_1800	GCA	25801	1
ILMN_1682	GCC1	79571	1
ILMN_1694	GCHFR	2644	1
ILMN_1745	GDF11	10220	1
ILMN_2188	GDF15	9518	1
ILMN_2367	GEM	2669	1
ILMN_2220	GFPT1	2673	1
ILMN_1709	GFPT2	9945	1
ILMN_1656	GFRA2	2675	1
ILMN_1686	GGA2	23062	1
ILMN_2195	GGH	8836	1
ILMN_1727	GJA1	2697	1
ILMN_1766	GLA	2717	1
ILMN_1652	GLIPR2	152007	1
ILMN_2188	GLS	2744	1
ILMN_1677	GLS2	27165	1
ILMN_1729	GMPR	2766	1
ILMN_1802	GNA11	2767	1
ILMN_1758	GNA13	10672	1

ILMN_168(	GNA14	9630	1
ILMN_211[	GNB3	2784	1
ILMN_172[	GNE	10020	1
ILMN_178[	GNG11	2791	1
ILMN_209[	GNGT1	2792	1
ILMN_174[	GNS	2799	1
ILMN_173[	GOLSYN	55638	1
ILMN_213[	GOLT1A	127845	1
ILMN_180[	GPC6	10082	1
ILMN_217[	GPI	2821	1
ILMN_240[	GPNMB	10457	1
ILMN_177[	GPR124	25960	1
ILMN_173(	GPR162	27239	1
ILMN_173[	GPR180	160897	1
ILMN_221[	GPR37	2861	1
ILMN_178[	GPR37L1	9283	1
ILMN_175[	GPR64	10149	1
ILMN_169(	GPR98	84059	1
ILMN_172[	GPRC5C	55890	1
ILMN_172(	GPX3	2878	1
ILMN_172(	GPX7	2882	1
ILMN_206[	GRAMD3	65983	1
ILMN_172[	GRM8	2918	1
ILMN_166[	GSDMD	79792	1
ILMN_180[	GSN	2934	1
ILMN_177[	GSTA4	2941	1
ILMN_171[	GSTM2	2946	1
ILMN_173(	GSTM3	2947	1
ILMN_174(	GSTO2	119391	1
ILMN_180[	GULP1	51454	1
ILMN_166[	GUSB	2990	1
ILMN_231[	GYG2	8908	1
ILMN_175[	H1F0	3005	1
ILMN_177[	H1FX	8971	1
ILMN_169[	H3F3B	3021	1
ILMN_171[	HADH	3033	1
ILMN_206[	HAND2	9464	1
ILMN_168[	HBP1	26959	1
ILMN_171[	HBZ	3050	1
ILMN_231[	HCFC1R1	54985	1
ILMN_180[	HCP5	10866	1
ILMN_171[	HEPH	9843	1
ILMN_172[	HERC5	51191	1
ILMN_237[	HERPUD1	9709	1
ILMN_171(	HES1	3280	1
ILMN_179[	HES5	388585	1
ILMN_169[	HHATL	57467	1

ILMN_165(	HIBCH	26275	1
ILMN_165:	HIC2	23119	1
ILMN_175'	HIST1H1C	3006	1
ILMN_179:	HIST1H2AC	8334	1
ILMN_165'	HIST1H2BD	3017	1
ILMN_171(	HIST1H2BG	8339	1
ILMN_181:	HIST1H2BK	85236	1
ILMN_172'	HIST1H3D	8351	1
ILMN_207:	HIST1H4C	8364	1
ILMN_165:	HIST2H2AA	8337	1
ILMN_324:	HIST2H2AA	723790	1
ILMN_176(	HIST2H2AC	8338	1
ILMN_173:	HIST2H2BE	8349	1
ILMN_177:	HIST3H2A	92815	1
ILMN_167'	HLA-A	3105	1
ILMN_216:	HLA-A29.1	649853	1
ILMN_177(	HLA-B	3106	1
ILMN_169:	HLA-DMA	3108	1
ILMN_176:	HLA-E	3133	1
ILMN_176:	HLA-F	3134	1
ILMN_165(	HLA-G	3135	1
ILMN_166(	HLA-H	3136	1
ILMN_172:	HLF	3131	1
ILMN_179(	HLTF	6596	1
ILMN_181:	HMGCS2	3158	1
ILMN_180(	HMOX1	3162	1
ILMN_235(	HPN	3249	1
ILMN_166'	HRASLS3	11145	1
ILMN_180:	HSD17B14	51171	1
ILMN_180(	HSD17B2	3294	1
ILMN_239:	HSF4	3299	1
ILMN_166(	HSPA1B	3304	1
ILMN_165'	HSPA1L	3305	1
ILMN_177:	HSPA5	3309	1
ILMN_180(	HSPA6	3310	1
ILMN_172(	HSPB3	8988	1
ILMN_179'	HSPB8	26353	1
ILMN_173:	HTR2B	3357	1
ILMN_209:	HTRA4	203100	1
ILMN_173:	HYAL1	3373	1
ILMN_181:	ICAM1	3383	1
ILMN_179:	ID2	3398	1
ILMN_173:	ID3	3399	1
ILMN_169(	IDH1	3417	1
ILMN_175'	IDH2	3418	1
ILMN_170(	IER2	9592	1
ILMN_168:	IER3	8870	1

ILMN_1721	IER5	51278	1
ILMN_3236	IFFO2	126917	1
ILMN_2347	IFI6	2537	1
ILMN_1781	IFIH1	64135	1
ILMN_1707	IFIT1	3434	1
ILMN_1739	IFIT2	3433	1
ILMN_1801	IFITM1	8519	1
ILMN_1764	IFNGR2	3460	1
ILMN_1703	IFP38	83880	1
ILMN_1667	IFRD1	3475	1
ILMN_1717	IGBP1	3476	1
ILMN_2188	IGFALS	3483	1
ILMN_1665	IGFBP4	3487	1
ILMN_2132	IGFBP5	3488	1
ILMN_1669	IGFBP6	3489	1
ILMN_1730	IGSF21	84966	1
ILMN_1704	IGSF3	3321	1
ILMN_2344	IGSF5	150084	1
ILMN_1720	IL11RA	3590	1
ILMN_1809	IL33	90865	1
ILMN_1713	IL34	146433	1
ILMN_1809	IMMP2L	83943	1
ILMN_1744	INPP5D	3635	1
ILMN_1655	INTS6	26512	1
ILMN_1769	IQGAP2	10788	1
ILMN_1708	IRF1	3659	1
ILMN_2394	IRF2BP2	359948	1
ILMN_1745	IRF9	10379	1
ILMN_1782	IRX2	153572	1
ILMN_2359	ITGA6	3655	1
ILMN_2169	ITGAV	3685	1
ILMN_1776	ITGB1BP3	27231	1
ILMN_2317	ITGB4	3691	1
ILMN_2076	ITM2A	9452	1
ILMN_1680	ITM2C	81618	1
ILMN_1805	ITPRIP	85450	1
ILMN_1672	JAM2	58494	1
ILMN_1682	JAZF1	221895	1
ILMN_1722	JMJD1A	55818	1
ILMN_3251	JMY	133746	1
ILMN_1739	JSRP1	126306	1
ILMN_1806	JUN	3725	1
ILMN_2086	JUNB	3726	1
ILMN_1810	JUND	3727	1
ILMN_1750	KAL1	3730	1
ILMN_1684	KAZALD1	81621	1
ILMN_1784	KBTBD11	9920	1

ILMN_1802	KBTBD9	114818	1
ILMN_1744	KCNAB1	7881	1
ILMN_1748	KCND2	3751	1
ILMN_1673	KCNG1	3755	1
ILMN_1709	KCNJ13	3769	1
ILMN_1800	KCNJ4	3761	1
ILMN_1711	KCNK12	56660	1
ILMN_1755	KDM5B	10765	1
ILMN_1692	KIAA1024	23251	1
ILMN_2158	KIAA1683	80726	1
ILMN_1801	KIAA1826	84437	1
ILMN_1852	KIAA1881	114782	1
ILMN_1681	KIF21A	55605	1
ILMN_2212	KIF5C	3800	1
ILMN_1673	KISS1R	84634	1
ILMN_1808	KITLG	4254	1
ILMN_2411	KLF10	7071	1
ILMN_1737	KLF6	1316	1
ILMN_1778	KLF9	687	1
ILMN_1741	KLHDC2	23588	1
ILMN_1695	KLHDC8B	200942	1
ILMN_1701	KLHDC9	126823	1
ILMN_1701	KLHL15	80311	1
ILMN_1692	KLHL21	9903	1
ILMN_1678	KLHL24	54800	1
ILMN_1770	KLHL3	26249	1
ILMN_1780	KLHL30	377007	1
ILMN_1772	KREMEN1	83999	1
ILMN_1730	KRT19	3880	1
ILMN_1807	KRT32	3882	1
ILMN_1704	KU-MEL-3	497048	1
ILMN_1788	LAMA2	3908	1
ILMN_1688	LAMA3	3909	1
ILMN_2214	LAMB1	3912	1
ILMN_3242	LAMB2L	22973	1
ILMN_2279	LAMP2	3920	1
ILMN_1703	LANCL1	10314	1
ILMN_1692	LCN2	3934	1
ILMN_1763	LCTL	197021	1
ILMN_3249	LDHA	3939	1
ILMN_1785	LEMD1	93273	1
ILMN_1705	LEPREL2	10536	1
ILMN_1752	LEPROTL1	23484	1
ILMN_1782	LETMD1	25875	1
ILMN_1659	LGALS3BP	3959	1
ILMN_2353	LGALS8	3964	1
ILMN_2412	LGALS9	3965	1

ILMN_2171	LGI1	9211	1
ILMN_2332	LGMN	5641	1
ILMN_1767	LHFP	10186	1
ILMN_1807	LHX2	9355	1
ILMN_2139	LIMCH1	22998	1
ILMN_1806	LIN7A	8825	1
ILMN_1663	LIN7B	64130	1
ILMN_1695	LINGO2	158038	1
ILMN_1670	LIPE	3991	1
ILMN_1689	LIPG	9388	1
ILMN_1652	LMBRD1	55788	1
ILMN_1662	LMO1	4004	1
ILMN_1668	LMTK3	114783	1
ILMN_3243	LOC100008	1E+08	1
ILMN_3192	LOC100128	1E+08	1
ILMN_3185	LOC100128	1E+08	1
ILMN_3267	LOC100129	1E+08	1
ILMN_3236	LOC100129	1E+08	1
ILMN_3191	LOC100129	1E+08	1
ILMN_3259	LOC100129	1E+08	1
ILMN_3182	LOC100129	1E+08	1
ILMN_3182	LOC100129	1E+08	1
ILMN_3270	LOC100129	1E+08	1
ILMN_3264	LOC100130	1E+08	1
ILMN_3271	LOC100130	1E+08	1
ILMN_3265	LOC100130	1E+08	1
ILMN_3241	LOC100130	1E+08	1
ILMN_3279	LOC100131	1E+08	1
ILMN_3292	LOC100131	1E+08	1
ILMN_3199	LOC100131	1E+08	1
ILMN_3203	LOC100132	1E+08	1
ILMN_3243	LOC100132	1E+08	1
ILMN_3244	LOC100133	1E+08	1
ILMN_3240	LOC100133	1E+08	1
ILMN_3239	LOC100134	1E+08	1
ILMN_3282	LOC202781	202781	1
ILMN_1795	LOC220433	220433	1
ILMN_1739	LOC284023	284023	1
ILMN_1733	LOC284988	284988	1
ILMN_1684	LOC286016	286016	1
ILMN_3274	LOC286512	286512	1
ILMN_1795	LOC338758	338758	1
ILMN_2098	LOC338799	338799	1
ILMN_3289	LOC339352	339352	1
ILMN_1764	LOC339766	339766	1
ILMN_3248	LOC340508	340508	1
ILMN_1757	LOC342934	342934	1

ILMN_170	LOC34737	347376	1
ILMN_320	LOC38779	387791	1
ILMN_171	LOC38788	387882	1
ILMN_174	LOC38858	388588	1
ILMN_166	LOC38978	389787	1
ILMN_168	LOC39059	390594	1
ILMN_324	LOC39995	399959	1
ILMN_178	LOC40002	400027	1
ILMN_178	LOC40075	400759	1
ILMN_172	LOC40250	402509	1
ILMN_327	LOC44018	440181	1
ILMN_170	LOC44035	440359	1
ILMN_321	LOC44107	441073	1
ILMN_324	LOC44120	441204	1
ILMN_320	LOC44145	441453	1
ILMN_170	LOC44146	441461	1
ILMN_169	LOC44232	442329	1
ILMN_178	LOC64180	641805	1
ILMN_166	LOC64182	641825	1
ILMN_167	LOC64184	641848	1
ILMN_177	LOC64234	642342	1
ILMN_166	LOC64253	642530	1
ILMN_179	LOC64275	642755	1
ILMN_328	LOC64282	642828	1
ILMN_165	LOC64298	642989	1
ILMN_171	LOC64301	643011	1
ILMN_174	LOC64303	643031	1
ILMN_328	LOC64418	644186	1
ILMN_177	LOC64477	644774	1
ILMN_323	LOC64514	645146	1
ILMN_329	LOC64515	645157	1
ILMN_177	LOC64619	646197	1
ILMN_166	LOC64717	647174	1
ILMN_328	LOC64730	647307	1
ILMN_169	LOC64783	647834	1
ILMN_179	LOC65232	652322	1
ILMN_169	LOC65268	652683	1
ILMN_324	LOC65290	652900	1
ILMN_175	LOC65306	653066	1
ILMN_175	LOC65312	653123	1
ILMN_327	LOC65315	653156	1
ILMN_176	LOC65334	653342	1
ILMN_169	LOC65334	653344	1
ILMN_169	LOC65338	653381	1
ILMN_178	LOC65350	653506	1
ILMN_169	LOC65361	653610	1
ILMN_177	LOC65375	653752	1

ILMN_169(	LOC653841	653841	1
ILMN_171:	LOC653879	653879	1
ILMN_171:	LOC654096	654096	1
ILMN_169:	LOC654244	654244	1
ILMN_323:	LOC678655	678655	1
ILMN_177(	LOC727820	727820	1
ILMN_178:	LOC728229	728229	1
ILMN_324:	LOC728735	728735	1
ILMN_323:	LOC729234	729234	1
ILMN_322:	LOC729568	729568	1
ILMN_330:	LOC729708	729708	1
ILMN_183:	LOC729776	729776	1
ILMN_330(	LOC729920	729920	1
ILMN_330:	LOC730101	730101	1
ILMN_330(	LOC730255	730255	1
ILMN_170:	LOC730256	730256	1
ILMN_323:	LOC730323	730323	1
ILMN_165:	LOC730525	730525	1
ILMN_171:	LOC730820	730820	1
ILMN_188(	LOC731496	731496	1
ILMN_166:	LOC732165	732165	1
ILMN_324:	LOC92973	92973	1
ILMN_170:	LONRF1	91694	1
ILMN_173:	LOXL3	84695	1
ILMN_170:	LPAR1	1902	1
ILMN_169:	LPHN2	23266	1
ILMN_175:	LPPR1	54886	1
ILMN_167:	LRAT	9227	1
ILMN_167(	LRP11	84918	1
ILMN_169(	LRP1B	53353	1
ILMN_170:	LRP5	4041	1
ILMN_230:	LRP8	7804	1
ILMN_173(	LRRC16	55604	1
ILMN_171:	LRRC39	127495	1
ILMN_172(	LRRN1	57633	1
ILMN_172:	LXN	56925	1
ILMN_174(	MACROD1	28992	1
ILMN_168(	MAFF	23764	1
ILMN_177:	MAGED1	9500	1
ILMN_232:	MAL	4118	1
ILMN_177(	MAL2	114569	1
ILMN_214:	MAN2A1	4124	1
ILMN_176:	MAN2B2	23324	1
ILMN_180(	MANBA	4126	1
ILMN_166:	MAOA	4128	1
ILMN_172:	MAOB	4129	1
ILMN_172:	MAP3K1	4214	1

ILMN_1671	MAP3K15	389840	1
ILMN_1694	MAP3K6	9064	1
ILMN_1741	MAP3K8	1326	1
ILMN_1665	MAP4K1	11184	1
ILMN_1723	MAP4K2	5871	1
ILMN_1717	Mar-07	64844	1
ILMN_1807	MARCKS	4082	1
ILMN_1714	MARCKSL1	65108	1
ILMN_1710	MARVELD3	91862	1
ILMN_1735	MCEE	84693	1
ILMN_1752	MCF2	4168	1
ILMN_1803	MCL1	4170	1
ILMN_1723	MDK	4192	1
ILMN_1718	MED26	9441	1
ILMN_2290	MEGF9	1955	1
ILMN_1770	MERTK	10461	1
ILMN_1806	MESP1	55897	1
ILMN_2278	MEST	4232	1
ILMN_1790	METRNL	284207	1
ILMN_1658	MEX3C	51320	1
ILMN_1723	MFAP3L	9848	1
ILMN_1756	MFGE8	4240	1
ILMN_1761	MGAT1	4245	1
ILMN_1769	MGC16169	93627	1
ILMN_1744	MGC18216	145815	1
ILMN_1651	MGP	4256	1
ILMN_1746	MIDN	90007	1
ILMN_3308	MIR1974	1E+08	1
ILMN_3310	MIR1978	1E+08	1
ILMN_3310	MIR221	407006	1
ILMN_1718	MIS12	79003	1
ILMN_2347	MKNK2	2872	1
ILMN_1710	MLANA	2315	1
ILMN_1759	MLLT11	10962	1
ILMN_1795	MLPH	79083	1
ILMN_1733	MMD	23531	1
ILMN_1655	MMP11	4320	1
ILMN_1718	MMP15	4324	1
ILMN_1792	MNT	4335	1
ILMN_1717	MOBKL2B	79817	1
ILMN_1654	MPP2	4355	1
ILMN_2167	MR1	3140	1
ILMN_1707	MST1	4485	1
ILMN_1688	MST1R	4486	1
ILMN_2328	MST4	51765	1
ILMN_1718	MT1F	4494	1
ILMN_1775	MT1X	4501	1

ILMN_218(	MTPN	136319	1
ILMN_167(	MTSS1	9788	1
ILMN_166:	MX1	4599	1
ILMN_221-	MXD1	4084	1
ILMN_180:	MXRA5	25878	1
ILMN_179:	MYBPC2	4606	1
ILMN_173:	MYBPHL	343263	1
ILMN_181:	MYH10	4628	1
ILMN_236:	MYH11	4629	1
ILMN_168:	MYL2	4633	1
ILMN_171:	MYL6B	140465	1
ILMN_177(	MYL9	10398	1
ILMN_165(	MYLIP	29116	1
ILMN_236-	MYLK	4638	1
ILMN_180:	MYO16	23026	1
ILMN_181:	MYO7A	4647	1
ILMN_205:	MYOC	4653	1
ILMN_166:	MYRIP	25924	1
ILMN_180-	MYST1	84148	1
ILMN_179:	N4BP2L1	90634	1
ILMN_174(	NAALAD2	10003	1
ILMN_171(	NAPRT1	93100	1
ILMN_233-	NARF	26502	1
ILMN_178-	NAT14	57106	1
ILMN_171-	NAV3	89795	1
ILMN_178:	NCALD	83988	1
ILMN_174:	NCAM2	4685	1
ILMN_171:	NCCRP1	342897	1
ILMN_168;	NCOA7	135112	1
ILMN_177:	NCRNA001	55857	1
ILMN_324-	NCRNA002	114915	1
ILMN_180:	NDRG1	10397	1
ILMN_167(	NDRG2	57447	1
ILMN_175(	NDUFA4L2	56901	1
ILMN_180:	NEBL	10529	1
ILMN_173:	NEDD4L	23327	1
ILMN_172:	NELL2	4753	1
ILMN_175:	NET1	10276	1
ILMN_171;	NFE2	4778	1
ILMN_173:	NFE2L1	4779	1
ILMN_204:	NFE2L3	9603	1
ILMN_170;	NFIL3	4783	1
ILMN_179:	NFKB2	4791	1
ILMN_177:	NFKBIA	4792	1
ILMN_168-	NFXL1	152518	1
ILMN_180;	NICN1	84276	1
ILMN_169:	NID2	22795	1

ILMN_1815	NINJ1	4814	1
ILMN_1739	NLGN1	22871	1
ILMN_1764	NLGN2	57555	1
ILMN_1728	NLGN4X	57502	1
ILMN_1669	NME3	4832	1
ILMN_1665	NMNAT3	349565	1
ILMN_2162	NMU	10874	1
ILMN_1652	NOG	9241	1
ILMN_1729	NOTCH1	4851	1
ILMN_1658	NOTCH3	4854	1
ILMN_1747	NPAS1	4861	1
ILMN_3246	NPW	283869	1
ILMN_1678	NR1H2	7376	1
ILMN_2210	NR3C2	4306	1
ILMN_3237	NRBF2	29982	1
ILMN_1733	NRBP2	340371	1
ILMN_1749	NSBP1	79366	1
ILMN_2205	NSUN7	79730	1
ILMN_1727	NTNG1	22854	1
ILMN_2357	NTRK2	4915	1
ILMN_1789	NUAK2	81788	1
ILMN_1722	NUCB1	4924	1
ILMN_1655	NUCB2	4925	1
ILMN_1669	NUDT14	256281	1
ILMN_3226	NUDT7	283927	1
ILMN_1765	NUFIP2	57532	1
ILMN_2404	NUPR1	26471	1
ILMN_1721	NWD1	284434	1
ILMN_1760	NXT1	29107	1
ILMN_3236	NYNRIN	57523	1
ILMN_1782	NYX	60506	1
ILMN_1749	OBSCN	84033	1
ILMN_2121	OC90	729330	1
ILMN_1746	OCA2	4948	1
ILMN_1729	ODAM	54959	1
ILMN_1714	OGDHL	55753	1
ILMN_1795	OKL38	29948	1
ILMN_1776	OLFML1	283298	1
ILMN_1739	OMG	4974	1
ILMN_1741	OPCML	4978	1
ILMN_1716	OPN3	23596	1
ILMN_1719	OR51E2	81285	1
ILMN_1802	OR7E156P	283491	1
ILMN_1706	OSBP	5007	1
ILMN_1773	OSBPL1A	114876	1
ILMN_1722	OTX2	5015	1
ILMN_1737	OXR1	55074	1

ILMN_2381	P4HA2	8974	1
ILMN_1672	P4HTM	54681	1
ILMN_1734	P76	196463	1
ILMN_1751	PACSIN1	29993	1
ILMN_2313	PAM	5066	1
ILMN_1658	PAN2	9924	1
ILMN_1783	PANK1	53354	1
ILMN_1694	PANX2	56666	1
ILMN_1710	PAPLN	89932	1
ILMN_1660	PAQR4	124222	1
ILMN_1674	PARD6G	84552	1
ILMN_1656	PARM1	25849	1
ILMN_1721	PARP10	84875	1
ILMN_1679	PCBP4	57060	1
ILMN_1781	PCDH17	27253	1
ILMN_2229	PCDH18	54510	1
ILMN_3230	PCLO	27445	1
ILMN_1737	PCMTD1	115294	1
ILMN_1767	PCMTD2	55251	1
ILMN_1707	PCOLCE	5118	1
ILMN_1755	PCSK1N	27344	1
ILMN_1767	PCSK5	5125	1
ILMN_1784	PCTK3	5129	1
ILMN_2113	PCYOX1	51449	1
ILMN_2340	PDE4B	5142	1
ILMN_1791	PDE4D	5144	1
ILMN_2342	PDGFA	5154	1
ILMN_2376	PDGFD	80310	1
ILMN_1815	PDGFRB	5159	1
ILMN_1680	PDGFRL	5157	1
ILMN_1695	PDIA5	10954	1
ILMN_1705	PDK2	5164	1
ILMN_1684	PDK4	5166	1
ILMN_1695	PDLIM3	27295	1
ILMN_1734	PEBP4	157310	1
ILMN_1780	PELI2	57161	1
ILMN_1660	PER3	8863	1
ILMN_1660	PEX5	5830	1
ILMN_1660	PFKFB3	5209	1
ILMN_1653	PFKFB4	5210	1
ILMN_1661	PGAM1	5223	1
ILMN_1668	PGAM2	5224	1
ILMN_2058	PGCP	10404	1
ILMN_2179	PHC3	80012	1
ILMN_1761	PHF13	148479	1
ILMN_1795	PHF15	23338	1
ILMN_1659	PHLDA3	23612	1

ILMN_180	PHTF1	10745	1
ILMN_167	PHYHIPL	84457	1
ILMN_166	PI15	51050	1
ILMN_170	PIGA	5277	1
ILMN_171	PIK3IP1	113791	1
ILMN_181	PIM1	5292	1
ILMN_174	PIM2	11040	1
ILMN_238	PIR	8544	1
ILMN_167	PITPNC1	26207	1
ILMN_168	PJA2	9867	1
ILMN_233	PKIA	5569	1
ILMN_180	PKNOX2	63876	1
ILMN_179	PLA1A	51365	1
ILMN_209	PLAC8	51316	1
ILMN_179	PLAC9	219348	1
ILMN_176	PLCD1	5333	1
ILMN_206	PLCH2	9651	1
ILMN_170	PLD5	200150	1
ILMN_324	PLD6	201164	1
ILMN_170	PLEKHA7	144100	1
ILMN_178	PLEKHB1	58473	1
ILMN_180	PLEKHH2	130271	1
ILMN_168	PLEKHO2	80301	1
ILMN_213	PLIN2	123	1
ILMN_208	PLLP	51090	1
ILMN_168	PLOD1	5351	1
ILMN_179	PLOD2	5352	1
ILMN_175	PLSCR4	57088	1
ILMN_171	PLTP	5360	1
ILMN_167	PLXND1	23129	1
ILMN_209	PMAIP1	5366	1
ILMN_178	PMM2	5373	1
ILMN_323	PMS2L4	5382	1
ILMN_169	PNCK	139728	1
ILMN_241	PODXL	5420	1
ILMN_177	POFUT2	23275	1
ILMN_174	POLR1D	51082	1
ILMN_235	PON2	5445	1
ILMN_175	PPARGC1A	10891	1
ILMN_166	PPFIA4	8497	1
ILMN_167	PPFIBP2	8495	1
ILMN_165	PPIL6	285755	1
ILMN_167	PPM1D	8493	1
ILMN_165	PPP1R10	5514	1
ILMN_176	PPP1R14A	94274	1
ILMN_165	PPP1R15A	23645	1
ILMN_173	PPP1R3E	90673	1

ILMN_167(	PPP3CA	5530	1
ILMN_177[	PPP4R4	57718	1
ILMN_179(	PPRC1	23082	1
ILMN_170[	PRELP	5549	1
ILMN_174[	PRICKLE1	144165	1
ILMN_167[	PRODH	5625	1
ILMN_177[	PROK2	60675	1
ILMN_178(	PROM1	8842	1
ILMN_167[	PROS1	5627	1
ILMN_172[	PRPH	5630	1
ILMN_168[	PRRC1	133619	1
ILMN_173[	PRRX1	5396	1
ILMN_167[	PRSS12	8492	1
ILMN_173(	PRSS33	260429	1
ILMN_179(	PRSS8	5652	1
ILMN_166[	PSD2	84249	1
ILMN_166[	PTGDS	5730	1
ILMN_174[	PTGFRN	5738	1
ILMN_173[	PTK2B	2185	1
ILMN_181[	PTN	5764	1
ILMN_235[	PTP4A3	11156	1
ILMN_231[	PTPRD	5789	1
ILMN_167(	PTPRZ1	5803	1
ILMN_169(	PYGL	5836	1
ILMN_172(	PYGM	5837	1
ILMN_170(	QPRT	23475	1
ILMN_205[	RAB17	64284	1
ILMN_169[	RAB18	22931	1
ILMN_171[	RAB24	53917	1
ILMN_179(	RAB26	25837	1
ILMN_232[	RAB27A	5873	1
ILMN_221[	RAB30	27314	1
ILMN_172[	RAB33A	9363	1
ILMN_172[	RAB33B	83452	1
ILMN_213[	RAB38	23682	1
ILMN_175[	RAB6B	51560	1
ILMN_167[	RALGPS1	9649	1
ILMN_177(	RAP1GAP	5909	1
ILMN_166[	RAPGEF4	11069	1
ILMN_323(	RAPGEF5	9771	1
ILMN_174[	RARRES1	5918	1
ILMN_181(	RARRES2	5919	1
ILMN_170[	RARRES3	5920	1
ILMN_174(	RASD1	51655	1
ILMN_217(	RASD2	23551	1
ILMN_172[	RASGRP3	25780	1
ILMN_214[	RASL11B	65997	1

ILMN_180(	RASL12	51285	1
ILMN_169(	RASSF4	83937	1
ILMN_168(	RAX	30062	1
ILMN_166(	RBM15	64783	1
ILMN_171:	RCAN1	1827	1
ILMN_179:	RCOR2	283248	1
ILMN_171-	RDH10	157506	1
ILMN_212(	RDH11	51109	1
ILMN_177:	RDH5	5959	1
ILMN_175:	REC8	9985	1
ILMN_173:	REEP1	65055	1
ILMN_166(	REEP2	51308	1
ILMN_170(	RELA	5970	1
ILMN_181:	RELB	5971	1
ILMN_323:	RELL1	768211	1
ILMN_180(	RELN	5649	1
ILMN_180(	RFTN1	23180	1
ILMN_165-	RGL1	23179	1
ILMN_171:	RGMA	56963	1
ILMN_181:	RGR	5995	1
ILMN_176:	RGS11	8786	1
ILMN_219:	RGS2	5997	1
ILMN_175(	RGS4	5999	1
ILMN_165-	RGS7BP	401190	1
ILMN_167(	RGS9BP	388531	1
ILMN_180:	RHOB	388	1
ILMN_174-	RHOBTB3	22836	1
ILMN_167(	RHOJ	57381	1
ILMN_324:	RHOU	58480	1
ILMN_174:	RIMS3	9783	1
ILMN_175(	RIPK2	8767	1
ILMN_175:	RLBP1	6017	1
ILMN_180:	RLF	6018	1
ILMN_179(	RNASE1	6035	1
ILMN_229-	RNASE4	6038	1
ILMN_221(	RNASEL	6041	1
ILMN_167:	RNASET2	8635	1
ILMN_169:	RNF122	79845	1
ILMN_177:	RNF144	9781	1
ILMN_176:	RNF150	57484	1
ILMN_329(	RNFT2	84900	1
ILMN_176(	RNMT	8731	1
ILMN_324(	RNU1-3	26869	1
ILMN_323(	RNU1-5	26863	1
ILMN_324-	RNU1G2	26864	1
ILMN_324(	RNU4ATAC	1E+08	1
ILMN_323:	RNY1	6084	1

ILMN_3246	RNY5	6090	1
ILMN_1722	ROGDI	79641	1
ILMN_2322	RORA	6095	1
ILMN_1746	RORB	6096	1
ILMN_1734	RORC	6097	1
ILMN_2047	RP11-529I1	25911	1
ILMN_1686	RPE65	6121	1
ILMN_1808	RPESP	157869	1
ILMN_3226	RPL12P6	440176	1
ILMN_1689	RPLP1	6176	1
ILMN_1704	RPPH1	85495	1
ILMN_1665	RPRM	56475	1
ILMN_1676	RPRML	388394	1
ILMN_1657	RPS6KA5	9252	1
ILMN_2186	RRAD	6236	1
ILMN_1780	RRAS	6237	1
ILMN_1791	RSBN1	54665	1
ILMN_2173	RTP4	64108	1
ILMN_1812	RWDD1	51389	1
ILMN_1722	RWDD2A	112611	1
ILMN_1796	RWDD3	25950	1
ILMN_1653	S100A1	6271	1
ILMN_1750	S100A9	6280	1
ILMN_1740	SALL2	6297	1
ILMN_1709	SAMD11	148398	1
ILMN_1760	SAMD14	201191	1
ILMN_2185	SASH1	23328	1
ILMN_1753	SAT1	6303	1
ILMN_1746	SAT2	112483	1
ILMN_2050	SAV1	60485	1
ILMN_1746	SCARA3	51435	1
ILMN_1805	SCARNA9	619383	1
ILMN_2065	SCG5	6447	1
ILMN_1813	SCIN	85477	1
ILMN_1776	SCML1	6322	1
ILMN_1676	SCN2B	6327	1
ILMN_1740	SCNN1B	6338	1
ILMN_1726	SCRG1	11341	1
ILMN_1663	SDC4	6385	1
ILMN_1705	SDCBP2	27111	1
ILMN_1749	SDF2L1	23753	1
ILMN_1744	SDHA	6389	1
ILMN_1676	SDK2	54549	1
ILMN_2126	SEC24A	10802	1
ILMN_1784	SECISBP2L	9728	1
ILMN_1797	SEL1L3	23231	1
ILMN_1680	SELENBP1	8991	1

ILMN_1651	SELM	140606	1
ILMN_1653	SEMA3B	7869	1
ILMN_1702	SEMA4A	64218	1
ILMN_1687	SEMA4D	10507	1
ILMN_1785	SEPP1	6414	1
ILMN_1746	Sep-03	55964	1
ILMN_1760	SERGEF	26297	1
ILMN_1741	SERINC1	57515	1
ILMN_1706	SERP1	27230	1
ILMN_2338	SERPINA1	5265	1
ILMN_1788	SERPINA3	12	1
ILMN_1759	SERPINA5	5104	1
ILMN_2141	SERPINF1	5176	1
ILMN_1740	SERPINF2	5345	1
ILMN_1670	SERPING1	710	1
ILMN_1751	SERPINH1	871	1
ILMN_1794	SERTAD1	29950	1
ILMN_1801	SERTAD3	29946	1
ILMN_1800	SESN1	27244	1
ILMN_1751	SESN2	83667	1
ILMN_1694	SESN3	143686	1
ILMN_1724	SESTD1	91404	1
ILMN_1682	SETMAR	6419	1
ILMN_1763	SETX	23064	1
ILMN_2413	SEZ6L2	26470	1
ILMN_2149	SFRP1	6422	1
ILMN_1790	SFRP5	6425	1
ILMN_1659	SGCG	6445	1
ILMN_1664	SGIP1	84251	1
ILMN_1702	SGK	6446	1
ILMN_1811	SGPP2	130367	1
ILMN_1702	SH3BGRL	6451	1
ILMN_1760	SH3GL3	6457	1
ILMN_1712	SH3YL1	26751	1
ILMN_1681	SHROOM2	357	1
ILMN_1665	SILV	6490	1
ILMN_1805	SIN3A	25942	1
ILMN_1732	SIPA1L2	57568	1
ILMN_1739	SIRT1	23411	1
ILMN_1799	SIX3	6496	1
ILMN_1743	SIX4	51804	1
ILMN_1793	SIX5	147912	1
ILMN_2085	SLC15A3	51296	1
ILMN_1782	SLC16A10	117247	1
ILMN_1736	SLC16A14	151473	1
ILMN_2102	SLC16A4	9122	1
ILMN_1729	SLC16A6	9120	1

ILMN_1731	SLC16A8	23539	1
ILMN_1732	SLC16A9	220963	1
ILMN_218(	SLC18A3	6572	1
ILMN_1704	SLC1A7	6512	1
ILMN_1786	SLC24A5	283652	1
ILMN_1675	SLC25A23	79085	1
ILMN_1791	SLC25A25	114789	1
ILMN_1705	SLC25A34	284723	1
ILMN_1715	SLC25A37	51312	1
ILMN_2222	SLC25A42	284439	1
ILMN_1787	SLC27A1	376497	1
ILMN_1700	SLC27A2	11001	1
ILMN_1715	SLC27A3	11000	1
ILMN_2325	SLC29A4	222962	1
ILMN_1655	SLC2A1	6513	1
ILMN_1663	SLC2A10	81031	1
ILMN_1766	SLC2A12	154091	1
ILMN_1775	SLC2A3	6515	1
ILMN_1702	SLC35D3	340146	1
ILMN_1678	SLC37A4	2542	1
ILMN_1672	SLC38A3	10991	1
ILMN_1718	SLC39A12	221074	1
ILMN_1710	SLC39A3	29985	1
ILMN_2053	SLC40A1	30061	1
ILMN_1787	SLC43A2	124935	1
ILMN_1771	SLC44A2	57153	1
ILMN_2320	SLC45A2	51151	1
ILMN_1745	SLC45A4	57210	1
ILMN_1670	SLC47A1	55244	1
ILMN_1787	SLC5A3	6526	1
ILMN_1707	SLC6A13	6540	1
ILMN_1806	SLC6A8	6535	1
ILMN_1812	SLC7A6	9057	1
ILMN_1785	SLITRK5	26050	1
ILMN_1767	SMAD6	4091	1
ILMN_1654	SMC6	79677	1
ILMN_1715	SMOC2	64094	1
ILMN_1775	SMOX	54498	1
ILMN_1715	SMPDL3B	27293	1
ILMN_1733	SNAP91	9892	1
ILMN_1701	SNCA	6622	1
ILMN_3305	SNHG8	1E+08	1
ILMN_1651	SNIP1	79753	1
ILMN_3238	SNORA12	677800	1
ILMN_3235	SNORA28	677811	1
ILMN_1892	SNORD13	692084	1
ILMN_2107	SNRK	54861	1

ILMN_1753	SNTA1	6640	1
ILMN_1793	SNTB1	6641	1
ILMN_1781	SOCS3	9021	1
ILMN_1690	SOD3	6649	1
ILMN_1729	SORCS2	57537	1
ILMN_2060	SORL1	6653	1
ILMN_1707	SORT1	6272	1
ILMN_1715	SOSTDC1	25928	1
ILMN_1653	SOX10	6663	1
ILMN_1773	SOX11	6664	1
ILMN_1683	SOX13	9580	1
ILMN_1784	SOX15	6665	1
ILMN_1815	SOX4	6659	1
ILMN_1789	SOX8	30812	1
ILMN_1805	SOX9	6662	1
ILMN_1721	SP4	6671	1
ILMN_1684	SPAG4	6676	1
ILMN_2233	SPANXA1	30014	1
ILMN_1653	SPANXA2	728712	1
ILMN_2211	SPANXB1	728695	1
ILMN_1795	SPARCL1	8404	1
ILMN_1687	SPATA20	64847	1
ILMN_1763	SPHKAP	80309	1
ILMN_2143	SPIB	6689	1
ILMN_1676	SPON2	10417	1
ILMN_2089	SPRY2	10253	1
ILMN_1728	SPTY2D1	144108	1
ILMN_2400	SRGAP3	9901	1
ILMN_2169	SRGN	5552	1
ILMN_1785	SRPR	6734	1
ILMN_1709	SRPX	8406	1
ILMN_1811	SRRM4	84530	1
ILMN_1711	SSBP2	23635	1
ILMN_1742	SSFA2	6744	1
ILMN_1755	SSH3	54961	1
ILMN_1775	SSPN	8082	1
ILMN_3237	SSPO	23145	1
ILMN_1812	SST	6750	1
ILMN_1720	SSX2IP	117178	1
ILMN_2388	ST3GAL5	8869	1
ILMN_1658	ST6GALNA(	10610	1
ILMN_1758	ST8SIA2	8128	1
ILMN_1717	STARD10	10809	1
ILMN_2410	STAT3	6774	1
ILMN_1758	STC1	6781	1
ILMN_1691	STC2	8614	1
ILMN_1727	STK35	140901	1

ILMN_176(	STOM	2040	1
ILMN_166{	STON1	11037	1
ILMN_170:	SULF1	23213	1
ILMN_233(	SULT1A4	445329	1
ILMN_168!	SUMF2	25870	1
ILMN_169=	SUSD2	56241	1
ILMN_180(	SV2B	9899	1
ILMN_175-	SYNE2	23224	1
ILMN_171:	SYNM	23336	1
ILMN_165{	SYT13	57586	1
ILMN_219-	TADA1L	117143	1
ILMN_175)	TAP1	6890	1
ILMN_174:	TAPBP	6892	1
ILMN_170=	TBC1D9	23158	1
ILMN_174=	TBCC	6903	1
ILMN_174-	TBL1X	6907	1
ILMN_172(	TCEA3	6920	1
ILMN_176!	TCEAL2	140597	1
ILMN_181-	TCFL5	10732	1
ILMN_175-	TCP10L	140290	1
ILMN_168!	TCTN1	79600	1
ILMN_228!	TDP1	55775	1
ILMN_168:	TEAD2	8463	1
ILMN_170(	TEF	7008	1
ILMN_179!	TEKT3	64518	1
ILMN_179)	TESK1	7016	1
ILMN_176{	TF	7018	1
ILMN_206{	TFPI2	7980	1
ILMN_168!	TGDS	23483	1
ILMN_208=	TGFA	7039	1
ILMN_166)	THRA	7067	1
ILMN_235/	THYN1	29087	1
ILMN_171:	TIA1	7072	1
ILMN_165)	TICAM2	353376	1
ILMN_172)	TIMP2	7077	1
ILMN_176!	TIPARP	25976	1
ILMN_172:	TLR5	7100	1
ILMN_169(	TM7SF2	7108	1
ILMN_173(	TMED10	10972	1
ILMN_173(	TMEFF2	23671	1
ILMN_172(	TMEM106E	54664	1
ILMN_169:	TMEM106(	79022	1
ILMN_166!	TMEM108	66000	1
ILMN_205:	TMEM116	89894	1
ILMN_180!	TMEM117	84216	1
ILMN_172-	TMEM123	114908	1
ILMN_168!	TMEM125	128218	1

ILMN_2317	TMEM132A	54972	1
ILMN_1732	TMEM143	55260	1
ILMN_1708	TMEM144	55314	1
ILMN_1785	TMEM14A	28978	1
ILMN_1809	TMEM155	132332	1
ILMN_1792	TMEM158	25907	1
ILMN_1655	TMEM159	57146	1
ILMN_1795	TMEM167B	56900	1
ILMN_1791	TMEM176A	55365	1
ILMN_2085	TMEM176B	28959	1
ILMN_2104	TMEM178	130733	1
ILMN_3251	TMEM19	55266	1
ILMN_1784	TMEM2	23670	1
ILMN_1772	TMEM27	57393	1
ILMN_1735	TMEM30A	55754	1
ILMN_1670	TMEM37	140738	1
ILMN_1765	TMEM38A	79041	1
ILMN_1770	TMEM45A	55076	1
ILMN_2129	TMEM47	83604	1
ILMN_1674	TMEM51	55092	1
ILMN_1792	TMEM59	9528	1
ILMN_1780	TMEM66	51669	1
ILMN_1797	TMEM86A	144110	1
ILMN_1757	TMEM88	92162	1
ILMN_1686	TMEM9	252839	1
ILMN_2206	TMEM90B	79953	1
ILMN_2211	TMEM91	641649	1
ILMN_1779	TMEM98	26022	1
ILMN_1736	TMOD1	7111	1
ILMN_1739	TMPRSS5	80975	1
ILMN_1727	TNFAIP2	7127	1
ILMN_1702	TNFAIP3	7128	1
ILMN_1697	TNFRSF14	8764	1
ILMN_1685	TNFRSF1A	7132	1
ILMN_1758	TNFSF13B	10673	1
ILMN_1751	TNFSF9	8744	1
ILMN_1726	TNRC6B	23112	1
ILMN_1672	TOB1	10140	1
ILMN_2214	TP53INP1	94241	1
ILMN_1714	TPD52L1	7164	1
ILMN_1729	TPP1	1200	1
ILMN_1758	TRAFD1	10906	1
ILMN_1747	TRAPPC2L	51693	1
ILMN_2211	TRAPPC2P1	10597	1
ILMN_1775	TRAPPC6A	79090	1
ILMN_1803	TRIB1	10221	1
ILMN_1714	TRIB2	28951	1

ILMN_1787	TRIB3	57761	1
ILMN_1775	TRIM22	10346	1
ILMN_2323	TRIM4	89122	1
ILMN_1702	TRIM63	84676	1
ILMN_1776	TRK1	7206	1
ILMN_1695	TRNP1	388610	1
ILMN_2295	TRO	7216	1
ILMN_1791	TRPM1	4308	1
ILMN_2302	TRPM3	80036	1
ILMN_1675	TRPM4	54795	1
ILMN_1814	TRPM6	140803	1
ILMN_2297	TRPV4	59341	1
ILMN_1696	TRQ1	7228	1
ILMN_1721	TSC22D4	81628	1
ILMN_1718	TSHZ1	10194	1
ILMN_1655	TSHZ2	128553	1
ILMN_1801	TSKU	25987	1
ILMN_1656	TSPAN10	83882	1
ILMN_1768	TSPAN12	23554	1
ILMN_1718	TSPAN32	10077	1
ILMN_1683	TSPAN8	7103	1
ILMN_1728	TTC3	7267	1
ILMN_1746	TTC39C	125488	1
ILMN_1746	TTLL4	9654	1
ILMN_2198	TTR	7276	1
ILMN_1758	TTYH1	57348	1
ILMN_1695	TTYH2	94015	1
ILMN_1680	TUBB2B	347733	1
ILMN_1682	TUBB4	10382	1
ILMN_1749	TUBD1	51174	1
ILMN_1701	TUBG2	27175	1
ILMN_1786	TUT1	64852	1
ILMN_1697	TXNIP	10628	1
ILMN_1788	TYR	7299	1
ILMN_2054	TYRP1	7306	1
ILMN_1794	UBA7	7318	1
ILMN_1678	UBD	10537	1
ILMN_1810	UBL3	5412	1
ILMN_1742	UBL4A	8266	1
ILMN_1685	UCP2	7351	1
ILMN_1705	ULK1	8408	1
ILMN_2353	UPK3B	80761	1
ILMN_1664	USE1	55850	1
ILMN_1697	USP36	57602	1
ILMN_1722	USP47	55031	1
ILMN_1662	USPL1	10208	1
ILMN_1713	VAMP2	6844	1

ILMN_1715	VANGL2	57216	1
ILMN_1796	VASH1	22846	1
ILMN_1667	VASN	114990	1
ILMN_1749	VAT1L	57687	1
ILMN_2375	VEGFA	7422	1
ILMN_1701	VEGFC	7424	1
ILMN_1684	VEPH1	79674	1
ILMN_1778	VILL	50853	1
ILMN_2361	VLDLR	7436	1
ILMN_1700	VPREB3	29802	1
ILMN_1692	VPS37D	155382	1
ILMN_1691	VTN	7448	1
ILMN_3309	VTRNA1-1	56664	1
ILMN_1719	WBSCR27	155368	1
ILMN_1658	WDR54	84058	1
ILMN_1700	WDR86	349136	1
ILMN_1695	WDYHV1	55093	1
ILMN_1778	WEE1	7465	1
ILMN_1662	WFIKKN2	124857	1
ILMN_1803	WNT3	7473	1
ILMN_1771	XAB2	56949	1
ILMN_2365	XBP1	7494	1
ILMN_1759	XK	7504	1
ILMN_1799	XYLT2	64132	1
ILMN_1714	YIPF5	81555	1
ILMN_1677	YPEL2	388403	1
ILMN_1791	YPEL3	83719	1
ILMN_2061	YRDC	79693	1
ILMN_1795	ZADH2	284273	1
ILMN_1731	ZBTB43	23099	1
ILMN_1710	ZBTB46	140685	1
ILMN_1757	ZBTB5	9925	1
ILMN_1672	ZC3H12A	80149	1
ILMN_3237	ZC3H12C	85463	1
ILMN_1795	ZFAND5	7763	1
ILMN_1800	ZFP106	64397	1
ILMN_1723	ZFP2	80108	1
ILMN_1720	ZFP36	7538	1
ILMN_1793	ZFP37	7539	1
ILMN_2184	ZHX2	22882	1
ILMN_2139	ZKSCAN1	7586	1
ILMN_1654	ZMAT3	64393	1
ILMN_1655	ZMYND12	84217	1
ILMN_2332	ZNF16	7564	1
ILMN_1806	ZNF165	7718	1
ILMN_1806	ZNF189	7743	1
ILMN_2079	ZNF204	7754	1

ILMN_1811	ZNF211	10520	1
ILMN_1692	ZNF226	7769	1
ILMN_1808	ZNF25	219749	1
ILMN_1757	ZNF250	58500	1
ILMN_2350	ZNF254	9534	1
ILMN_1757	ZNF256	10172	1
ILMN_1692	ZNF263	10127	1
ILMN_1795	ZNF264	9422	1
ILMN_1753	ZNF266	10781	1
ILMN_1688	ZNF274	10782	1
ILMN_2243	ZNF275	10838	1
ILMN_1681	ZNF277	11179	1
ILMN_2414	ZNF302	55900	1
ILMN_1656	ZNF304	57343	1
ILMN_1689	ZNF329	79673	1
ILMN_1711	ZNF331	55422	1
ILMN_2124	ZNF34	80778	1
ILMN_1807	ZNF394	84124	1
ILMN_1779	ZNF467	168544	1
ILMN_1653	ZNF483	158399	1
ILMN_1787	ZNF503	84858	1
ILMN_1742	ZNF518A	9849	1
ILMN_2225	ZNF521	25925	1
ILMN_1716	ZNF543	125919	1
ILMN_1728	ZNF548	147694	1
ILMN_2162	ZNF597	146434	1
ILMN_1681	ZNF606	80095	1
ILMN_1672	ZNF615	284370	1
ILMN_1665	ZNF672	79894	1
ILMN_1730	ZNF680	340252	1
ILMN_1751	ZNF684	127396	1
ILMN_1805	ZNF721	170960	1
ILMN_1758	ZNF791	163049	1
ILMN_1665	ZNF792	126375	1
ILMN_2225	ZNF805	390980	1
ILMN_1802	ZNF91	7644	1
ILMN_1654	ZSCAN18	65982	1
ILMN_3237	AAGAB	79719	2
ILMN_1703	AATF	26574	2
ILMN_1766	ABCA1	19	2
ILMN_2330	ABCE1	6059	2
ILMN_1745	ABHD12	26090	2
ILMN_2403	ABHD2	11057	2
ILMN_1801	ABHD3	171586	2
ILMN_1655	ABHD5	51099	2
ILMN_1719	ABHD7	253152	2
ILMN_1775	ACAD9	28976	2

ILMN_3187	ACCS	84680	2
ILMN_2371	ACLY	47	2
ILMN_2367	ACOT9	23597	2
ILMN_2125	ACTA1	58	2
ILMN_1658	ACTC1	70	2
ILMN_1795	ACTG2	72	2
ILMN_2232	ACTN1	87	2
ILMN_1725	ACTN4	81	2
ILMN_2060	ADAM23	8745	2
ILMN_1676	ADCY3	109	2
ILMN_1790	ADSL	158	2
ILMN_1662	AGPAT5	55326	2
ILMN_1709	AGXT	189	2
ILMN_1714	AHNAK	79026	2
ILMN_3243	AHNAK2	113146	2
ILMN_1798	AHSA2	130872	2
ILMN_1673	AIMP2	7965	2
ILMN_1684	AKAP12	9590	2
ILMN_1701	AKR1B1	231	2
ILMN_2150	ALDH1B1	219	2
ILMN_2244	ALDH4A1	8659	2
ILMN_1718	ALG1	56052	2
ILMN_1761	ALG13	79868	2
ILMN_1743	ALG14	199857	2
ILMN_2365	ALG8	79053	2
ILMN_1680	ALOX5	240	2
ILMN_1797	ALOX5AP	241	2
ILMN_1811	ALPK2	115701	2
ILMN_1693	ALPP	250	2
ILMN_1800	ALS2CR4	65062	2
ILMN_1713	AMTN	401138	2
ILMN_2195	ANAPC7	51434	2
ILMN_1813	ANGPTL7	10218	2
ILMN_3249	ANKLE2	23141	2
ILMN_1716	ANKRD1	27063	2
ILMN_1739	ANLN	54443	2
ILMN_1674	ANO6	196527	2
ILMN_1812	ANTXR2	118429	2
ILMN_2184	ANXA1	301	2
ILMN_2380	ANXA11	311	2
ILMN_1711	ANXA2	302	2
ILMN_1698	ANXA2P1	303	2
ILMN_1798	ANXA2P3	305	2
ILMN_1694	ANXA3	306	2
ILMN_1778	ANXA8	244	2
ILMN_2095	ANXA8	653145	2
ILMN_1767	AOX1	316	2

ILMN_170[illegible]	AP1M2	10053	2
ILMN_175[illegible]	AP1S1	1174	2
ILMN_176[illegible]	AP3B1	8546	2
ILMN_168[illegible]	APCDD1L	164284	2
ILMN_172[illegible]	APOA1BP	128240	2
ILMN_221[illegible]	APOBEC3B	9582	2
ILMN_172[illegible]	APRT	353	2
ILMN_324[illegible]	ARAP3	64411	2
ILMN_172[illegible]	ARD1A	8260	2
ILMN_178[illegible]	ARGLU1	55082	2
ILMN_173[illegible]	ARHGAP10	79658	2
ILMN_167[illegible]	ARHGAP22	58504	2
ILMN_176[illegible]	ARHGAP23	57636	2
ILMN_173[illegible]	ARHGDIA	396	2
ILMN_218[illegible]	ARL16	339231	2
ILMN_170[illegible]	ARL4A	10124	2
ILMN_169[illegible]	ARMC6	93436	2
ILMN_208[illegible]	ARPC1B	10095	2
ILMN_204[illegible]	ARPC5L	81873	2
ILMN_235[illegible]	ARS2	51593	2
ILMN_172[illegible]	ARSI	340075	2
ILMN_165[illegible]	ASAM	79827	2
ILMN_327[illegible]	ASAP2	8853	2
ILMN_167[illegible]	ASCC2	84164	2
ILMN_169[illegible]	ASF1B	55723	2
ILMN_179[illegible]	ASNS	440	2
ILMN_181[illegible]	ASPM	259266	2
ILMN_204[illegible]	ATAD2	29028	2
ILMN_173[illegible]	ATAD3A	55210	2
ILMN_213[illegible]	ATAD3B	83858	2
ILMN_167[illegible]	ATF4	468	2
ILMN_166[illegible]	ATF5	22809	2
ILMN_175[illegible]	ATL3	25923	2
ILMN_171[illegible]	ATP5G1	516	2
ILMN_170[illegible]	ATP6V0A2	23545	2
ILMN_168[illegible]	AURKA	6790	2
ILMN_168[illegible]	AURKB	9212	2
ILMN_171[illegible]	AVEN	57099	2
ILMN_170[illegible]	AXL	558	2
ILMN_174[illegible]	AZI1	22994	2
ILMN_166[illegible]	B4GALT7	11285	2
ILMN_323[illegible]	B9D1	27077	2
ILMN_177[illegible]	BAIAP2L2	80115	2
ILMN_174[illegible]	BAT2D1	23215	2
ILMN_177[illegible]	BCCIP	56647	2
ILMN_239[illegible]	BCKDHB	594	2
ILMN_225[illegible]	BCL11A	53335	2

ILMN_1678	BCYRN1	618	2
ILMN_2206	BGN	633	2
ILMN_2372	BID	637	2
ILMN_2405	BIRC3	330	2
ILMN_2349	BIRC5	332	2
ILMN_1709	BLM	641	2
ILMN_2106	BLZF1	8548	2
ILMN_2299	BMP2K	55589	2
ILMN_2070	BMPR2	659	2
ILMN_3238	BMS1P5	399761	2
ILMN_1656	BNC2	54796	2
ILMN_1782	BOLA2	552900	2
ILMN_1786	BOLA3	388962	2
ILMN_1715	BOP1	23246	2
ILMN_1657	BPHL	670	2
ILMN_1708	BPIL2	254240	2
ILMN_2311	BRCA1	672	2
ILMN_1697	BRCC3	79184	2
ILMN_2398	BRMS1	25855	2
ILMN_1760	BSN	8927	2
ILMN_2202	BUB1	699	2
ILMN_1797	BUB1B	701	2
ILMN_1682	BYSL	705	2
ILMN_1704	C10orf125	282969	2
ILMN_1772	C10orf32	119032	2
ILMN_2205	C10orf54	64115	2
ILMN_1739	C11orf48	79081	2
ILMN_1726	C11orf51	25906	2
ILMN_1757	C11orf68	83638	2
ILMN_1781	C11orf73	51501	2
ILMN_1790	C11orf82	220042	2
ILMN_2180	C12orf24	29902	2
ILMN_2122	C12orf31	84298	2
ILMN_1751	C12orf4	57102	2
ILMN_1727	C12orf48	55010	2
ILMN_1736	C13orf3	221150	2
ILMN_1666	C14orf106	55320	2
ILMN_1704	C14orf126	112487	2
ILMN_1661	C14orf156	81892	2
ILMN_1653	C14orf80	283643	2
ILMN_1690	C14orf82	145438	2
ILMN_2134	C14orf85	319085	2
ILMN_1652	C15orf23	90417	2
ILMN_1775	C15orf52	388115	2
ILMN_1801	C16orf33	79622	2
ILMN_1656	C16orf59	80178	2
ILMN_1729	C16orf62	57020	2

ILMN_165	C16orf68	79091	2
ILMN_179	C16orf75	116028	2
ILMN_217	C16orf93	90835	2
ILMN_177	C17orf53	78995	2
ILMN_222	C17orf85	55421	2
ILMN_239	C17orf91	84981	2
ILMN_169	C18orf45	85019	2
ILMN_171	C19orf33	64073	2
ILMN_239	C19orf62	29086	2
ILMN_176	C19orf70	125988	2
ILMN_208	C1orf107	27042	2
ILMN_172	C1orf112	55732	2
ILMN_324	C1orf133	574036	2
ILMN_178	C1orf135	79000	2
ILMN_170	C1orf144	26099	2
ILMN_167	C1orf159	54991	2
ILMN_178	C1orf188	148646	2
ILMN_173	C1orf19	116461	2
ILMN_169	C1orf212	113444	2
ILMN_166	C1orf53	388722	2
ILMN_168	C1orf59	113802	2
ILMN_174	C1orf63	57035	2
ILMN_169	C1orf85	112770	2
ILMN_166	C20orf127	140851	2
ILMN_169	C20orf27	54976	2
ILMN_169	C21orf7	56911	2
ILMN_210	C21orf70	85395	2
ILMN_319	C22orf27	150291	2
ILMN_222	C2orf7	84279	2
ILMN_170	C3orf26	84319	2
ILMN_218	C3orf52	79669	2
ILMN_167	C4orf18	51313	2
ILMN_176	C5orf23	79614	2
ILMN_215	C5orf28	64417	2
ILMN_171	C5orf46	389336	2
ILMN_167	C5orf5	51306	2
ILMN_172	C6orf115	58527	2
ILMN_179	C6orf125	84300	2
ILMN_181	C6orf153	88745	2
ILMN_176	C6orf173	387103	2
ILMN_213	C6orf26	401251	2
ILMN_166	C6orf89	221477	2
ILMN_324	C7orf40	285958	2
ILMN_165	C7orf54	27099	2
ILMN_324	C8orf30B	728071	2
ILMN_172	C8orf38	137682	2
ILMN_211	C8orf45	157777	2

ILMN_180	C9orf114	51490	2
ILMN_172	C9orf116	138162	2
ILMN_170	C9orf140	89958	2
ILMN_181	C9orf167	54863	2
ILMN_181	C9orf169	375791	2
ILMN_167	C9orf3	84909	2
ILMN_171	C9orf30	91283	2
ILMN_324	C9orf69	90120	2
ILMN_165	CABLES1	91768	2
ILMN_173	CALD1	800	2
ILMN_166	CAMK2A	815	2
ILMN_169	CAP2	10486	2
ILMN_171	CAPN2	824	2
ILMN_174	CARD10	29775	2
ILMN_214	CAV1	857	2
ILMN_180	CBS	875	2
ILMN_215	CBWD5	220869	2
ILMN_212	CCBE1	147372	2
ILMN_180	CCDC109B	55013	2
ILMN_171	CCDC132	55610	2
ILMN_206	CCDC56	28958	2
ILMN_168	CCDC58	131076	2
ILMN_167	CCDC74A	90557	2
ILMN_180	CCDC80	151887	2
ILMN_170	CCDC84	338657	2
ILMN_166	CCDC85A	114800	2
ILMN_179	CCDC86	79080	2
ILMN_169	CCDC99	54908	2
ILMN_172	CCL2	6347	2
ILMN_165	CCL26	10344	2
ILMN_215	CCNA1	8900	2
ILMN_178	CCNA2	890	2
ILMN_171	CCNB1	891	2
ILMN_180	CCNB2	9133	2
ILMN_168	CCND1	595	2
ILMN_166	CCND3	896	2
ILMN_177	CCNF	899	2
ILMN_167	CCT2	10576	2
ILMN_165	CCT3	7203	2
ILMN_170	CCT5	22948	2
ILMN_171	CCT6A	908	2
ILMN_234	CCT7	10574	2
ILMN_166	CD151	977	2
ILMN_174	CD3EAP	10849	2
ILMN_233	CD59	966	2
ILMN_167	CDC123	8872	2
ILMN_233	CDC16	8881	2

ILMN_1747	CDC2	983	2
ILMN_1663	CDC20	991	2
ILMN_1711	CDC25A	993	2
ILMN_1725	CDC25C	995	2
ILMN_1668	CDC37	11140	2
ILMN_1652	CDC42EP2	10435	2
ILMN_1670	CDC45L	8318	2
ILMN_1741	CDC7	8317	2
ILMN_1802	CDCA1	83540	2
ILMN_1660	CDCA2	157313	2
ILMN_1737	CDCA3	83461	2
ILMN_1683	CDCA5	113130	2
ILMN_1737	CDCA7	83879	2
ILMN_1709	CDCA8	55143	2
ILMN_1770	CDH1	999	2
ILMN_1672	CDH11	1009	2
ILMN_1781	CDK5	1020	2
ILMN_2376	CDKN2B	1030	2
ILMN_1666	CDKN3	1033	2
ILMN_1651	CDT1	81620	2
ILMN_1810	CDV3	55573	2
ILMN_1801	CENPA	1058	2
ILMN_2225	CENPE	1062	2
ILMN_1664	CENPF	1063	2
ILMN_1737	CENPK	64105	2
ILMN_2368	CENPM	79019	2
ILMN_1720	CENPN	55839	2
ILMN_1787	CENPO	79172	2
ILMN_3246	CENPV	201161	2
ILMN_1693	CEP135	9662	2
ILMN_1747	CEP55	55165	2
ILMN_1750	CERCAM	51148	2
ILMN_1705	CFL1	1072	2
ILMN_2387	CGGBP1	8545	2
ILMN_1746	CGN	57530	2
ILMN_1669	CHAF1A	10036	2
ILMN_1674	CHAF1B	8208	2
ILMN_1673	CHCHD3	54927	2
ILMN_1786	CHD1L	9557	2
ILMN_1664	CHEK1	1111	2
ILMN_1776	CHORDC1	26973	2
ILMN_1770	CHRNA5	1138	2
ILMN_1734	CHST13	166012	2
ILMN_1794	CHST2	9435	2
ILMN_1674	CKAP2	26586	2
ILMN_1751	CKAP2L	150468	2
ILMN_1732	CKMT1A	548596	2

ILMN_2072	CKS2	1164	2
ILMN_1661	CLCF1	23529	2
ILMN_1724	CLDN1	9076	2
ILMN_1754	CLDN11	5010	2
ILMN_1756	CLIC1	1192	2
ILMN_1796	CLIC3	9022	2
ILMN_1689	CLK1	1195	2
ILMN_1707	CMC1	152100	2
ILMN_1698	CNIH2	254263	2
ILMN_1810	CNN1	1264	2
ILMN_1733	COL12A1	1303	2
ILMN_1651	COL17A1	1308	2
ILMN_1701	COL1A1	1277	2
ILMN_1785	COL1A2	1278	2
ILMN_1784	COL22A1	169044	2
ILMN_1788	COL27A1	85301	2
ILMN_1773	COL3A1	1281	2
ILMN_1653	COL4A1	1282	2
ILMN_1724	COL4A2	1284	2
ILMN_1706	COL5A1	1289	2
ILMN_1729	COL5A2	1290	2
ILMN_1751	COL7A1	1294	2
ILMN_1808	COMMD9	29099	2
ILMN_1764	COPS6	10980	2
ILMN_1756	COQ2	27235	2
ILMN_1745	CORO1C	23603	2
ILMN_1788	COTL1	23406	2
ILMN_1784	CPA4	51200	2
ILMN_2087	CPSF3	51692	2
ILMN_2146	CRIM1	51232	2
ILMN_1694	CRIP2	1397	2
ILMN_1790	CRISPLD2	83716	2
ILMN_1789	CRMP1	1400	2
ILMN_1728	CROP	51747	2
ILMN_1760	CRYBB2	1415	2
ILMN_2119	CSAD	51380	2
ILMN_1806	CSDC2	27254	2
ILMN_1698	CST6	1474	2
ILMN_1653	CSTF2	1478	2
ILMN_2397	CSTF3	1479	2
ILMN_1806	CTAGE6	340307	2
ILMN_2115	CTGF	1490	2
ILMN_1725	CTHRC1	115908	2
ILMN_1783	CTPS	1503	2
ILMN_1719	CTSA	5476	2
ILMN_1748	CTSL2	1515	2
ILMN_1666	CTSZ	1522	2

ILMN_1744	CTTN	2017	2
ILMN_1759	CTXN1	404217	2
ILMN_1798	CXCR7	57007	2
ILMN_3247	CXorf64	1E+08	2
ILMN_1688	CYB5R4	51167	2
ILMN_2129	CYBASC3	220002	2
ILMN_1730	CYCS	54205	2
ILMN_1693	CYP1B1	1545	2
ILMN_1685	CYP24A1	1591	2
ILMN_1664	CYP51A1	1595	2
ILMN_2160	CYTH3	9265	2
ILMN_1733	DACT3	147906	2
ILMN_1658	DAGLB	221955	2
ILMN_1676	DARS2	55157	2
ILMN_1769	DBN1	1627	2
ILMN_1698	DBNL	28988	2
ILMN_1735	DCBLD2	131566	2
ILMN_1740	DCPS	28960	2
ILMN_3242	DCTPP1	79077	2
ILMN_1668	DDAH1	23576	2
ILMN_1735	DDX21	9188	2
ILMN_1747	DDX39	10212	2
ILMN_1727	DDX46	9879	2
ILMN_1812	DDX54	79039	2
ILMN_1679	DDX56	54606	2
ILMN_1656	DEF8	54849	2
ILMN_1747	DEK	7913	2
ILMN_2117	DEM1	64789	2
ILMN_1727	DENND1A	57706	2
ILMN_2103	DEPDC1B	55789	2
ILMN_1761	DERL2	51009	2
ILMN_1725	DHCR24	1718	2
ILMN_2165	DHCR7	1717	2
ILMN_1807	DHRS1	115817	2
ILMN_1697	DHX29	54505	2
ILMN_2192	DHX37	57647	2
ILMN_2373	DIAPH3	81624	2
ILMN_1671	DKC1	1736	2
ILMN_1749	DLGAP5	9787	2
ILMN_1752	DNAJC13	23317	2
ILMN_1663	DNAJC7	7266	2
ILMN_1799	DNAJC9	23234	2
ILMN_1730	DNAL1	83544	2
ILMN_1795	DNCL1	8655	2
ILMN_2112	DNLZ	728489	2
ILMN_1760	DNMT1	1786	2
ILMN_1715	DOCK1	1793	2

ILMN_179	DOCK2	1794	2
ILMN_175	DOCK5	80005	2
ILMN_170	DPP3	10072	2
ILMN_167	DPP9	91039	2
ILMN_167	DPYSL3	1809	2
ILMN_166	DRAM1	55332	2
ILMN_211	DRAP1	10589	2
ILMN_177	DTL	51514	2
ILMN_172	DUS3L	56931	2
ILMN_172	DUSP19	142679	2
ILMN_165	DUSP23	54935	2
ILMN_179	DUSP3	1845	2
ILMN_178	DYNC1H1	1778	2
ILMN_181	DYSF	8291	2
ILMN_177	E2F2	1870	2
ILMN_180	EBI3	10148	2
ILMN_176	EBNA1BP2	10969	2
ILMN_207	EBP	10682	2
ILMN_176	ECE2	9718	2
ILMN_210	ECGF1	1890	2
ILMN_165	ECM1	1893	2
ILMN_171	ECT2	1894	2
ILMN_171	EDEM2	55741	2
ILMN_168	EDN1	1906	2
ILMN_168	EDN2	1907	2
ILMN_168	EEF1B2	1933	2
ILMN_172	EEF1E1	9521	2
ILMN_173	EFHA1	221154	2
ILMN_176	EFHD2	79180	2
ILMN_173	EFTUD2	9343	2
ILMN_165	EHD1	10938	2
ILMN_205	EID2B	126272	2
ILMN_237	EIF3B	8662	2
ILMN_176	EIF4EBP1	1978	2
ILMN_237	EIF4G1	1981	2
ILMN_178	EIF6	3692	2
ILMN_169	ELK3	2004	2
ILMN_165	ELL2	22936	2
ILMN_179	ELOVL1	64834	2
ILMN_179	EMG1	10436	2
ILMN_172	EML1	2009	2
ILMN_180	EMP1	2012	2
ILMN_176	EMP3	2014	2
ILMN_177	ENC1	8507	2
ILMN_180	ENOSF1	55556	2
ILMN_169	EPHB1	2047	2
ILMN_236	EPHB2	2048	2

ILMN_2377	ERCC1	2067	2
ILMN_1665	ERRFI1	54206	2
ILMN_2212	ESM1	11082	2
ILMN_1720	EVC	2121	2
ILMN_1697	EWSR1	2130	2
ILMN_1673	EXO1	9156	2
ILMN_2402	EXOSC10	5394	2
ILMN_1697	EXOSC2	23404	2
ILMN_1659	EXOSC5	56915	2
ILMN_1756	EXOSC8	11340	2
ILMN_2129	EXT1	2131	2
ILMN_1652	EZH2	2146	2
ILMN_1742	F2R	2149	2
ILMN_2129	F3	2152	2
ILMN_2136	FABP3	2170	2
ILMN_3266	FABP5L2	729163	2
ILMN_1758	FADD	8772	2
ILMN_2075	FADS2	9415	2
ILMN_1775	FAIM3	9214	2
ILMN_1714	FAM101B	359845	2
ILMN_2049	FAM119A	151194	2
ILMN_2189	FAM122B	159090	2
ILMN_1773	FAM173A	65990	2
ILMN_1691	FAM173B	134145	2
ILMN_3237	FAM175A	84142	2
ILMN_3194	FAM176A	84141	2
ILMN_1735	FAM181B	220382	2
ILMN_1808	FAM36A	116228	2
ILMN_1752	FAM38A	9780	2
ILMN_1706	FAM43A	131583	2
ILMN_1808	FAM46B	115572	2
ILMN_1725	FAM50A	9130	2
ILMN_1728	FAM64A	54478	2
ILMN_2123	FAM73A	374986	2
ILMN_1781	FAM83D	81610	2
ILMN_1780	FAM86A	196483	2
ILMN_1769	FAM86B1	85002	2
ILMN_1753	FAM86C	55199	2
ILMN_3236	FAM86D	692099	2
ILMN_2235	FANCD2	2177	2
ILMN_1758	FANCG	2189	2
ILMN_1655	FANCI	55215	2
ILMN_2232	FAP	2191	2
ILMN_1793	FARS2	10667	2
ILMN_1778	FARSA	2193	2
ILMN_1784	FASN	2194	2
ILMN_1783	FBN1	2200	2

ILMN_1688	FBXL2	25827	2
ILMN_1795	FBXL6	26233	2
ILMN_1652	FBXO32	114907	2
ILMN_1710	FBXO5	26271	2
ILMN_2275	FCAR	2204	2
ILMN_1741	FDFT1	2222	2
ILMN_1804	FDPS	2224	2
ILMN_1744	FDX1L	112812	2
ILMN_1755	FEN1	2237	2
ILMN_1810	FER1L3	26509	2
ILMN_2105	FGF2	2247	2
ILMN_2355	FHL2	2274	2
ILMN_1761	FHOD3	80206	2
ILMN_1657	FIBP	9158	2
ILMN_1746	FJX1	24147	2
ILMN_1787	FKBP11	51303	2
ILMN_2150	FKBP14	55033	2
ILMN_2089	FKBP9L	360132	2
ILMN_1737	FLII	2314	2
ILMN_2072	FLJ12684	79584	2
ILMN_1697	FLJ14213	79899	2
ILMN_1763	FLJ20718	55027	2
ILMN_1763	FLJ35258	284297	2
ILMN_3181	FLJ36131	338999	2
ILMN_2041	FLJ40504	284085	2
ILMN_2230	FLJ44124	641737	2
ILMN_1769	FLRT2	23768	2
ILMN_1734	FNDC1	84624	2
ILMN_1730	FOLR3	2352	2
ILMN_1771	FOSL1	8061	2
ILMN_1738	FOXC1	2296	2
ILMN_2344	FOXM1	2305	2
ILMN_1669	FOXQ1	94234	2
ILMN_1806	FRAS1	80144	2
ILMN_1756	FREQ	23413	2
ILMN_2330	FRMD6	122786	2
ILMN_2201	FSTL1	11167	2
ILMN_1730	FSTL3	10272	2
ILMN_2134	FTHL11	2503	2
ILMN_2173	FTHL3	2498	2
ILMN_1776	FUBP1	8880	2
ILMN_2306	FUS	2521	2
ILMN_1704	FXYD5	53827	2
ILMN_1659	FZD6	8323	2
ILMN_1704	FZD9	8326	2
ILMN_1707	GABRA5	2558	2
ILMN_1694	GADD45A	1647	2

ILMN_1718	GADD45B	4616	2
ILMN_1651	GADD45G	10912	2
ILMN_1682	GAL	51083	2
ILMN_1735	GALNT12	79695	2
ILMN_1653	GALNT9	50614	2
ILMN_1733	GALR2	8811	2
ILMN_1679	GART	2618	2
ILMN_2211	GAS2L3	283431	2
ILMN_1779	GAS6	2621	2
ILMN_1695	GATS	352954	2
ILMN_1755	GBA	2629	2
ILMN_1789	GBE1	2632	2
ILMN_1652	GBGT1	26301	2
ILMN_1788	GCLM	2730	2
ILMN_1796	GDF5	8200	2
ILMN_1809	GINS2	51659	2
ILMN_1754	GINS3	64785	2
ILMN_1807	GINS4	84296	2
ILMN_1769	GLIPR1	11010	2
ILMN_1737	GLRX	2745	2
ILMN_2258	GLRX2	51022	2
ILMN_3247	GLRX3	10539	2
ILMN_1791	GLYCTK	132158	2
ILMN_1720	GMNN	51053	2
ILMN_2412	GMPPB	29925	2
ILMN_2216	GNA12	2768	2
ILMN_1757	GNG10	2790	2
ILMN_1673	GNG12	55970	2
ILMN_1708	GNL3L	54552	2
ILMN_1764	GNPTG	84572	2
ILMN_1789	GPC4	2239	2
ILMN_2384	GPER	2852	2
ILMN_2107	GPR1	2825	2
ILMN_2041	GPR172A	79581	2
ILMN_1748	GPR176	11245	2
ILMN_1660	GPR177	79971	2
ILMN_1682	GPRC5A	9052	2
ILMN_1815	GPS2	2874	2
ILMN_2139	GPSM2	29899	2
ILMN_2124	GREM1	26585	2
ILMN_1742	GRWD1	83743	2
ILMN_1709	GSG2	83903	2
ILMN_1683	GSS	2937	2
ILMN_2227	GSTO1	9446	2
ILMN_2355	GSTT2	653689	2
ILMN_1789	GSTT2	2953	2
ILMN_1658	GTF3A	2971	2

ILMN_177(	GTPBP6	8225	2
ILMN_1771	GTSE1	51512	2
ILMN_166:	GUCA1A	2978	2
ILMN_170:	H2AFZ	3015	2
ILMN_179:	HABP4	22927	2
ILMN_169:	HADH2	3028	2
ILMN_165-	HAPLN3	145864	2
ILMN_176:	HARS	3035	2
ILMN_317(	HAUS8	93323	2
ILMN_2121	HBEGF	1839	2
ILMN_169(	HBQ1	3049	2
ILMN_176!	HDGF	3068	2
ILMN_178:	HEATR1	55127	2
ILMN_181:	HERC2	8924	2
ILMN_169-	HES6	55502	2
ILMN_323!	HIATL2	84278	2
ILMN_237!	HIF1A	3091	2
ILMN_1751	HIST1H4H	8365	2
ILMN_170:	HJURP	55355	2
ILMN_175:	HKDC1	80201	2
ILMN_221!	HMGB2	3148	2
ILMN_165:	HMGCR	3156	2
ILMN_179:	HMGCS1	3157	2
ILMN_240!	HMMR	3161	2
ILMN_238-	HN1	51155	2
ILMN_166:	HNRNPA1	3178	2
ILMN_1761	HNRNPA3	220988	2
ILMN_1751	HNRNPD	3184	2
ILMN_238!	HNRNPL	3191	2
ILMN_319:	HNRNPM	4670	2
ILMN_317:	HNRNPR	10236	2
ILMN_177:	HRAS	3265	2
ILMN_180!	HRIHFB212	11078	2
ILMN_219:	HRK	8739	2
ILMN_169:	HS3ST3A1	9955	2
ILMN_166:	HSBP1	3281	2
ILMN_1671	HSD17B7	51478	2
ILMN_1671	HSPB2	3316	2
ILMN_220(	HSPB7	27129	2
ILMN_170-	HSPC111	51491	2
ILMN_170(	HSPC171	29100	2
ILMN_209:	HSPE1	3336	2
ILMN_171:	HSPH1	10808	2
ILMN_167(	HTRA1	5654	2
ILMN_170(	HYI	81888	2
ILMN_173:	IARS	3376	2
ILMN_221:	ICAM3	3385	2

ILMN_169	IDH3A	3419	2
ILMN_175	IDI1	3422	2
ILMN_205	IFI27	3429	2
ILMN_172	IFI44L	10964	2
ILMN_223	IFIT3	3437	2
ILMN_174	IFRD2	7866	2
ILMN_181	IFT57	55081	2
ILMN_180	IGF2BP3	10643	2
ILMN_172	IGFBP2	3485	2
ILMN_174	IGFBP3	3486	2
ILMN_206	IGFBP7	3490	2
ILMN_172	IKBKB	3551	2
ILMN_170	IKBKG	8517	2
ILMN_167	IL12A	3592	2
ILMN_168	IL13RA2	3598	2
ILMN_177	IL32	9235	2
ILMN_169	IL6	3569	2
ILMN_234	IL7R	3575	2
ILMN_169	ILF3	3609	2
ILMN_168	ILKAP	80895	2
ILMN_215	IMP4	92856	2
ILMN_169	IMPAD1	54928	2
ILMN_324	INO80	54617	2
ILMN_179	INSIG1	3638	2
ILMN_175	INTS3	65123	2
ILMN_179	IPO4	79711	2
ILMN_216	IPO5	3843	2
ILMN_173	IPPK	64768	2
ILMN_237	IRAK1	3654	2
ILMN_174	IRAK2	3656	2
ILMN_208	IRS2	8660	2
ILMN_205	ISG15	9636	2
ILMN_180	ITGA1	3672	2
ILMN_240	ITGA11	22801	2
ILMN_179	ITGA5	3678	2
ILMN_171	ITGB1	3688	2
ILMN_166	ITGB1BP1	9270	2
ILMN_231	ITGB5	3693	2
ILMN_240	ITPA	3704	2
ILMN_181	ITPR3	3710	2
ILMN_239	IVNS1ABP	10625	2
ILMN_179	JAK1	3716	2
ILMN_168	JMJD8	339123	2
ILMN_168	JUB	84962	2
ILMN_178	KAT2A	2648	2
ILMN_173	KATNB1	10300	2
ILMN_171	KCNB1	3745	2

ILMN_1665	KIAA0020	9933	2
ILMN_2153	KIAA0090	23065	2
ILMN_2285	KIAA0101	9768	2
ILMN_3248	KIAA0114	57291	2
ILMN_1728	KIAA0196	9897	2
ILMN_1697	KIAA0258	9827	2
ILMN_1810	KIAA0367	23273	2
ILMN_1770	KIAA0664	23277	2
ILMN_1784	KIAA1688	80728	2
ILMN_1675	KIDINS220	57498	2
ILMN_2143	KIF11	3832	2
ILMN_1808	KIF14	9928	2
ILMN_2132	KIF18A	81930	2
ILMN_1796	KIF1C	10749	2
ILMN_1695	KIF20A	10112	2
ILMN_1712	KIF20B	9585	2
ILMN_1685	KIF2C	11004	2
ILMN_1795	KIF4A	24137	2
ILMN_2222	KIFC1	3833	2
ILMN_1735	KLF2	10365	2
ILMN_3251	KLHL28	54813	2
ILMN_1663	KLK3	354	2
ILMN_1730	KMO	8564	2
ILMN_1732	KNTC1	9735	2
ILMN_1721	KPNA2	3838	2
ILMN_1703	KPNB1	3837	2
ILMN_1666	KRT17	3872	2
ILMN_3195	KRT17P3	729682	2
ILMN_3263	KRT18P13	392371	2
ILMN_2163	KRT7	3855	2
ILMN_1753	KRT8	3856	2
ILMN_2366	KRT80	144501	2
ILMN_1801	KRT81	3887	2
ILMN_2178	KRT86	3892	2
ILMN_2339	KTN1	3895	2
ILMN_1765	LACTB	114294	2
ILMN_1782	LAD1	3898	2
ILMN_2140	LAMA4	3910	2
ILMN_1653	LAMC2	3918	2
ILMN_1782	LAMP1	3916	2
ILMN_1708	LANCL2	55915	2
ILMN_2392	LARP7	51574	2
ILMN_1662	LCP1	3936	2
ILMN_2053	LDLR	3949	2
ILMN_2207	LEP	3952	2
ILMN_1664	LEPRE1	64175	2
ILMN_1710	LETM1	3954	2

ILMN_1714	LETM2	137994	2
ILMN_1723	LGALS1	3956	2
ILMN_1747	LHFPL2	10184	2
ILMN_1738	LIF	3976	2
ILMN_1704	LIMA1	51474	2
ILMN_1797	LIMK1	3984	2
ILMN_1754	LMCD1	29995	2
ILMN_1737	LMNA	4000	2
ILMN_2126	LMNB1	4001	2
ILMN_1708	LMNB2	84823	2
ILMN_1703	LMO4	8543	2
ILMN_1785	LMOD3	56203	2
ILMN_3179	LOC100128	1E+08	2
ILMN_3187	LOC100128	1E+08	2
ILMN_3260	LOC100128	1E+08	2
ILMN_3235	LOC100128	1E+08	2
ILMN_3255	LOC100128	1E+08	2
ILMN_3262	LOC100128	1E+08	2
ILMN_3263	LOC100128	1E+08	2
ILMN_3191	LOC100128	1E+08	2
ILMN_3238	LOC100129	1E+08	2
ILMN_3264	LOC100129	1E+08	2
ILMN_3265	LOC100129	1E+08	2
ILMN_3179	LOC100129	1E+08	2
ILMN_3254	LOC100129	1E+08	2
ILMN_3268	LOC100129	1E+08	2
ILMN_3182	LOC100129	1E+08	2
ILMN_3258	LOC100130	1E+08	2
ILMN_3272	LOC100130	1E+08	2
ILMN_3261	LOC100130	1E+08	2
ILMN_3231	LOC100130	1E+08	2
ILMN_3258	LOC100130	1E+08	2
ILMN_3231	LOC100131	1E+08	2
ILMN_3215	LOC100131	1E+08	2
ILMN_3245	LOC100132	1E+08	2
ILMN_3239	LOC100132	1E+08	2
ILMN_3237	LOC100132	1E+08	2
ILMN_3205	LOC100132	1E+08	2
ILMN_3287	LOC100133	1E+08	2
ILMN_3246	LOC100133	1E+08	2
ILMN_3203	LOC100133	1E+08	2
ILMN_3237	LOC100134	1E+08	2
ILMN_3294	LOC100190	1E+08	2
ILMN_3246	LOC100190	1E+08	2
ILMN_3214	LOC128192	128192	2
ILMN_2205	LOC134997	134997	2
ILMN_3244	LOC148413	148413	2

ILMN_177(	LOC148915	148915	2
ILMN_1767	LOC158301	158301	2
ILMN_169:	LOC205251	205251	2
ILMN_320(	LOC255167	255167	2
ILMN_176(	LOC283050	283050	2
ILMN_171(	LOC283932	283932	2
ILMN_327:	LOC340274	340274	2
ILMN_167-	LOC387841	387841	2
ILMN_323:	LOC388796	388796	2
ILMN_321(	LOC389049	389049	2
ILMN_329-	LOC389765	389765	2
ILMN_329:	LOC391532	391532	2
ILMN_174(	LOC391811	391811	2
ILMN_320:	LOC392285	392285	2
ILMN_324:	LOC392871	392871	2
ILMN_328-	LOC399748	399748	2
ILMN_170:	LOC399900	399900	2
ILMN_176:	LOC399942	399942	2
ILMN_329-	LOC401098	401098	2
ILMN_168(	LOC402644	402644	2
ILMN_321:	LOC439953	439953	2
ILMN_320:	LOC440063	440063	2
ILMN_175:	LOC440132	440132	2
ILMN_176:	LOC441019	441019	2
ILMN_223:	LOC441294	441294	2
ILMN_165:	LOC442597	442597	2
ILMN_165:	LOC642031	642031	2
ILMN_327(	LOC642469	642469	2
ILMN_175-	LOC642489	642489	2
ILMN_320(	LOC642590	642590	2
ILMN_176(	LOC643319	643319	2
ILMN_181:	LOC643668	643668	2
ILMN_167:	LOC643997	643997	2
ILMN_173:	LOC644033	644033	2
ILMN_320:	LOC644214	644214	2
ILMN_176-	LOC644330	644330	2
ILMN_171:	LOC644422	644422	2
ILMN_321-	LOC644517	644517	2
ILMN_320-	LOC644563	644563	2
ILMN_167:	LOC644584	644584	2
ILMN_323(	LOC644632	644632	2
ILMN_178:	LOC644640	644640	2
ILMN_165:	LOC644689	644689	2
ILMN_167:	LOC644743	644743	2
ILMN_172-	LOC644852	644852	2
ILMN_329(	LOC644877	644877	2
ILMN_328:	LOC644879	644879	2

ILMN_320	LOC645094	645094	2
ILMN_323	LOC645166	645166	2
ILMN_321	LOC645175	645175	2
ILMN_172	LOC645236	645236	2
ILMN_323	LOC645332	645332	2
ILMN_321	LOC645452	645452	2
ILMN_167	LOC645553	645553	2
ILMN_171	LOC645895	645895	2
ILMN_170	LOC646345	646345	2
ILMN_319	LOC646347	646347	2
ILMN_169	LOC646723	646723	2
ILMN_170	LOC646817	646817	2
ILMN_170	LOC647000	647000	2
ILMN_165	LOC647322	647322	2
ILMN_178	LOC647389	647389	2
ILMN_320	LOC647597	647597	2
ILMN_168	LOC647954	647954	2
ILMN_166	LOC648024	648024	2
ILMN_171	LOC648526	648526	2
ILMN_172	LOC648638	648638	2
ILMN_167	LOC648852	648852	2
ILMN_320	LOC649553	649553	2
ILMN_166	LOC649604	649604	2
ILMN_171	LOC649970	649970	2
ILMN_167	LOC650128	650128	2
ILMN_166	LOC650152	650152	2
ILMN_175	LOC650494	650494	2
ILMN_328	LOC650515	650515	2
ILMN_178	LOC650832	650832	2
ILMN_172	LOC651816	651816	2
ILMN_181	LOC652545	652545	2
ILMN_170	LOC652595	652595	2
ILMN_180	LOC652826	652826	2
ILMN_179	LOC652846	652846	2
ILMN_172	LOC652903	652903	2
ILMN_165	LOC653113	653113	2
ILMN_172	LOC653147	653147	2
ILMN_165	LOC653158	653158	2
ILMN_177	LOC653377	653377	2
ILMN_177	LOC653505	653505	2
ILMN_177	LOC653874	653874	2
ILMN_165	LOC653884	653884	2
ILMN_180	LOC653888	653888	2
ILMN_171	LOC727761	727761	2
ILMN_321	LOC727803	727803	2
ILMN_323	LOC727980	727980	2
ILMN_321	LOC728263	728263	2

ILMN_1718	LOC728499	728499	2
ILMN_1790	LOC728556	728556	2
ILMN_3232	LOC728620	728620	2
ILMN_3223	LOC728666	728666	2
ILMN_2134	LOC728758	728758	2
ILMN_3305	LOC728809	728809	2
ILMN_3244	LOC728877	728877	2
ILMN_3236	LOC728908	728908	2
ILMN_3227	LOC729009	729009	2
ILMN_3239	LOC729057	729057	2
ILMN_3298	LOC729120	729120	2
ILMN_3239	LOC729375	729375	2
ILMN_3299	LOC729406	729406	2
ILMN_3306	LOC729535	729535	2
ILMN_3302	LOC729774	729774	2
ILMN_3232	LOC729816	729816	2
ILMN_3305	LOC729970	729970	2
ILMN_1728	LOC730273	730273	2
ILMN_3241	LOC730278	730278	2
ILMN_3237	LOC730313	730313	2
ILMN_1689	LOC730534	730534	2
ILMN_1808	LOC731049	731049	2
ILMN_1785	LOC731314	731314	2
ILMN_3227	LOC731542	731542	2
ILMN_3235	LOC731751	731751	2
ILMN_1873	LOC731895	731895	2
ILMN_1754	LOC85389	85389	2
ILMN_3224	LOC92755	92755	2
ILMN_2052	LOH3CR2A	29931	2
ILMN_1695	LOX	4015	2
ILMN_2179	LOXL4	84171	2
ILMN_1651	LPP	4026	2
ILMN_1652	LRRC17	10234	2
ILMN_2129	LRRC32	2615	2
ILMN_2214	LRRFIP1	9208	2
ILMN_2376	LTB	4050	2
ILMN_3248	LTBP2	4053	2
ILMN_1805	LTV1	84946	2
ILMN_1790	LUM	4060	2
ILMN_1724	LY96	23643	2
ILMN_2221	LYAR	55646	2
ILMN_1693	LYPD6B	130576	2
ILMN_1764	LYPLA2	11313	2
ILMN_1724	LYSMD2	256586	2
ILMN_1777	MAD2L1	4085	2
ILMN_1721	MAGT1	84061	2
ILMN_1730	MALT1	10892	2

ILMN_167	MAMDC2	256691	2
ILMN_168	MAMLD1	10046	2
ILMN_174	MAPK13	5603	2
ILMN_173	MAPKAPK3	7867	2
ILMN_178	Mar-04	57574	2
ILMN_179	MARS	4141	2
ILMN_166	MATN3	4148	2
ILMN_180	MAX	4149	2
ILMN_174	MCAT	27349	2
ILMN_176	MCCC1	56922	2
ILMN_241	MCM10	55388	2
ILMN_168	MCM2	4171	2
ILMN_180	MCM3	4172	2
ILMN_241	MCM4	4173	2
ILMN_181	MCM5	4174	2
ILMN_170	MCM7	4176	2
ILMN_176	MCOLN1	57192	2
ILMN_166	MCOLN2	255231	2
ILMN_204	ME2	4200	2
ILMN_177	MED20	9477	2
ILMN_324	MEGF6	1953	2
ILMN_221	MELK	9833	2
ILMN_174	MEMO1	51072	2
ILMN_178	METAP1	23173	2
ILMN_178	METT11D1	64745	2
ILMN_330	METTL1	4234	2
ILMN_323	METTL12	751071	2
ILMN_165	METTL3	56339	2
ILMN_176	MFAP4	4239	2
ILMN_173	MFAP5	8076	2
ILMN_178	MFSD1	64747	2
ILMN_167	MFSD10	10227	2
ILMN_171	MFSD3	113655	2
ILMN_330	MGC11082	84777	2
ILMN_181	MGC24103	158295	2
ILMN_175	MGC3731	79159	2
ILMN_173	MGC39900	286527	2
ILMN_174	MGC4294	79160	2
ILMN_215	MGC72080	389538	2
ILMN_173	MGLL	11343	2
ILMN_178	MICAL2	9645	2
ILMN_181	MICALL1	85377	2
ILMN_330	MIR1228	1E+08	2
ILMN_324	MIR155HG	114614	2
ILMN_331	MIR586	693171	2
ILMN_173	MKI67	4288	2
ILMN_178	MKI67IP	84365	2

ILMN_227	MKKS	8195	2
ILMN_167	MLF1IP	79682	2
ILMN_180	MMACHC	25974	2
ILMN_214	MND1	84057	2
ILMN_175	MORN2	378464	2
ILMN_179	MOSC1	64757	2
ILMN_168	MOXD1	26002	2
ILMN_207	MPDU1	9526	2
ILMN_170	MPP4	58538	2
ILMN_167	MPRIP	23164	2
ILMN_165	MRLC2	103910	2
ILMN_169	MRPL11	65003	2
ILMN_169	MRPL12	6182	2
ILMN_218	MRPL20	55052	2
ILMN_234	MRPL21	219927	2
ILMN_166	MRPL22	29093	2
ILMN_180	MRPL23	6150	2
ILMN_239	MRPL24	79590	2
ILMN_172	MRPL33	9553	2
ILMN_171	MRPL52	122704	2
ILMN_165	MRPL54	116541	2
ILMN_172	MRPS11	64963	2
ILMN_177	MRPS16	51021	2
ILMN_218	MRPS35	60488	2
ILMN_241	MRRF	92399	2
ILMN_168	MRTO4	51154	2
ILMN_174	MSC	9242	2
ILMN_165	MSN	4478	2
ILMN_222	MSRA	4482	2
ILMN_233	MSRB3	253827	2
ILMN_170	MSTO1	55154	2
ILMN_169	MT1A	4489	2
ILMN_171	MT1G	4495	2
ILMN_165	MT1M	4499	2
ILMN_168	MT2A	4502	2
ILMN_177	MTG1	92170	2
ILMN_167	MTHFD2	10797	2
ILMN_325	MTMR10	54893	2
ILMN_217	MTRF1L	54516	2
ILMN_176	MUM1	84939	2
ILMN_165	MVD	4597	2
ILMN_171	MXD3	83463	2
ILMN_168	MYC	4609	2
ILMN_221	MYCN	4613	2
ILMN_208	MYH9	4627	2
ILMN_167	MYL12A	10627	2
ILMN_232	MYO1C	4641	2

ILMN_1808	MYO5C	55930	2
ILMN_1672	MYO9B	4650	2
ILMN_2315	N6AMT1	29104	2
ILMN_1809	NACC2	138151	2
ILMN_1716	NAGK	55577	2
ILMN_1675	NAGPA	51172	2
ILMN_1815	NANS	54187	2
ILMN_1703	NAV1	89796	2
ILMN_2399	NAV2	89797	2
ILMN_1775	NCAPD2	9918	2
ILMN_1751	NCAPG	64151	2
ILMN_1777	NCBP1	4686	2
ILMN_3237	NCLN	56926	2
ILMN_1664	NDC80	10403	2
ILMN_1807	NDST1	3340	2
ILMN_2175	NDUFA11	126328	2
ILMN_1760	NDUFA9	4704	2
ILMN_1682	NDUFAF2	91942	2
ILMN_2117	NDUFB2	4708	2
ILMN_1763	NDUFB6	4712	2
ILMN_1705	NEFH	4744	2
ILMN_1757	NEIL3	55247	2
ILMN_1653	NEK2	4751	2
ILMN_1760	NETO2	81831	2
ILMN_1783	NEXN	91624	2
ILMN_1671	NF2	4771	2
ILMN_1717	NFKBIE	4794	2
ILMN_1716	NGF	4803	2
ILMN_3231	NHP2	55651	2
ILMN_1704	NIP7	51388	2
ILMN_1805	NIPSNAP1	8508	2
ILMN_1813	NKAIN4	128414	2
ILMN_2330	NKTR	4820	2
ILMN_2075	NLRP8	126205	2
ILMN_1741	NME1	4830	2
ILMN_1784	NME5	8382	2
ILMN_2369	NME7	29922	2
ILMN_1715	NNMT	4837	2
ILMN_1792	NOC2L	26155	2
ILMN_2187	NOC3L	64318	2
ILMN_1703	NOC4L	79050	2
ILMN_2320	NOL6	65083	2
ILMN_1803	NOL7	51406	2
ILMN_1723	NOP2	4839	2
ILMN_1787	NOP56	10528	2
ILMN_1748	NOP58	51602	2
ILMN_1787	NOV	4856	2

ILMN_173[illegible]	NOX4	50507	2
ILMN_217[illegible]	NP	4860	2
ILMN_172[illegible]	NPEPL1	79716	2
ILMN_211[illegible]	NPM3	10360	2
ILMN_176[illegible]	NPPB	4879	2
ILMN_168[illegible]	NPTX2	4885	2
ILMN_168[illegible]	NPTXR	23467	2
ILMN_213[illegible]	NR2C2AP	126382	2
ILMN_169[illegible]	NSDHL	50814	2
ILMN_168[illegible]	NSUN2	54888	2
ILMN_168[illegible]	NT5C2	22978	2
ILMN_169[illegible]	NT5E	4907	2
ILMN_180[illegible]	NTF3	4908	2
ILMN_179[illegible]	NTM	50863	2
ILMN_168[illegible]	NUAK1	9891	2
ILMN_209[illegible]	NUDC	10726	2
ILMN_181[illegible]	NUP107	57122	2
ILMN_171[illegible]	NUP188	23511	2
ILMN_181[illegible]	NUP35	129401	2
ILMN_166[illegible]	NUP85	79902	2
ILMN_173[illegible]	NUP88	4927	2
ILMN_172[illegible]	NUSAP1	51203	2
ILMN_165[illegible]	NUTF2	10204	2
ILMN_235[illegible]	NXF1	10482	2
ILMN_166[illegible]	OAF	220323	2
ILMN_178[illegible]	OBFC2A	64859	2
ILMN_177[illegible]	OCIAD2	132299	2
ILMN_174[illegible]	ODC1	4953	2
ILMN_233[illegible]	ODZ3	55714	2
ILMN_171[illegible]	OGFRL1	79627	2
ILMN_175[illegible]	OIP5	11339	2
ILMN_207[illegible]	OR2A1	346528	2
ILMN_172[illegible]	ORAI1	84876	2
ILMN_176[illegible]	ORAOV1	220064	2
ILMN_175[illegible]	OSGEP	55644	2
ILMN_219[illegible]	OSR1	130497	2
ILMN_181[illegible]	OXCT1	5019	2
ILMN_180[illegible]	OXTR	5021	2
ILMN_172[illegible]	PA2G4	5036	2
ILMN_330[illegible]	PABPC1L	80336	2
ILMN_324[illegible]	PABPC4L	132430	2
ILMN_175[illegible]	PABPN1	8106	2
ILMN_172[illegible]	PAFAH1B1	5048	2
ILMN_174[illegible]	PAFAH1B3	5050	2
ILMN_179[illegible]	PAPOLA	10914	2
ILMN_172[illegible]	PAPPA	5069	2
ILMN_241[illegible]	PAPSS2	9060	2

ILMN_1654	PARD6A	50855	2
ILMN_3238	PATE3	1E+08	2
ILMN_1806	PAWR	5074	2
ILMN_1673	PBK	55872	2
ILMN_1723	PBRM1	55193	2
ILMN_1710	PCDH7	5099	2
ILMN_1788	PCID2	55795	2
ILMN_1810	PCNT	5116	2
ILMN_1695	PCSK7	9159	2
ILMN_1758	PDCD2	5134	2
ILMN_2228	PDCD5	9141	2
ILMN_1667	PDCL3	79031	2
ILMN_1698	PDF	64146	2
ILMN_1663	PDLIM4	8572	2
ILMN_1814	PDLIM7	9260	2
ILMN_1771	PEA15	8682	2
ILMN_1717	PEPD	5184	2
ILMN_1753	PET112L	5188	2
ILMN_1755	PFAS	5198	2
ILMN_1661	PFDN6	10471	2
ILMN_1712	PFN1	5216	2
ILMN_1788	PGAM5	192111	2
ILMN_2216	PGK1	5230	2
ILMN_1790	PHACTR2	9749	2
ILMN_1692	PHB	5245	2
ILMN_1666	PHLDB1	23187	2
ILMN_1750	PI4K2A	55361	2
ILMN_2373	PICK1	9463	2
ILMN_1795	PIGM	93183	2
ILMN_1725	PIN4	5303	2
ILMN_3236	PIP4K2A	5305	2
ILMN_1793	PISD	23761	2
ILMN_2052	PKD2	5311	2
ILMN_1766	PKMYT1	9088	2
ILMN_1746	PLA2G3	50487	2
ILMN_1810	PLA2G4C	8605	2
ILMN_1738	PLAT	5327	2
ILMN_1656	PLAU	5328	2
ILMN_1691	PLAUR	5329	2
ILMN_1744	PLEC1	5339	2
ILMN_1706	PLEKHA9	51054	2
ILMN_1736	PLK1	5347	2
ILMN_1717	PLK2	10769	2
ILMN_1789	PLK4	10733	2
ILMN_1738	PLP2	5355	2
ILMN_1703	PLSCR3	57048	2
ILMN_1791	PLXNA1	5361	2

ILMN_1734	PMEPA1	56937	2
ILMN_1774	PNKD	25953	2
ILMN_1790	PNMA2	10687	2
ILMN_1753	PNO1	56902	2
ILMN_1684	PNPO	55163	2
ILMN_1810	PNPT1	87178	2
ILMN_1770	PODN	127435	2
ILMN_2276	POFUT1	23509	2
ILMN_1696	POLA2	23649	2
ILMN_1652	POLD1	5424	2
ILMN_3305	POLD2	5425	2
ILMN_1743	POLDIP2	26073	2
ILMN_1774	POLE2	5427	2
ILMN_1660	POLE4	56655	2
ILMN_1740	POLQ	10721	2
ILMN_1746	POLR1C	9533	2
ILMN_1657	POLR2J	5439	2
ILMN_1670	POLR2L	5441	2
ILMN_3241	POLR3E	55718	2
ILMN_1786	POLR3H	171568	2
ILMN_1768	POP1	10940	2
ILMN_1687	POP5	51367	2
ILMN_1798	PPAN	56342	2
ILMN_3236	PPIAL4A	164022	2
ILMN_1669	PPIC	5480	2
ILMN_2054	PPIL1	51645	2
ILMN_1806	PPL	5493	2
ILMN_1695	PPP1CA	5499	2
ILMN_1747	PPP1R11	6992	2
ILMN_1685	PPP1R12C	54776	2
ILMN_1669	PPP1R13L	10848	2
ILMN_1659	PPP1R14B	26472	2
ILMN_1664	PPP1R14C	81706	2
ILMN_1736	PPP1R3C	5507	2
ILMN_1724	PPP4R1	9989	2
ILMN_1737	PPPDE2	27351	2
ILMN_1814	PQLC3	130814	2
ILMN_1728	PRC1	9055	2
ILMN_2395	PRDX3	10935	2
ILMN_2179	PRELID1	27166	2
ILMN_2210	PRIM1	5557	2
ILMN_1797	PRKAG2	51422	2
ILMN_1674	PRKAR1B	5575	2
ILMN_1771	PRKCA	5578	2
ILMN_1793	PRKCDBP	112464	2
ILMN_1785	PRKD1	5587	2
ILMN_1769	PRKDC	5591	2

ILMN_240	PRMT5	10419	2
ILMN_171	PROCR	10544	2
ILMN_176	PRPF19	27339	2
ILMN_166	PRPS1	5631	2
ILMN_178	PRR11	55771	2
ILMN_179	PRSS23	11098	2
ILMN_166	PSMB6	5694	2
ILMN_180	PSMC3	5702	2
ILMN_239	PSMC4	5704	2
ILMN_178	PSMC5	5705	2
ILMN_171	PSMD2	5708	2
ILMN_177	PSMD6	9861	2
ILMN_173	PSMD8	5714	2
ILMN_234	PSME3	10197	2
ILMN_176	PSME4	23198	2
ILMN_165	PSMG1	8624	2
ILMN_179	PSPC1	55269	2
ILMN_167	PSRC1	84722	2
ILMN_168	PTDSS1	9791	2
ILMN_179	PTGER4	5734	2
ILMN_171	PTGES	9536	2
ILMN_166	PTGIS	5740	2
ILMN_172	PTPLA	9200	2
ILMN_173	PTPRE	5791	2
ILMN_167	PTPRR	5801	2
ILMN_175	PTRF	284119	2
ILMN_176	PTRH1	138428	2
ILMN_231	PTRH2	51651	2
ILMN_175	PTTG1	9232	2
ILMN_204	PTTG3P	26255	2
ILMN_180	PTX3	5806	2
ILMN_166	PUS1	80324	2
ILMN_177	PUS7	54517	2
ILMN_236	PXDN	7837	2
ILMN_215	PXDNL	137902	2
ILMN_179	PXMP2	5827	2
ILMN_178	QSOX2	169714	2
ILMN_178	QTRT1	81890	2
ILMN_166	RAB31	11031	2
ILMN_211	RAB32	10981	2
ILMN_174	RABEPK	10244	2
ILMN_207	RACGAP1	29127	2
ILMN_175	RAD50	10111	2
ILMN_167	RAD51AP1	10635	2
ILMN_165	RAD54L	8438	2
ILMN_174	RAGE	5891	2
ILMN_330	RAN	5901	2

ILMN_210	RANBP1	5902	2
ILMN_166	RANGAP1	5905	2
ILMN_173	RASSF7	8045	2
ILMN_176	RBM25	58517	2
ILMN_179	RBM28	55131	2
ILMN_169	RBM3	5935	2
ILMN_241	RBM39	9584	2
ILMN_168	RBM45	129831	2
ILMN_171	RBP7	116362	2
ILMN_176	RDBP	7936	2
ILMN_181	RER1	11079	2
ILMN_174	REXO2	25996	2
ILMN_165	RFC3	5983	2
ILMN_172	RFC4	5984	2
ILMN_165	RFC5	5985	2
ILMN_171	RGMB	285704	2
ILMN_172	RGS17	26575	2
ILMN_205	RHBDL2	54933	2
ILMN_181	RNASEH2A	10535	2
ILMN_175	RND3	390	2
ILMN_175	RNF144B	255488	2
ILMN_324	RNU1A3	26871	2
ILMN_330	RNU6-1	26827	2
ILMN_331	RNU6-15	1E+08	2
ILMN_165	RPAP2	79871	2
ILMN_170	RPL13	6137	2
ILMN_179	RPL22L1	200916	2
ILMN_167	RPL28	6158	2
ILMN_173	RPL29	6159	2
ILMN_170	RPL34	6164	2
ILMN_181	RPL8	6132	2
ILMN_181	RPP40	10799	2
ILMN_217	RPS19BP1	91582	2
ILMN_180	RPS21	6227	2
ILMN_239	RPS24	6229	2
ILMN_175	RPS26	6231	2
ILMN_175	RPS6KA4	8986	2
ILMN_207	RPS7	6201	2
ILMN_168	RPUSD1	113000	2
ILMN_204	RQCD1	9125	2
ILMN_207	RRAS2	22800	2
ILMN_167	RRM2	6241	2
ILMN_176	RRP12	23223	2
ILMN_168	RRP15	51018	2
ILMN_168	RRP9	9136	2
ILMN_176	RRS1	23212	2
ILMN_168	RSPO3	84870	2

ILMN_1721	RSU1	6251	2
ILMN_2352	RTN4	57142	2
ILMN_1810	RUSC2	9853	2
ILMN_2120	RUVBL2	10856	2
ILMN_2046	S100A10	6281	2
ILMN_1750	S100A11	6282	2
ILMN_1728	S100A16	140576	2
ILMN_1725	S100A2	6273	2
ILMN_1712	S100A3	6274	2
ILMN_1688	S100A4	6275	2
ILMN_1713	S100A6	6277	2
ILMN_1657	SAE1	10055	2
ILMN_2119	SAMD4A	23034	2
ILMN_1712	SBSN	374897	2
ILMN_1655	SC65	10609	2
ILMN_3246	SCARNA10	692148	2
ILMN_3240	SCXA	1E+08	2
ILMN_2380	SDCCAG3	10807	2
ILMN_1701	SEC11C	90701	2
ILMN_1656	SEC24D	9871	2
ILMN_1708	SEH1L	81929	2
ILMN_1696	SELI	85465	2
ILMN_2154	SEMA3E	9723	2
ILMN_1696	SERP2	387923	2
ILMN_2397	SERPINB8	5271	2
ILMN_1744	SERPINE1	5054	2
ILMN_1655	SERPINE2	5270	2
ILMN_1730	SERTAD4	56256	2
ILMN_1810	SFRP4	6424	2
ILMN_1795	SFRS1	6426	2
ILMN_1742	SFRS10	6434	2
ILMN_1696	SFRS2	6427	2
ILMN_3310	SFTA1P	207107	2
ILMN_1685	SGMS2	166929	2
ILMN_1730	SGOL1	151648	2
ILMN_1679	SH2D4A	63898	2
ILMN_1743	SH3PXD2A	9644	2
ILMN_1661	SH3RF2	153769	2
ILMN_1661	SHMT2	6472	2
ILMN_1717	SIK1	150094	2
ILMN_2291	SIRT5	23408	2
ILMN_1771	SKA1	220134	2
ILMN_1665	SKP2	6502	2
ILMN_1703	SLC16A2	6567	2
ILMN_1707	SLC1A5	6510	2
ILMN_1672	SLC20A1	6574	2
ILMN_1668	SLC25A13	10165	2

ILMN_174	SLC25A14	9016	2
ILMN_166	SLC25A15	10166	2
ILMN_166	SLC25A19	60386	2
ILMN_168	SLC25A22	79751	2
ILMN_214	SLC25A43	203427	2
ILMN_173	SLC29A2	3177	2
ILMN_174	SLC2A4RG	56731	2
ILMN_177	SLC2A6	11182	2
ILMN_172	SLC2A8	29988	2
ILMN_174	SLC30A1	7779	2
ILMN_207	SLC35F2	54733	2
ILMN_165	SLC39A10	57181	2
ILMN_233	SLC43A3	29015	2
ILMN_179	SLC4A3	6508	2
ILMN_220	SLC4A7	9497	2
ILMN_172	SLC6A17	388662	2
ILMN_181	SLC7A7	9056	2
ILMN_180	SLC9A1	6548	2
ILMN_219	SLITRK4	139065	2
ILMN_212	SMG5	23381	2
ILMN_222	SMS	6611	2
ILMN_172	SMYD2	56950	2
ILMN_209	SNAPC1	6617	2
ILMN_176	SNF8	11267	2
ILMN_323	SNHG1	23642	2
ILMN_170	SNHG3-RC	751867	2
ILMN_323	SNHG9	735301	2
ILMN_324	SNORA24	677809	2
ILMN_324	SNORA6	574040	2
ILMN_324	SNORA61	677838	2
ILMN_178	SNORA65	26783	2
ILMN_324	SNORA67	26781	2
ILMN_173	SNORA70	26778	2
ILMN_324	SNORD104	692227	2
ILMN_166	SNORD16	595097	2
ILMN_207	SNORD31	9298	2
ILMN_208	SNORD68	606500	2
ILMN_324	SNORD80	26774	2
ILMN_324	SNORD83B	116938	2
ILMN_324	SNORD96A	619571	2
ILMN_177	SNRPB	6628	2
ILMN_176	SNRPD1	6632	2
ILMN_167	SNRPF	6636	2
ILMN_167	SNX5	27131	2
ILMN_240	SOD2	6648	2
ILMN_167	SPA17	53340	2
ILMN_168	SPATS2L	26010	2

ILMN_2181	SPC24	147841	2
ILMN_1814	SPC25	57405	2
ILMN_3307	SPCS3	60559	2
ILMN_1675	SPG7	6687	2
ILMN_1800	SPINT2	10653	2
ILMN_1668	SPNS3	201305	2
ILMN_1784	SPOCD1	90853	2
ILMN_1746	SPOCK1	6695	2
ILMN_2249	SPTLC1	10558	2
ILMN_2041	SQLE	6713	2
ILMN_1677	SRGAP1	57522	2
ILMN_1661	SRM	6723	2
ILMN_1798	SRPK1	6732	2
ILMN_1657	SRPK2	6733	2
ILMN_1676	SRPX2	27286	2
ILMN_1666	SRRD	402055	2
ILMN_1804	SRXN1	140809	2
ILMN_1672	SSB	6741	2
ILMN_1727	SSH1	54434	2
ILMN_1728	SSSCA1	10534	2
ILMN_2152	SSTR2	6752	2
ILMN_2350	ST5	6764	2
ILMN_2127	ST6GALNA(	256435	2
ILMN_1773	ST6GALNA(	81849	2
ILMN_3239	STAG3L3	442578	2
ILMN_2413	STIL	6491	2
ILMN_1789	STIP1	10963	2
ILMN_1668	STK25	10494	2
ILMN_1778	STK33	65975	2
ILMN_1693	STK36	27148	2
ILMN_2152	STK38	11329	2
ILMN_3244	STMN3	50861	2
ILMN_1769	STRA13	201254	2
ILMN_1653	STS-1	84959	2
ILMN_2345	SULF2	55959	2
ILMN_1753	SUMF1	285362	2
ILMN_1709	SUSD1	64420	2
ILMN_1781	SUV39H1	6839	2
ILMN_1727	SYNCRIP	10492	2
ILMN_1724	TACC3	10460	2
ILMN_1739	TACSTD2	4070	2
ILMN_1778	TAGLN	6876	2
ILMN_1691	TAGLN2	8407	2
ILMN_1759	TAP2	6891	2
ILMN_1803	TARBP1	6894	2
ILMN_2310	TARBP2	6895	2
ILMN_1803	TAX1BP3	30851	2

ILMN_176	TBC1D2	55357	2
ILMN_179	TBCB	1155	2
ILMN_172	TBCE	6905	2
ILMN_241	TBRG4	9238	2
ILMN_237	TCEB2	6923	2
ILMN_181	TCF4	6925	2
ILMN_171	TCIRG1	10312	2
ILMN_170	TCTA	6988	2
ILMN_168	TELO2	9894	2
ILMN_165	TEX10	54881	2
ILMN_169	TEX261	113419	2
ILMN_211	TFDP1	7027	2
ILMN_166	TFPI	7035	2
ILMN_167	TFRC	7037	2
ILMN_168	TGFB3	7043	2
ILMN_166	TGFBI	7045	2
ILMN_172	TGM1	7051	2
ILMN_170	TGM2	7052	2
ILMN_166	TH1L	51497	2
ILMN_181	THADA	63892	2
ILMN_168	THBS1	7057	2
ILMN_167	THBS2	7058	2
ILMN_180	THBS3	7059	2
ILMN_180	THOC1	9984	2
ILMN_175	THOC4	10189	2
ILMN_167	THOC6	79228	2
ILMN_172	THOP1	7064	2
ILMN_177	THY1	7070	2
ILMN_173	TIMELESS	8914	2
ILMN_176	TIMM10	26519	2
ILMN_180	TK1	7083	2
ILMN_178	TLCD1	116238	2
ILMN_175	TLE1	7088	2
ILMN_170	TLN2	83660	2
ILMN_177	TM4SF1	4071	2
ILMN_216	TM4SF18	116441	2
ILMN_179	TM4SF4	7104	2
ILMN_324	TMEM106A	113277	2
ILMN_221	TMEM126A	84233	2
ILMN_174	TMEM130	222865	2
ILMN_168	TMEM139	135932	2
ILMN_177	TMEM165	55858	2
ILMN_221	TMEM17	200728	2
ILMN_175	TMEM177	80775	2
ILMN_168	TMEM198	130612	2
ILMN_174	TMEM199	147007	2
ILMN_169	TMEM20	159371	2

ILMN_169	TMEM43	79188	2
ILMN_174	TMEM48	55706	2
ILMN_174	TMEM50A	23585	2
ILMN_173	TMEM70	54968	2
ILMN_171	TMEM97	27346	2
ILMN_181	TMSB10	9168	2
ILMN_168	TMSB15A	11013	2
ILMN_324	TMSL3	7117	2
ILMN_171	TNC	3371	2
ILMN_168	TNFAIP8L1	126282	2
ILMN_166	TNFRSF10D	8793	2
ILMN_168	TNFRSF12A	51330	2
ILMN_233	TNFRSF6B	8771	2
ILMN_168	TNIK	23043	2
ILMN_180	TNNC1	7134	2
ILMN_180	TNS1	7145	2
ILMN_171	TOMM22	56993	2
ILMN_168	TOMM40	10452	2
ILMN_180	TOMM5	401505	2
ILMN_168	TOP2A	7153	2
ILMN_176	TOP3B	8940	2
ILMN_176	TOR3A	64222	2
ILMN_166	TP53BP1	7158	2
ILMN_177	TP53BP2	7159	2
ILMN_235	TP53I3	9540	2
ILMN_172	TPCN2	219931	2
ILMN_171	TPM1	7168	2
ILMN_178	TPM2	7169	2
ILMN_169	TPM3	7170	2
ILMN_174	TPMT	7172	2
ILMN_169	TPST2	8459	2
ILMN_179	TPX2	22974	2
ILMN_173	TRA2A	29896	2
ILMN_175	TRABD	80305	2
ILMN_178	TRAK1	22906	2
ILMN_178	TRAK2	66008	2
ILMN_226	TRIM13	10206	2
ILMN_181	TRIM25	7706	2
ILMN_180	TRIO	7204	2
ILMN_179	TRIP13	9319	2
ILMN_181	TRMT1	55621	2
ILMN_216	TRMT5	57570	2
ILMN_167	TRMT61A	115708	2
ILMN_170	TROAP	10024	2
ILMN_241	TSC22D1	8848	2
ILMN_212	TSC22D2	9819	2
ILMN_174	TSEN2	80746	2

ILMN_213(	TSPAN13	27075	2
ILMN_169	TSTA3	7264	2
ILMN_174	TTC13	79573	2
ILMN_239(	TTC14	151613	2
ILMN_167(	TTC26	79989	2
ILMN_175	TTC27	55622	2
ILMN_179	TTC37	9652	2
ILMN_181(	TTF2	8458	2
ILMN_178	TTK	7272	2
ILMN_175	TTLL5	23093	2
ILMN_169	TTYH3	80727	2
ILMN_174	TUBA1A	7846	2
ILMN_180(	TUBA1B	10376	2
ILMN_174	TUBA1C	84790	2
ILMN_178	TUBA4A	7277	2
ILMN_166	TUBB	203068	2
ILMN_203	TUBB2A	7280	2
ILMN_178(	TUBB2C	10383	2
ILMN_179	TUBB3	10381	2
ILMN_170	TUBB6	84617	2
ILMN_178	TUFT1	7286	2
ILMN_203	TXN	7295	2
ILMN_179	TXNDC14	51075	2
ILMN_165	TXNDC17	84817	2
ILMN_171	TXNRD1	7296	2
ILMN_165	TXNRD2	10587	2
ILMN_180	TYMS	7298	2
ILMN_174(	TYRO3	7301	2
ILMN_176	U2AF2	11338	2
ILMN_170	UACA	55075	2
ILMN_174	UAP1	6675	2
ILMN_230	UBE2C	11065	2
ILMN_178	UBE2G2	7327	2
ILMN_171	UBE2T	29089	2
ILMN_165	UBIAD1	29914	2
ILMN_179	UBQLN3	50613	2
ILMN_173	UBXN8	7993	2
ILMN_175	UCHL1	7345	2
ILMN_166(	UCHL3	7347	2
ILMN_176	UCK2	7371	2
ILMN_173	UGCG	7357	2
ILMN_239	UPF3B	65109	2
ILMN_174	UQCR	10975	2
ILMN_168(	USP49	25862	2
ILMN_209	UTP14A	10813	2
ILMN_168	VCAN	1462	2
ILMN_175	VGF	7425	2

ILMN_1704	VPS29	51699	2
ILMN_1805	VRK1	7443	2
ILMN_1752	VWF	7450	2
ILMN_1727	WARS	7453	2
ILMN_1697	WBSCR22	114049	2
ILMN_1675	WDR1	9948	2
ILMN_1685	WDR34	89891	2
ILMN_1789	WDR35	57539	2
ILMN_1656	WDR4	10785	2
ILMN_1671	WDR43	23160	2
ILMN_1756	WDR45	11152	2
ILMN_2212	WDR46	9277	2
ILMN_1780	WDR51A	25886	2
ILMN_1678	WDR55	54853	2
ILMN_1793	WDR60	55112	2
ILMN_1665	WDR61	80349	2
ILMN_1809	WDR74	54663	2
ILMN_1742	WDR77	79084	2
ILMN_1662	WDR92	116143	2
ILMN_1800	WNT5A	7474	2
ILMN_1658	WWC1	23286	2
ILMN_1755	XPO6	23214	2
ILMN_2204	XRCC2	7516	2
ILMN_1766	YARS	8565	2
ILMN_1694	YWHAB	7529	2
ILMN_2335	ZC3H14	79882	2
ILMN_2362	ZDHHC16	84287	2
ILMN_2046	ZDHHC6	64429	2
ILMN_1808	ZFHX3	463	2
ILMN_1675	ZFP36L1	677	2
ILMN_1726	ZNF135	7694	2
ILMN_1753	ZNF259	8882	2
ILMN_1706	ZNF271	10778	2
ILMN_1794	ZNF469	84627	2
ILMN_2176	ZNF69	7620	2
ILMN_1789	ZNF789	285989	2
ILMN_2190	ZNF83	55769	2
ILMN_1809	ZSCAN16	80345	2
ILMN_2371	ZYX	7791	2

Gene Ontology terms derived from comparing gene expression data of RPE seeded at 20000 cells/cm2 in tl

ID	up.FDR	dn.FDR	mx.FDR	term	ontology
GO:190161	2.93E-12	1	0.00017	organic hydroxy compound metabolic process	BP
GO:004428	4.42E-11	1	0.002263	small molecule catabolic process	BP
GO:001605	1.12E-08	1	0.009777	organic acid catabolic process	BP
GO:004639	1.12E-08	1	0.009777	carboxylic acid catabolic process	BP
GO:000906	1.58E-08	1	0.037714	cellular amino acid catabolic process	BP
GO:000705	2.00E-07	1	0.258102	chromosome segregation	BP
GO:000706	2.77E-07	1	0.079368	mitotic nuclear division	BP
GO:000606	4.39E-07	1	0.009254	alcohol metabolic process	BP
GO:190161	9.79E-06	1	0.082887	organic hydroxy compound catabolic process	BP
GO:19016C	1.41E-05	1	0.145533	alpha-amino acid catabolic process	BP
GO:007182	1.43E-05	1	0.043816	protein-lipid complex subunit organization	BP
GO:001974	2.32E-05	1	3.52E-07	secondary metabolic process	BP
GO:003111	3.23E-05	1	0.11038	regulation of microtubule polymerization or dep	BP
GO:00343C	3.61E-05	1	2.62E-05	primary alcohol metabolic process	BP
GO:005095	4.08E-05	1	0.071441	sensory perception of light stimulus	BP
GO:000908	4.16E-05	1	0.058766	branched-chain amino acid catabolic process	BP
GO:190161	4.32E-05	1	0.002931	organic hydroxy compound biosynthetic process	BP
GO:004616	4.81E-05	1	0.085481	alcohol catabolic process	BP
GO:007182	4.88E-05	1	0.047132	plasma lipoprotein particle organization	BP
GO:00076C	5.31E-05	1	0.059793	visual perception	BP
GO:000245	6.08E-05	1	0.046003	humoral immune response mediated by circulati	BP
GO:00705C	6.36E-05	1	0.054153	regulation of microtubule cytoskeleton organizat	BP
GO:000657	6.49E-05	1	0.012817	cellular modified amino acid metabolic process	BP
GO:003433	7.70E-05	1	0.010312	cell junction maintenance	BP
GO:004244	9.10E-05	1	0.019981	pigment metabolic process	BP
GO:005118	9.10E-05	1	0.154509	cofactor metabolic process	BP
GO:004369	9.32E-05	1	0.015928	reverse cholesterol transport	BP
GO:004428	9.49E-05	1	0.00213	small molecule biosynthetic process	BP
GO:00970C	0.000103	1	0.097365	regulation of plasma lipoprotein particle levels	BP
GO:00311C	0.000113	1	0.240483	microtubule polymerization or depolymerization	BP
GO:000007	0.000118	1	0.250392	mitotic sister chromatid segregation	BP
GO:004395	0.000152	1	0.438828	cellular component maintenance	BP
GO:005087	0.000156	1	0.006572	brown fat cell differentiation	BP
GO:000676	0.000215	1	0.013412	vitamin metabolic process	BP
GO:000673	0.000222	1	0.151493	coenzyme metabolic process	BP
GO:004478	0.000225	1	0.503954	cilium organization	BP
GO:003288	0.000236	1	0.047584	regulation of microtubule-based process	BP
GO:19016C	0.000257	1	0.007444	alpha-amino acid metabolic process	BP
GO:002261	0.000268	1	0.438671	DNA strand elongation	BP
GO:000701	0.000272	1	0.087457	microtubule depolymerization	BP
GO:000081	0.000305	1	0.23304	sister chromatid segregation	BP
GO:000908	0.000312	1	0.14558	branched-chain amino acid metabolic process	BP
GO:001571	0.000335	1	0.003621	organic anion transport	BP
GO:001895	0.000335	1	0.125141	phenol-containing compound metabolic process	BP
GO:004614	0.000358	1	0.053141	pigment biosynthetic process	BP

GO:000652	0.000414	1	0.006592	cellular amino acid metabolic process	BP
GO:003026	0.000453	1	0.547212	chromosome condensation	BP
GO:000631	0.000471	1	0.902242	DNA recombination	BP
GO:000682	0.000492	1	0.000414	anion transport	BP
GO:000695	0.000509	1	0.050892	complement activation, classical pathway	BP
GO:000627	0.000533	1	0.386653	DNA strand elongation involved in DNA replicatic	BP
GO:003111	0.000584	1	0.121348	negative regulation of microtubule polymerizatic	BP
GO:000009	0.000647	1	0.368923	sulfur amino acid metabolic process	BP
GO:003437	0.000721	1	0.044579	high-density lipoprotein particle remodeling	BP
GO:001605	0.000774	1	0.780692	carbohydrate catabolic process	BP
GO:003436	0.000816	1	0.017031	macromolecular complex remodeling	BP
GO:003436	0.000816	1	0.017031	protein-lipid complex remodeling	BP
GO:003436	0.000816	1	0.017031	plasma lipoprotein particle remodeling	BP
GO:000663	0.000832	1	0.017947	fatty acid metabolic process	BP
GO:004472	0.000898	1	0.739163	single-organism carbohydrate catabolic process	BP
GO:000658	0.000966	1	7.30E-05	melanin metabolic process	BP
GO:003105	0.001	1	0.310853	chromatin remodeling at centromere	BP
GO:006027	0.001062	1	0.478125	cilium morphogenesis	BP
GO:000676	0.001199	1	0.141344	water-soluble vitamin metabolic process	BP
GO:000680	0.001226	1	0.006221	xenobiotic metabolic process	BP
GO:000702	0.001226	1	0.123191	negative regulation of microtubule depolymeriza	BP
GO:007146	0.001226	1	0.006221	cellular response to xenobiotic stimulus	BP
GO:190304	0.001226	1	0.683949	meiotic cell cycle process	BP
GO:003450	0.001256	1	0.391878	centromere complex assembly	BP
GO:190137	0.001306	1	0.498682	regulation of potassium ion transmembrane tran	BP
GO:000911	0.001619	1	0.406133	purine nucleobase biosynthetic process	BP
GO:004238	0.001703	1	0.576318	cilium assembly	BP
GO:009706	0.001774	1	0.065497	cellular response to thyroid hormone stimulus	BP
GO:001604	0.001856	1	0.099453	lipid catabolic process	BP
GO:000628	0.001884	1	0.833241	DNA repair	BP
GO:000609	0.001923	1	0.950707	tricarboxylic acid cycle	BP
GO:000641	0.001923	1	1	translational termination	BP
GO:001612	0.00207	1	0.132192	sterol metabolic process	BP
GO:000609	0.002073	1	0.678514	pyruvate metabolic process	BP
GO:000610	0.002078	1	0.536971	2-oxoglutarate metabolic process	BP
GO:000916	0.002475	1	1	ribonucleoside monophosphate metabolic proce	BP
GO:001087	0.002489	1	0.105148	cholesterol storage	BP
GO:003370	0.002511	1	0.131008	phospholipid efflux	BP
GO:000608	0.00275	1	6.65E-05	cellular aldehyde metabolic process	BP
GO:003111	0.002774	1	0.241597	regulation of microtubule depolymerization	BP
GO:000941	0.002926	1	0.006427	response to xenobiotic stimulus	BP
GO:000633	0.002991	1	0.518331	DNA replication-independent nucleosome assem	BP
GO:003472	0.002991	1	0.518331	DNA replication-independent nucleosome organi	BP
GO:000912	0.00309	1	1	purine nucleoside monophosphate metabolic pr	BP
GO:000916	0.00309	1	1	purine ribonucleoside monophosphate metaboli	BP
GO:000606	0.003268	1	0.119241	ethanol oxidation	BP
GO:004483	0.003326	1	0.291271	cell cycle G2/M phase transition	BP

GO:000674	0.003327	1	0.045138	glutathione metabolic process	BP
GO:004243	0.003339	1	0.000108	melanin biosynthetic process	BP
GO:007232	0.003369	1	0.065993	monocarboxylic acid catabolic process	BP
GO:003408	0.003464	1	0.34497	CENP-A containing nucleosome assembly	BP
GO:006164	0.003464	1	0.34497	CENP-A containing chromatin organization	BP
GO:004647	0.003583	1	0.530882	phosphatidylcholine metabolic process	BP
GO:000627	0.003597	1	0.268081	DNA replication initiation	BP
GO:000008	0.003634	1	0.304246	G2/M transition of mitotic cell cycle	BP
GO:004871	0.003649	1	0.176709	negative regulation of astrocyte differentiation	BP
GO:004326	0.003678	1	0.298474	regulation of potassium ion transport	BP
GO:004455	0.003726	1	6.08E-05	secondary metabolite biosynthetic process	BP
GO:000906	0.003752	1	0.927741	aerobic respiration	BP
GO:004616	0.003867	1	0.15834	alcohol biosynthetic process	BP
GO:000713	0.00403	1	1	reciprocal meiotic recombination	BP
GO:003582	0.00403	1	1	reciprocal DNA recombination	BP
GO:000695	0.004174	1	0.150685	complement activation	BP
GO:004611	0.004235	1	0.627265	nucleobase biosynthetic process	BP
GO:003237	0.004283	1	0.065847	positive regulation of sterol transport	BP
GO:003237	0.004283	1	0.065847	positive regulation of cholesterol transport	BP
GO:000712	0.004557	1	0.879553	meiotic nuclear division	BP
GO:004665	0.004557	1	0.15776	folic acid metabolic process	BP
GO:003334	0.004639	1	0.166234	cholesterol efflux	BP
GO:004364	0.005157	1	0.433678	dicarboxylic acid metabolic process	BP
GO:000708	0.005166	1	0.300971	regulation of mitosis	BP
GO:000673	0.005188	1	0.622461	oxidoreduction coenzyme metabolic process	BP
GO:001074	0.005235	1	0.141063	negative regulation of macrophage derived foam	BP
GO:001088	0.005257	1	0.153065	regulation of cholesterol storage	BP
GO:001939	0.005262	1	0.328246	fatty acid oxidation	BP
GO:000022	0.005336	1	0.115782	microtubule cytoskeleton organization	BP
GO:007233	0.005425	1	0.364794	modified amino acid transport	BP
GO:005066	0.005552	1	0.441374	homocysteine metabolic process	BP
GO:200017	0.00563	1	0.136952	positive regulation of neural precursor cell prolif	BP
GO:000629	0.0057	1	0.771975	mismatch repair	BP
GO:001076	0.0057	1	0.095484	positive regulation of sodium ion transport	BP
GO:190101	0.005717	1	0.731569	regulation of potassium ion transmembrane tran	BP
GO:000609	0.005734	1	0.69149	glycolytic process	BP
GO:000672	0.00587	1	0.000193	isoprenoid metabolic process	BP
GO:000333	0.005871	1	0.035314	amino acid transmembrane transport	BP
GO:007187	0.005873	1	0.027937	response to epinephrine	BP
GO:006500	0.005875	1	0.541208	protein-lipid complex assembly	BP
GO:004694	0.006059	1	0.008481	carboxylic acid transport	BP
GO:004348	0.006074	1	0.28565	histone exchange	BP
GO:004243	0.006178	1	0.479505	ethanolamine-containing compound metabolic p	BP
GO:004275	0.006178	1	0.125408	negative regulation of circadian rhythm	BP
GO:007187	0.006392	1	0.314448	adrenergic receptor signaling pathway	BP
GO:000009	0.00645	1	0.245485	sulfur amino acid catabolic process	BP
GO:000820	0.006816	1	0.142462	cholesterol metabolic process	BP

GO:001074	0.007102	1	0.186422	macrophage derived foam cell differentiation	BP
GO:009007	0.007102	1	0.186422	foam cell differentiation	BP
GO:001584	0.007413	1	0.007849	organic acid transport	BP
GO:004871	0.007466	1	0.008213	regulation of astrocyte differentiation	BP
GO:003444	0.007706	1	0.298237	lipid oxidation	BP
GO:000907	0.007908	1	0.704198	serine family amino acid biosynthetic process	BP
GO:000606	0.008175	1	0.032526	ethanol metabolic process	BP
GO:004568	0.008213	1	0.03292	regulation of glial cell differentiation	BP
GO:005132	0.008392	1	0.791268	meiotic cell cycle	BP
GO:000657	0.008571	1	0.538139	cellular biogenic amine metabolic process	BP
GO:004324	0.008799	1	0.84473	protein complex disassembly	BP
GO:190293	0.008805	1	0.096018	positive regulation of alcohol biosynthetic proces	BP
GO:004691	0.008832	1	0.516754	cellular transition metal ion homeostasis	BP
GO:001605	0.008894	1	0.022671	organic acid biosynthetic process	BP
GO:004639	0.008894	1	0.022671	carboxylic acid biosynthetic process	BP
GO:000705	0.00892	1	0.061413	spindle organization	BP
GO:001612	0.009027	1	0.609909	sterol biosynthetic process	BP
GO:000686	0.009071	1	0.000694	amino acid transport	BP
GO:000641	0.009175	1	1	translational elongation	BP
GO:001567	0.009309	1	0.058139	monovalent inorganic cation transport	BP
GO:003541	0.00944	1	0.169143	protein localization to synapse	BP
GO:003317	0.009584	1	0.204049	calcineurin-NFAT signaling cascade	BP
GO:000018	1	0.004988	0.595475	inactivation of MAPK activity	BP
GO:000076	1	0.009337	0.240799	syncytium formation by plasma membrane fusio	BP
GO:00015C	1	2.18E-06	3.74E-05	skeletal system development	BP
GO:000152	1	1.38E-06	1.85E-08	angiogenesis	BP
GO:000156	1	6.08E-05	0.001478	patterning of blood vessels	BP
GO:000166	1	0.000417	2.45E-07	ameboidal cell migration	BP
GO:00017C	1	0.00111	0.003684	formation of primary germ layer	BP
GO:000176	1	0.000266	1.17E-06	morphogenesis of a branching structure	BP
GO:000181	1	0.001386	0.040764	regulation of cytokine production	BP
GO:000193	1	0.002133	0.001452	negative regulation of protein phosphorylation	BP
GO:000195	1	0.007647	0.027937	regulation of cell-matrix adhesion	BP
GO:00020C	1	0.006484	1.64E-09	morphogenesis of an epithelium	BP
GO:000206	1	0.000262	0.081645	chondrocyte development	BP
GO:000236	1	0.007992	0.300971	T cell cytokine production	BP
GO:000242	1	0.00018	0.482575	immune response-activating cell surface recepto	BP
GO:000243	1	6.37E-06	0.898861	Fc receptor mediated stimulatory signaling pathv	BP
GO:000243	1	6.36E-06	0.924106	immune response-regulating cell surface recepto	BP
GO:000247	1	0.00035	0.537427	antigen processing and presentation of peptide a	BP
GO:000247	1	0.001509	0.004735	antigen processing and presentation of exogenou	BP
GO:000247	1	0.001628	0.450224	antigen processing and presentation of exogenou	BP
GO:000252	1	0.006959	0.017595	leukocyte differentiation	BP
GO:000269	1	0.006754	0.164184	regulation of leukocyte activation	BP
GO:000269	1	9.90E-05	0.432886	positive regulation of leukocyte activation	BP
GO:00027C	1	0.006869	0.874259	positive regulation of production of molecular m	BP
GO:000272	1	0.00854	0.923761	positive regulation of cytokine production involv	BP

GO:000275	1	0.000281	0.518726	immune response-activating signal transduction	BP
GO:000276	1	9.81E-06	0.142808	immune response-regulating signaling pathway	BP
GO:000276	1	4.23E-05	0.19906	immune response-regulating cell surface receptc	BP
GO:000309	1	0.000566	0.044497	glomerular filtration	BP
GO:000602	1	0.000259	0.006965	proteoglycan metabolic process	BP
GO:000646	1	0.001433	0.02517	negative regulation of protein kinase activity	BP
GO:000648	1	0.000186	0.402251	protein glycosylation	BP
GO:000648	1	1.16E-05	0.157727	protein N-linked glycosylation	BP
GO:000688	1	4.97E-05	0.049947	ER to Golgi vesicle-mediated transport	BP
GO:000689	1	0.001012	0.906512	retrograde vesicle-mediated transport, Golgi to E	BP
GO:000689	1	0.002143	0.796339	post-Golgi vesicle-mediated transport	BP
GO:000689	1	0.004334	0.92091	Golgi to endosome transport	BP
GO:000690	1	0.00034	0.083326	membrane budding	BP
GO:000690	1	0.000164	0.069687	vesicle coating	BP
GO:000690	1	0.000158	0.04932	vesicle targeting	BP
GO:000690	1	0.000185	0.010056	phagocytosis	BP
GO:000691	1	0.005742	0.685629	autophagy	BP
GO:000697	1	0.007736	0.233809	DNA damage response, signal transduction by p5	BP
GO:000698	1	8.33E-11	5.05E-06	ER-nucleus signaling pathway	BP
GO:000698	1	1.56E-10	0.001293	response to unfolded protein	BP
GO:000698	1	7.24E-13	1.96E-05	activation of signaling protein activity involved in	BP
GO:000701	1	7.14E-05	0.001476	actin filament organization	BP
GO:000702	1	0.001923	0.001121	endoplasmic reticulum organization	BP
GO:000705	1	0.008278	0.006015	cell cycle arrest	BP
GO:000715	1	0.000706	0.043068	leukocyte cell-cell adhesion	BP
GO:000716	1	9.49E-05	0.000164	cell-matrix adhesion	BP
GO:000716	1	0.000125	0.008967	negative regulation of cell adhesion	BP
GO:000717	1	0.000564	0.016963	epidermal growth factor receptor signaling pathv	BP
GO:000717	1	5.22E-05	0.000371	transmembrane receptor protein serine/threonir	BP
GO:000717	1	0.000984	0.011293	transforming growth factor beta receptor signali	BP
GO:000724	1	0.007153	0.86915	I-kappaB kinase/NF-kappaB signaling	BP
GO:000725	1	0.001036	0.098349	activation of NF-kappaB-inducing kinase activity	BP
GO:000725	1	0.000374	0.166036	I-kappaB phosphorylation	BP
GO:000726	1	0.005273	0.00077	Ras protein signal transduction	BP
GO:000736	1	0.006329	0.000492	gastrulation	BP
GO:000750	1	0.003736	4.86E-07	heart development	BP
GO:000751	1	1.37E-06	0.013551	muscle organ development	BP
GO:000751	1	9.20E-05	0.491457	skeletal muscle tissue development	BP
GO:000752	1	0.007338	0.362032	myoblast fusion	BP
GO:000806	1	1.63E-05	0.020553	regulation of actin polymerization or depolymeri	BP
GO:000815	1	0.000234	0.001178	actin polymerization or depolymerization	BP
GO:000836	1	0.005336	0.047538	regulation of cell size	BP
GO:000854	1	3.19E-05	0.138167	fibroblast growth factor receptor signaling pathv	BP
GO:000862	1	0.007226	0.202811	extrinsic apoptotic signaling pathway via death d	BP
GO:000863	1	0.005336	0.000414	intrinsic apoptotic signaling pathway in response	BP
GO:000910	1	2.87E-07	0.033899	glycoprotein metabolic process	BP
GO:000910	1	9.07E-06	0.066893	glycoprotein biosynthetic process	BP

GO:000922	1	0.004762	0.101281	nucleotide-sugar metabolic process	BP
GO:000922	1	0.00228	0.127075	nucleotide-sugar biosynthetic process	BP
GO:00093C	1	0.006959	0.10632	protein secretion	BP
GO:00094C	1	0.005577	0.135238	response to heat	BP
GO:000961	1	8.76E-05	3.63E-05	response to mechanical stimulus	BP
GO:00100C	1	0.000721	0.142722	cardioblast differentiation	BP
GO:001056	1	5.89E-05	0.000627	negative regulation of phosphorus metabolic pro	BP
GO:001063	1	0.004969	3.11E-05	epithelial cell migration	BP
GO:001095	1	0.004521	0.000366	positive regulation of peptidase activity	BP
GO:00147C	1	8.37E-05	0.007739	striated muscle tissue development	BP
GO:001605	1	0.001029	0.014164	vesicle organization	BP
GO:001605	1	0.00554	0.077508	Wnt signaling pathway	BP
GO:001619	1	0.002626	0.910158	endosomal transport	BP
GO:001633	1	7.97E-10	2.24E-08	single organismal cell-cell adhesion	BP
GO:001648	1	0.004237	0.032829	peptide hormone processing	BP
GO:001652	1	0.009999	0.073957	negative regulation of angiogenesis	BP
GO:001701	1	0.007793	0.01803	regulation of transforming growth factor beta re	BP
GO:001812	1	0.01	0.12411	protein hydroxylation	BP
GO:001814	1	6.36E-05	0.003178	peptide cross-linking	BP
GO:001819	1	6.14E-06	0.117724	peptidyl-asparagine modification	BP
GO:00182C	1	0.005279	0.514836	peptidyl-proline modification	BP
GO:00182C	1	0.004846	0.023974	peptidyl-serine modification	BP
GO:001827	1	9.75E-06	0.134584	protein N-linked glycosylation via asparagine	BP
GO:001988	1	0.001576	0.013422	antigen processing and presentation	BP
GO:001988	1	0.000762	0.004572	antigen processing and presentation of exogenou	BP
GO:00224C	1	0.002163	0.804615	membrane docking	BP
GO:00224C	1	0.003268	0.007736	negative regulation of cell-cell adhesion	BP
GO:00226C	1	0.001036	1.73E-07	regulation of cell morphogenesis	BP
GO:002261	1	0.00103	0.000196	gland morphogenesis	BP
GO:002261	1	0.003088	3.32E-06	extracellular matrix disassembly	BP
GO:003003	1	7.07E-09	4.42E-09	actin cytoskeleton organization	BP
GO:003004	1	0.009664	0.032548	actin filament polymerization	BP
GO:003004	1	0.005554	0.1046	actin filament depolymerization	BP
GO:003015	1	0.000122	1.48E-12	regulation of cell adhesion	BP
GO:003016	1	0.005875	0.020936	proteoglycan biosynthetic process	BP
GO:003016	1	0.000274	0.000257	platelet activation	BP
GO:003019	1	3.51E-10	4.19E-22	extracellular matrix organization	BP
GO:003019	1	1.38E-05	0.012168	collagen fibril organization	BP
GO:00302C	1	0.006329	0.000847	glycosaminoglycan metabolic process	BP
GO:00302C	1	7.63E-05	0.030828	chondroitin sulfate metabolic process	BP
GO:00302C	1	0.000766	0.086814	chondroitin sulfate biosynthetic process	BP
GO:003033	1	0.000113	0.047539	DNA damage response, signal transduction by p5	BP
GO:003051	1	4.02E-05	5.90E-05	regulation of axon extension	BP
GO:003051	1	0.006142	0.002332	negative regulation of axon extension	BP
GO:003083	1	1.38E-05	0.021805	regulation of actin filament length	BP
GO:003083	1	0.000195	0.155364	regulation of actin filament polymerization	BP
GO:003083	1	0.00501	0.583753	positive regulation of actin filament polymerizati	BP

GO:003096	1	8.33E-11	4.06E-05	endoplasmic reticulum unfolded protein respons	BP
GO:003134	1	0.006044	0.000271	positive regulation of cell projection organizatior	BP
GO:003134	1	0.001956	0.69149	positive regulation of defense response	BP
GO:00314C	1	0.00645	0.013717	negative regulation of protein modification proce	BP
GO:003157	1	0.004969	0.17994	mitotic G1 DNA damage checkpoint	BP
GO:003158	1	6.26E-06	1.87E-08	cell-substrate adhesion	BP
GO:003167	1	0.000932	0.011776	cellular response to nutrient	BP
GO:003206	1	1.16E-11	0.000203	regulation of nuclease activity	BP
GO:003207	1	3.02E-12	6.84E-06	positive regulation of nuclease activity	BP
GO:003209	1	0.004174	0.034315	positive regulation of protein binding	BP
GO:00321C	1	0.006484	0.125672	positive regulation of response to external stimu	BP
GO:003231	1	0.009337	0.003882	regulation of Rho GTPase activity	BP
GO:003232	1	0.000252	0.008322	positive regulation of Rho GTPase activity	BP
GO:003253	1	3.52E-07	0.006434	regulation of cellular component size	BP
GO:003261	1	0.005315	0.05584	interleukin-1 production	BP
GO:003263	1	0.001375	0.064587	interleukin-6 production	BP
GO:003263	1	0.00606	0.507663	interleukin-8 production	BP
GO:003265	1	0.001898	0.060206	regulation of interleukin-1 production	BP
GO:003267	1	0.001885	0.052361	regulation of interleukin-6 production	BP
GO:003267	1	0.002146	0.675179	regulation of interleukin-8 production	BP
GO:003273	1	0.001763	0.125048	positive regulation of interleukin-1 production	BP
GO:003294	1	0.001796	0.013621	mononuclear cell proliferation	BP
GO:003294	1	0.000627	0.372415	positive regulation of mononuclear cell prolifera	BP
GO:003295	1	0.000168	0.00323	regulation of actin cytoskeleton organization	BP
GO:003297	1	0.000172	5.60E-05	regulation of actin filament-based process	BP
GO:00332C	1	0.00237	0.474224	tumor necrosis factor-mediated signaling pathwa	BP
GO:003367	1	0.005873	0.018038	negative regulation of kinase activity	BP
GO:003367	1	0.000344	1.97E-08	positive regulation of kinase activity	BP
GO:003411	1	0.002401	0.075589	heterotypic cell-cell adhesion	BP
GO:003431	1	0.007507	0.657549	Arp2/3 complex-mediated actin nucleation	BP
GO:003432	1	0.003476	0.00023	cell junction assembly	BP
GO:003433	1	0.002936	4.14E-06	cell junction organization	BP
GO:003434	1	0.000467	0.057203	glial cell apoptotic process	BP
GO:003444	1	0.000105	0.000947	substrate adhesion-dependent cell spreading	BP
GO:00345C	1	0.008032	0.008213	protein localization to nucleus	BP
GO:003462	1	5.11E-11	4.26E-05	cellular response to unfolded protein	BP
GO:003497	1	2.44E-11	0.000544	response to endoplasmic reticulum stress	BP
GO:003596	1	0.00594	0.306857	COPI-coated vesicle budding	BP
GO:003596	1	7.05E-10	0.002063	response to topologically incorrect protein	BP
GO:003596	1	5.62E-11	0.000165	cellular response to topologically incorrect prote	BP
GO:003803	1	0.000868	0.158152	signal transduction in absence of ligand	BP
GO:003809	1	1.17E-06	0.637993	Fc receptor signaling pathway	BP
GO:003809	1	6.36E-06	0.924106	Fc-gamma receptor signaling pathway	BP
GO:003809	1	0.0003	0.26465	Fc-epsilon receptor signaling pathway	BP
GO:003809	1	6.36E-06	0.924106	Fc-gamma receptor signaling pathway involved i	BP
GO:003812	1	0.000128	0.019666	ERBB signaling pathway	BP
GO:003817	1	0.000566	0.212366	neurotrophin signaling pathway	BP

GO:004209	1	0.001295	0.001354	T cell proliferation	BP
GO:00421C	1	0.001893	0.157021	positive regulation of T cell proliferation	BP
GO:004211	1	3.82E-05	0.024723	T cell activation	BP
GO:004232	1	0.000268	0.000348	negative regulation of phosphorylation	BP
GO:004259	1	0.003157	0.41787	antigen processing and presentation of exogenoı	BP
GO:004269	1	0.007457	0.007153	muscle cell differentiation	BP
GO:004277	1	0.000202	0.052881	signal transduction in response to DNA damage	BP
GO:004301	1	0.004062	0.529951	myeloid dendritic cell differentiation	BP
GO:004306	1	3.51E-10	4.19E-22	extracellular structure organization	BP
GO:004306	1	0.006764	0.000119	positive regulation of apoptotic process	BP
GO:004306	1	0.00439	9.49E-05	positive regulation of programmed cell death	BP
GO:004312	1	0.009027	0.844844	regulation of I-kappaB kinase/NF-kappaB signalir	BP
GO:004312	1	0.008554	0.809643	positive regulation of I-kappaB kinase/NF-kappaE	BP
GO:004341	1	0.000186	0.402251	macromolecule glycosylation	BP
GO:004351	1	0.001619	0.263843	regulation of DNA damage response, signal trans	BP
GO:004352	1	0.007721	0.901251	positive regulation of neuron apoptotic process	BP
GO:004354	1	0.003265	3.19E-05	endothelial cell migration	BP
GO:004358	1	0.004212	0.019554	skin morphogenesis	BP
GO:004368	1	0.005717	0.230603	post-translational protein modification	BP
GO:004434	1	0.000113	0.040323	cellular response to fibroblast growth factor stim	BP
GO:004478	1	0.006329	0.237627	G1 DNA damage checkpoint	BP
GO:004481	1	0.004137	0.179847	mitotic G1/S transition checkpoint	BP
GO:00451C	1	0.006442	0.344566	intermediate filament-based process	BP
GO:004512	1	3.73E-05	0.090706	cellular extravasation	BP
GO:004545	1	0.004632	0.18133	cell redox homeostasis	BP
GO:004577	1	0.000164	0.000274	positive regulation of axon extension	BP
GO:004578	1	0.01	9.46E-10	positive regulation of cell adhesion	BP
GO:004586	1	0.001513	2.84E-08	positive regulation of protein kinase activity	BP
GO:004593	1	5.89E-05	0.000627	negative regulation of phosphate metabolic proc	BP
GO:004633	1	0.003326	0.204674	positive regulation of JNK cascade	BP
GO:004665	1	0.002237	0.011998	lymphocyte proliferation	BP
GO:004682	1	0.006852	0.057497	regulation of protein export from nucleus	BP
GO:00480C	1	0.000868	0.025681	antigen processing and presentation of peptide a	BP
GO:004801	1	0.00036	0.203121	neurotrophin TRK receptor signaling pathway	BP
GO:004819	1	7.22E-10	0.286095	Golgi vesicle transport	BP
GO:004819	1	7.45E-06	0.11361	vesicle targeting, to, from or within Golgi	BP
GO:00482C	1	0.00594	0.306857	Golgi transport vesicle coating	BP
GO:00482C	1	0.00594	0.306857	COPI coating of Golgi vesicle	BP
GO:00482C	1	0.001004	0.138865	vesicle targeting, rough ER to cis-Golgi	BP
GO:00482C	1	0.001004	0.138865	COPII vesicle coating	BP
GO:004827	1	0.002074	1	vesicle docking	BP
GO:004851	1	7.17E-07	8.63E-10	blood vessel morphogenesis	BP
GO:004863	1	0.000847	9.20E-05	positive regulation of developmental growth	BP
GO:004867	1	9.11E-05	0.00035	axon extension	BP
GO:00487C	1	0.006125	0.034917	skeletal system morphogenesis	BP
GO:004875	1	0.001923	0.000137	branching morphogenesis of an epithelial tube	BP
GO:005065	1	0.001628	0.017497	chondroitin sulfate proteoglycan biosynthetic pr	BP

GO:005065	1	0.00019	0.011739	chondroitin sulfate proteoglycan metabolic proc	BP
GO:005066	1	0.001824	0.098837	cytokine secretion	BP
GO:005067	1	0.000863	0.345673	positive regulation of lymphocyte proliferation	BP
GO:00507C	1	0.00035	0.084885	interleukin-1 secretion	BP
GO:00507C	1	0.000215	0.064776	regulation of interleukin-1 secretion	BP
GO:00507C	1	0.001461	0.030183	regulation of cytokine secretion	BP
GO:00507C	1	0.007021	0.068069	regulation of protein secretion	BP
GO:005071	1	0.007759	0.118706	negative regulation of cytokine secretion	BP
GO:005071	1	0.003318	0.28321	positive regulation of interleukin-1 secretion	BP
GO:005073	1	0.004705	0.000982	regulation of peptidyl-tyrosine phosphorylation	BP
GO:005073	1	0.002952	0.249107	negative regulation of peptidyl-tyrosine phospho	BP
GO:005077	1	0.003476	4.41E-05	positive regulation of axonogenesis	BP
GO:005085	1	0.006851	0.087974	T cell receptor signaling pathway	BP
GO:005086	1	0.00068	0.423152	regulation of T cell activation	BP
GO:005086	1	0.00947	0.060405	regulation of cell activation	BP
GO:005086	1	0.000548	0.332661	positive regulation of cell activation	BP
GO:005087	1	0.00027	0.359681	positive regulation of T cell activation	BP
GO:00509C	1	3.03E-05	0.067848	leukocyte tethering or rolling	BP
GO:005109	1	0.00045	0.02412	positive regulation of binding	BP
GO:005121	1	0.004766	0.000116	cartilage development	BP
GO:005122	1	0.002746	0.002304	regulation of protein transport	BP
GO:005122	1	0.005279	0.053757	negative regulation of protein transport	BP
GO:005124	1	0.000628	0.417826	regulation of lymphocyte activation	BP
GO:005125	1	0.000104	0.421044	positive regulation of lymphocyte activation	BP
GO:005134	1	0.000398	0.040678	negative regulation of transferase activity	BP
GO:005159	1	0.006919	0.00028	response to calcium ion	BP
GO:006032	1	0.004988	0.085416	cell chemotaxis	BP
GO:006034	1	0.003861	0.008574	bone development	BP
GO:006053	1	1.38E-05	0.002257	muscle tissue development	BP
GO:006053	1	0.000118	0.523101	skeletal muscle organ development	BP
GO:006056	1	0.007108	2.40E-05	developmental growth involved in morphogenes	BP
GO:006056	1	0.004705	0.064652	apoptotic process involved in morphogenesis	BP
GO:006113	1	0.000279	8.72E-07	morphogenesis of a branching epithelium	BP
GO:006138	1	0.004274	6.39E-05	regulation of extent of cell growth	BP
GO:006144	1	0.007356	1.46E-06	connective tissue development	BP
GO:007008	1	6.71E-05	0.407438	glycosylation	BP
GO:00702C	1	0.0019	0.000706	regulation of establishment of protein localizatio	BP
GO:007052	1	0.005493	0.282279	platelet aggregation	BP
GO:007066	1	0.001226	0.00549	leukocyte proliferation	BP
GO:007066	1	0.005336	0.030169	regulation of leukocyte proliferation	BP
GO:007066	1	0.000566	0.373577	positive regulation of leukocyte proliferation	BP
GO:007115	1	0.002837	0.055893	positive regulation of cell cycle arrest	BP
GO:007126	1	0.000414	0.015974	cellular response to mechanical stimulus	BP
GO:007129	1	0.001098	0.018833	cellular response to vitamin	BP
GO:007149	1	0.000597	0.003561	cellular response to external stimulus	BP
GO:007155	1	0.001264	0.0111	response to transforming growth factor beta	BP
GO:007156	1	0.001264	0.0111	cellular response to transforming growth factor b	BP

GO:007177	1	7.04E-05	0.033579	response to fibroblast growth factor	BP
GO:007201	1	0.006724	0.013925	glomerulus vasculature development	BP
GO:007221	1	0.000414	0.001923	metanephric nephron development	BP
GO:007222	1	0.007739	0.359781	metanephric glomerulus development	BP
GO:007233	1	0.000141	0.011461	signal transduction by p53 class mediator	BP
GO:007238	1	0.001893	0.639679	organelle transport along microtubule	BP
GO:009006	1	6.24E-05	6.86E-05	regulation of anatomical structure size	BP
GO:009009	1	0.003504	0.000428	regulation of transmembrane receptor protein se	BP
GO:009011	1	0.005251	0.075219	COPII-coated vesicle budding	BP
GO:009013	1	0.006329	3.19E-05	tissue migration	BP
GO:009013	1	0.004969	3.11E-05	epithelium migration	BP
GO:009028	1	0.005225	0.003726	regulation of cellular response to growth factor s	BP
GO:009719	1	4.80E-07	0.073232	extrinsic apoptotic signaling pathway	BP
GO:009719	1	0.000868	0.158152	extrinsic apoptotic signaling pathway in absence	BP
GO:009720	1	0.000164	0.023057	renal filtration	BP
GO:009728	1	0.00113	0.000242	cell-type specific apoptotic process	BP
GO:009860	1	5.11E-11	3.60E-10	single organism cell adhesion	BP
GO:190018	1	0.009399	0.01576	regulation of protein localization to nucleus	BP
GO:190259	1	4.61E-05	0.03292	single-organism membrane budding	BP
GO:190274	1	0.003319	0.024854	apoptotic process involved in development	BP
GO:190280	1	0.003396	0.061689	negative regulation of cell cycle G1/S phase trans	BP
GO:190303	1	0.009917	0.000533	regulation of response to wounding	BP
GO:199013	1	0.000213	0.000225	neuron projection extension	BP
GO:200013	1	0.003396	0.061689	negative regulation of G1/S transition of mitotic	BP
GO:200020	1	0.003839	0.00023	regulation of anoikis	BP
GO:200035	1	0.009071	0.14098	negative regulation of endothelial cell apoptotic	BP
GO:200123	1	0.007767	0.034613	regulation of apoptotic signaling pathway	BP
GO:200123	1	2.94E-05	0.034603	regulation of extrinsic apoptotic signaling pathwa	BP
GO:200123	1	6.65E-05	0.167836	positive regulation of extrinsic apoptotic signalin	BP
GO:200123	1	0.000254	0.104853	regulation of extrinsic apoptotic signaling pathwa	BP

ne presence vs absence of dbcAMP at Day35 in culture.

dir
U
U
U
U
U
U
U
U
U
U
U
U
U
U
U
U
U
U
U
U
U
U
U
U
U
U
U
U
U
U
U
U
U
U
U
U
U
U
U
U
U
U
U
U
U

U
U
U
U
U
U
U
U
U
U
U
U
U
U
U
U
U
U
U
U
U
U
U
U
U
U
U
U
U
U
U
U
U
U
U
U
U
U
U
U
U
U
U
U
U
U
U

U
U
U
U
U
U
U
U
U
U
U
U
U
U
U
U
U
U
U
U
U
U
U
U
U
U
U
U
U
U
U
U
U
U
U
U
U
U
U
U
U
U
U
U
U
U
U

U
U
U
U
U
U
U
U
U
U
U
U
U
U
U
U
U
U
U
U
U
U
U
D
D
D
D
D
D
D
D
D
D
D
D
D
D
D
D
D
D
D
D
D
D
D
D
D
D
D
D
D

D
D
D
D
D
D
D
D
D
D
D
D
D
D
D
D
D
D
D
D
D
D
D
D
D
D
D
D
D
D
D
D
D
D
D
D
D
D
D
D
D
D
D
D
D
D
D

D
D
D
D
D
D
D
D
D
D
D
D
D
D
D
D
D
D
D
D
D
D
D
D
D
D
D
D
D
D
D
D
D
D
D
D
D
D
D
D
D
D
D
D
D
D
D

D
D
D
D
D
D
D
D
D
D
D
D
D
D
D
D
D
D
D
D
D
D
D
D
D
D
D
D
D
D
D
D
D
D
D
D
D
D
D
D
D
D
D
D
D
D
D

D
D
D
D
D
D
D
D
D
D
D
D
D
D
D
D
D
D
D
D
D
D
D
D
D
D
D
D
D
D
D
D
D
D
D
D
D
D
D
D
D
D
D
D
D
D
D

D
D
D
D
D
D
D
D
D
D
D
D
D
D
D
D
D
D
D
D
D
D
D
D
D
D
D
D
D
D
D
D
D
D
D
D
D
D
D
D
D
D
D
D
D
D
D

D
D
D
D
D
D
D
D
D
D
D
D
D
D
D
D
D
D
D
D
D
D
D
D
D
D
D
D
D
D
D
D